THE UNIVERSITY OF
SYDNEY

Smart Grid Communications in High Traffic Environments

By

ROBERT EDWARD DOUGLAS WEBSTER

B. Eng. (Hons), B. Sc., University of Sydney, Australia, 2012

A THESIS SUBMITTED IN FULFILLMENT OF THE REQUIREMENTS FOR THE DEGREE OF MASTER OF PHILOSOPHY

In

THE SCHOOL OF ELECTRICAL AND INFORMATION ENGINEERING

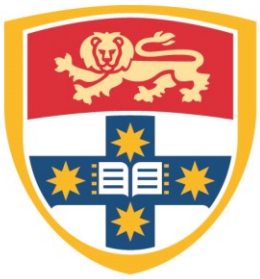

THE UNIVERSITY OF SYDNEY

2014

Statement of Originality

The novel research results reported in this thesis represent an original work by the author, at the School of Electrical and Information Engineering, The University of Sydney, under the guidance and instruction of Professor Abbas Jamalipour and Dr. Kumudu Munasinghe. The presented results rely on numerous research results taken from well-known references as well as on results taken from recent publications. None of the content of this thesis has been previously submitted for the consideration for a degree or any qualification. Some of the results have been published or submitted for publication in conference proceedings as listed in this thesis.

Robert Edward Douglas Webster
2014

Abstract

The establishment of a previously non-existent data class known as the Smart Grid will pose many difficulties on current and future communication infrastructure. It is imperative that the Smart Grid, as the reactionary and monitory arm of the Power Grid, be able to communicate effectively between grid controllers and individual User Equipment (UE). By doing so, the successful implementation of Smart Grid applications can occur, including support for higher capacities of Renewable Energy Resources.

As the Smart Grid matures, the number of UEs required is expected to rise. This will increase the traffic in an already burdened communications network. This thesis aims to optimally allocate radio resources such that the Smart Grid Quality of Service requirements are satisfied, with minimal effect on pre-existing traffic caused by the imposition of Smart Grid UEs.

To address this resource allocation problem, a Lotka-Volterra based resource allocation and scheduler was developed due to its ability to easily adapt to the dynamics of a telecommunications environment. Each 'species' in the Lotka-Volterra scheme was modelled as either Data, Voice or Smart Grid traffic class in a Rayleigh-Fading channel. Unlike previous resource allocation algorithms, the Lotka-Volterra scheme allocated telecommunications resources to each class as a function of its growth rate. Subcarrier power allocation was non-uniform and the total power allocated to each class is based on the size of its queued traffic. By doing so, the Quality of Service requirements of the Smart Grid were satisfied, with minimal effect on pre-existing traffic. Class queue latencies were reduced by intelligent scheduling of periodic traffic and forward allocation of resources.

By allocating resources based on growth rates and queue sizes, the system produced fairer performance for all UEs. This produced higher average throughput rates than examined in other common opportunistic schedulers.

The overall results and analysis of this research concludes that the Smart Grid will have a large effect on the telecommunications environment if not successfully controlled and monitored. This effect can be minimized by utilizing the proposed Lotka-Volterra based resource allocation and scheduler system. Furthermore, it was shown that the allocation of periodic Smart Grid radio channels was optimized by continual updates of the Lotka-Volterra model. This not only ensures the Quality of Service requirements of the Smart Grid are accomplished but provides enhanced performance. Successful integration of Smart Grid UEs in a wireless network can pave the way for increases in total capacity of Renewable and Intermittent Energy Resources operating on the Power Grid.

Acknowledgments

First and foremost, I would like to extend my sincere gratitude and appreciation to my primary supervisor, Professor Abbas Jamalipour. Professor Jamalipour has provided me with a great amount of support, both technical and personal, and without whom this thesis would not be possible. Secondly, my deepest respect and thanks to Dr. Kumudu Munasinghe, my secondary supervisor, who provided invaluable knowledge and expertise, and who helped shaped my thesis.

To all members, past and present, of the Wireless Networking Group at the University of Sydney, my many thanks. All members provided such a warm and encouraging research office and ensured technical rigor to all research conducted there.

To my partner, Lauren Anderson, who has had to deal with having no dining room table for the last two years, we can now eat at the table again! My many thanks to her for the support, encouragement and English & grammatical wizardry.

To my parents who are always a source of guidance and encouragement. To Glenn and Michelle Anderson, for always taking an interest in my research.

My heartfelt thanks to all my friends who stood by me and encouraged me every step of the way.

Table of Contents

List of Publications

International Conferences

[1] R. Webster, K. Munasinghe, A. Jamalipour, “A Scalable Distributed Microgrid Control Structure,” *IEEE TENCON Spring 2013*, Sydney, Australia, April 2013

[2] R. Webster, K. Munasinghe, A. Jamalipour, “A population theory inspired solution to the optimal bandwidth allocation for smart grid applications,” *IEEE WCNC 2014*, Istanbul, Turkey, April 2014

[3] R. Webster, K. Munasinghe, A. Jamalipour, “Optimal resource allocation for smart grid applications in high traffic wireless networks”, *IEEE SmartGridComm 2014*, Venice, Italy, November 2014

List of Figures

List of Tables

List of Algorithms

Acronyms

3GPP	Third Generation Partnership Project
ADC	Analog to Digital Conversion
APS	American Physical Society
BER	Bit Error Rate
BPL	Broadband over Power Line
CCI	Co-Channel Interference
CSI	Channel State Information
DA	Distribution Automation
DAN	Distribution Automation Network
DOE	Department of Energy (United States of America Government)
DRX	Delay Responsive Cross Layer
DwPTS	Downlink Pilot Time Slot
E-UTRAN	Evolved Universal Terrestrial Access Network
E_B/N_0	Energy per Bit / Noise Power Spectral Density Ratio
ECC	Error Correction Control
EMI	Electro-Magnetic Interference
eNB	Evolved Node-B
EPIA	European Photovoltaic Industry Association

FEC	Forward Error Correction
FFT	Fast Fourier Transform
FIFO	First In First Out
GP	Guard Period
H-ARQ	Hybrid Automatic Repeat reQuest
Hz	Hertz (s^{-1})
ICI	Inter-Carrier Interference
IEA	International Energy Agency
IED	Intelligent Electronic Device
IEEE	Institute of Electrical and Electronic Engineers
ISI	Inter Symbol Interference
L-V	Lotka-Volterra
LOS	Line Of Sight
LSP	Label Switched Paths
LTE	Long Term Evolution
LTE-A	Long Term Evolution Advanced
M2M	Machine To Machine
MAS	Multi-Agent System
MFS	Maximum Fairness Scheduler
MIMO	Multiple Input, Multiple Output
MSR	Maximum Sum Rate
NAPSI	North American SynchroPhasor Initiative
NBS	Nash Bargaining Solution

ODE	Ordinary Differential Equation
OFDM	Orthogonal Frequency Division Multiplexing
OFDMA	Orthogonal Frequency Division Multiple Access
PAPR	Peak-To-Average-Power Ratio
PC	Personal Computer
PDC	Phasor Data Concentrator
PER	Packet Error Rate
PLL	Phase Locked Loop
PMU	Phasor Measurement Unit
PRC	Proportional Rates Constraints
PV	Photo Voltaic
QAM	Quadrature Amplitude Modulation
QOS	Quality of Service
QPSK	Quadrature Phase Shift Keying
R&D	Research & Development
RET	Department of Resources, Energy and Tourism (Australian Government)
ROCOF	Rate of Change of Frequency
RPF	Rate Proportional Fairness
RRM	Radio Resource Management
SC-FDMA	Single Carrier – Frequency Division Multiple Access
SG	Smart Grid
SINR	Signal to Interference Plus Noise Ratio

SMI	Smart Metering Infrastructure
SNR	Signal to Noise Ratio
TCP/IP	Transport Control Protocol / Internet Protocol
TSO	Transmission System Operator
UCTE	Union for the Co-ordination of Transmission of Electricity
UE	User Equipment
UPF	Utility Proportional Fairness
UpPTS	Uplink Pilot Time Slot
USM	Utility Sum Maximization
VCO	Voltage Controlled Oscillator
VNI	Visual Networking Index
WAMPAC	Wide Area Monitoring, Protection, and Control
WiMAX	Worldwide Interoperability for Microwave Access
WSN	Wireless Sensor Network
WSO	Wireless Service Operators
WWEA	World Wind Energy Association

Chapter 1.
Introduction

The Smart Grid is the complete modernisation of the current power grid, by enabling it to provide complex functions and features with a higher degree of autonomy [1]. The three objectives of the smart grid are higher power efficiency, reliability and security. There still remains significant uncertainty about how Smart Grid technologies will emerge and ultimately be implemented. It is very apparent that an efficient and robust communications infrastructure is required to facilitate the transformation of the power grid [2] and it is this infrastructure that takes the central focus of this thesis.

The increase in distributed generation warrants the need for a communication network to monitor the stability of the distribution grid. It is required that the smart grid will encompass a high speed, two-way communications network which will facilitate the large amount of data monitoring in real time. The expected response time of the Smart Grid will be within milliseconds [3,4] providing unprecedented control and monitoring functions for grid operators to ensure power stability. The communications network will also provide the framework for driving autonomous functions utilising smart algorithms in real time. As such, no standardized communication network for Smart Grid applications exists. Due to the omnipresence of the Smart Grid, the fundamental

solution will be a wireless telecommunications network to ensure complete connectivity.

The integration of large amounts of distributed generation currently lies outside of the scope of the power grid. This is primarily due to the complexity of scheduling multiple small scale generators. To combat such environmental issues such as global warming there must be a reduction in the reliance on carbon intensive energy production such as coal power stations. Distributed generation composed of renewable energy generators such as wind and solar can be utilized to reduce spinning reserves of such coal power stations if they can be scheduled and monitored with high accuracy and do not diminish power quality and security [5,6,7,8]. In order to do this, communication must freely flow to and from Distributed Generators operating on the Smart Grid and grid controllers. This inclusion of a previously non-existent data class required by the Smart Grid poses many difficulties on current and future communication infrastructure. It is imperative that the Smart Grid, as the reactionary and monitory arm of the power grid, be able to communicate effectively between grid controllers and individual devices. This paradigm ensures that whilst the Smart Grid will be new in the field of communications theory, its effect will be large. Therefore, it is this thesis's goal to examine the resource allocation between differing service classes in a wireless communication environment and ensure the continual operation of current and future communication services.

The existence of multiple differing service classes is borne from a Multi-User communications environment with differing applications that require different bandwidth, latency, Quality of Service (QoS) etc. The differentiation of such services and the users that utilise them is known as Multi-User Diversity. Multi-User Diversity is defined as differing users requiring differing amount of resources and QoS dependent on their application, channel conditions, mobility, timing etc [9]. Multi-User Diversity has heralded a new age in the resource allocation problem by allowing Wireless Service Operators (WSO) to use opportunistic scheduling methods which can share resources more equally (or when required, unequally) between users [10]. The rate of growth of wireless access users is increasing at a rapid rate yet communications technology evolves discretely over time [11,12]. This disparity can be solved by finding an optimal operating point by exploiting the Multi-User Diversity environment. In this way, Multi-User Gain can be used to ensure current

communications infrastructure is capable of adapting to future or evolving requirements. The Smart Grid is such an evolving requirement that without proper integration will cause decreased performance in existing telecommunications infrastructure. This thesis seeks to address the proper integration of Smart Grid communications in pre-existing wireless networks by maximizing Multi-User Gain, whilst minimizing the imposition of Smart Grid traffic on that network. However, this must still be done so in a manner that upholds the strict QoS requirements of Smart Grid applications.

This thesis proposes that a solution to achieving optimal resource allocation is by use of a Radio Resource Management (RRM) and Opportunistic Scheduling scheme [13,14,15,16,17]. Radio Resource Management can be summarized as methods for the allocation of subcarriers to users, in addition to rate adaptation and transmit power control [18]. In a Multi-User environment, a subcarrier of low quality to one User Equipment (UE) may be of high quality to another UE. This forms the basis of the resource allocation problem which this thesis seeks to address. It argues that an optimal operating point can be found when viewing the system as a population dynamics problem. By doing so, the fluctuations of a wireless communications environment can be solved by non-linear differential equations used to describe the dynamics of biological systems.

This chapter will provide an introduction and background of the Smart Grid. This will contextualise the wireless resource allocation problem, which takes the focus of this thesis. Furthermore, this chapter will establish the motivation, purpose and scope of this thesis. It does this by firstly introducing the limitations of the current power grid architecture. This is followed by an explanation of the challenges facing integration of Smart Grid data packets into existing wireless communication networks. This chapter then briefly introduces Radio Resource Management, particularly in terms of Orthogonal Frequency Division Multiple Access (OFDMA). Finally, it outlines the overall structure of this thesis.

1.1 EVOLUTION OF THE POWER GRID

The current electrical power infrastructure has served us well for a long amount of time. However, the current power grid is rapidly approaching its limitations [4], which this chapter will now briefly explore. Global electrical grids are facing the largest technological transformation since the introduction to electricity to the home [19]. The challenges encountered during this transformation are currently being addressed by many academics and industry experts [20,21,22], providing insights into what the smart grid is likely to be able to achieve.

For example, Elsworth [4] describes the transition from the current power grid to the smart grid of the future as a two-step process. The first step in the advancement to the smart grid involves what she calls the 'smarter grid'. The 'smarter grid' provides higher efficiency by utilising technologies, tools and techniques that are available today. The second step is the complete transition to the smart grid. This is a much longer term goal that requires many evolutionary steps. This evolutionary process has also been taken up by Hart [23], who explains its evolutionary nature as dependent on the scope and stage of Research and Development (R&D) initiatives.

It should be noted that, despite the concept of a smart grid as a future possibility, there may in fact exist a smart grid of sorts today. However, Miller [24] notes that this present smart grid exists only in small pockets, and as a mere fraction of what it will be in the future.

1.2 THE CALL FOR A SMART GRID

It is important to note that the smart grid is not a single technology. To define it this way would impede its revolutionary power in the future. Rather, the smart grid is better described as the three aforementioned objectives: which, according to Elsworth [4], are most notably the increase of:

- Power efficiency

- Power reliability and
- Power security.

There are many pressures driving the need to achieve these goals, and the boundaries distinguishing these pressures are becoming increasingly blurred [4]. For example, pressures such as increased awareness of environmental issues, including climate change, are being coupled with social pressures for nations to reduce their carbon footprint. This topic has been explored by many academics, and whilst many solutions have been proposed, it is implicit that the Smart Grid will be the solution.

1.2.1 Distributed Generation Including Renewables

Elsworth [4] and He [25] define the two basic features of current day electrical power generation as the centralisation of large scale generation coupled with high voltage, long distance AC/DC transmission lines. Distribution grids were designed to transport power in a unidirectional flow from higher to lower voltage levels. This current model of electrical power production and transportation has served us well globally, and allowed countries and their economies to flourish with heightened productivity [4]. However, there are also evident deficiencies with the current power grid model. The Department of Resources, Energy and Tourism (RET) calculated that approximately ten per cent of electrical power generated is lost during its transportation [26]. Clearly, this is a significant figure that must be addressed.

Another issue is the problem of increasing global energy demand. This issue is exacerbated by the fact that climate change and greenhouse gas emissions are increasingly becoming influential concerns for societies around the world. This has been highlighted in a recent Australian Government report, which stated that the electrical power generating sector is currently facing the competing stresses of meeting increased energy demand and reducing the impact of greenhouse gases [5]

A novel solution to this problem that many governments are adopting is the subsidisation of small scale renewables for homes and businesses. This provides the ability for consumers to break into the power generating market, which has largely been monopolised by large scale generating power plants. To further address this issue, the Australian Government has recently expanded its Renewable Energy Target

to twenty per cent renewables powering the grid by the year 2020 [27]. Renewable energy sources such as wind and solar farms are regarded as crucial if Australia is to achieve its target of an eighty per cent reduction of emissions on 2000 levels [27].

The International Energy Agency (IEA) forecasts that global renewable installed capacity will exceed fifty per cent by 2050 [28]. This all points towards the need for a power grid that is capable of integrating a much larger percentage of distributed generation, most of which will be renewable. Higher renewable generating capacity on the Power Grid will only be possible with the addition of increased monitoring and protection capabilities. This is only possible if such increased capacity is facilitated along with a communications network capable of carrying such traffic.

1.2.1.1 Photovoltaic Generation

Photovoltaics are becoming a major part of electricity systems around the world. For the third year in a row, in 2013, photovoltaics were amongst the two most installed sources of electricity in the European Union. According to the European Photovoltaic Industry Association (EPIA), the installed capacity of photovoltaic (PV) cells in 2013 was 38.4 GW pushing the global cumulative total to 138.9 GW. This corresponded to a growth in the industry of twenty eight per cent. In Australia, the installed capacity of Photovoltaics is rated at 3226.4 MW [29] and represents a 0.6 per cent share of the total Australian Electrical Generation [30]. Whilst this number may seem small, estimated generation from solar has increased substantially by ninety-five per cent over the last five years [30]. The PV regional installation per inhabitant (EPIA) has Oceania as second in the world with 108.3 Watts per inhabitant. This is slightly below Europe's 125.1 Watts per inhabitant and well above North America's at 29.6 Watts per inhabitant.

The relative ease of installation of Photovoltaic Cells has caused a sudden increase in de-centralized power generation. This sudden increase has not been adequately combined with enhanced monitoring, control and scheduling capabilities supported by a communications network. Whilst PV cells are installed with monitoring devices, these are predominantly simple devices that do not have communication abilities. This provides no scheduling, power quality, or quantity details to grid operators.

1.2.1.2 Wind Generation

According to the World Wind Energy Association (WWEA), the global wind industry had an installed capacity of 318.5 GW with an annual growth rate of 12.8 per cent [31]. The wind industry now contributes close to 4 per cent of the global energy demand and could increase to as much as 12% by 2020 [31,32,33]. As of April 2012, Australia had an installed capacity of Wind Generation of 2.48 GW. However, proposals for thirty-one future wind farms could push this number to 14.87 GW pushing its contribution well above the global 4 per cent average [34].

Wind generation tends to be installed in larger capacities than average PV cell installations. Such installations are referred to as Wind Farms and are usually connected with monitoring and control devices that are able to communicate to grid operators. Unlike most PV installations that operate on the distribution grid, Wind Farms are generally connected to the transmission grid and as such can affect system wide power quality and security considerably.

1.2.2 Support For Large Percentages of Distributed Generation

The Department of Resources, Energy and Tourism [26], Ummels [5], He [25] and the American Physical Society (APS) [27] have all stated that current grid approaches are unable to support large percentages of distributed generation. This highlights a conflicting argument between the need to increase the amount of renewable–and thus distributed– generation sources as proposed by RET and others, and the amount of renewables that the current power grid can support. RET has thus concluded that existing grid infrastructure require upgrades and redesign to facilitate this shift from centralized to distributed power generation [26]. This includes the inclusion of a communications network to apply monitoring and control functionality.

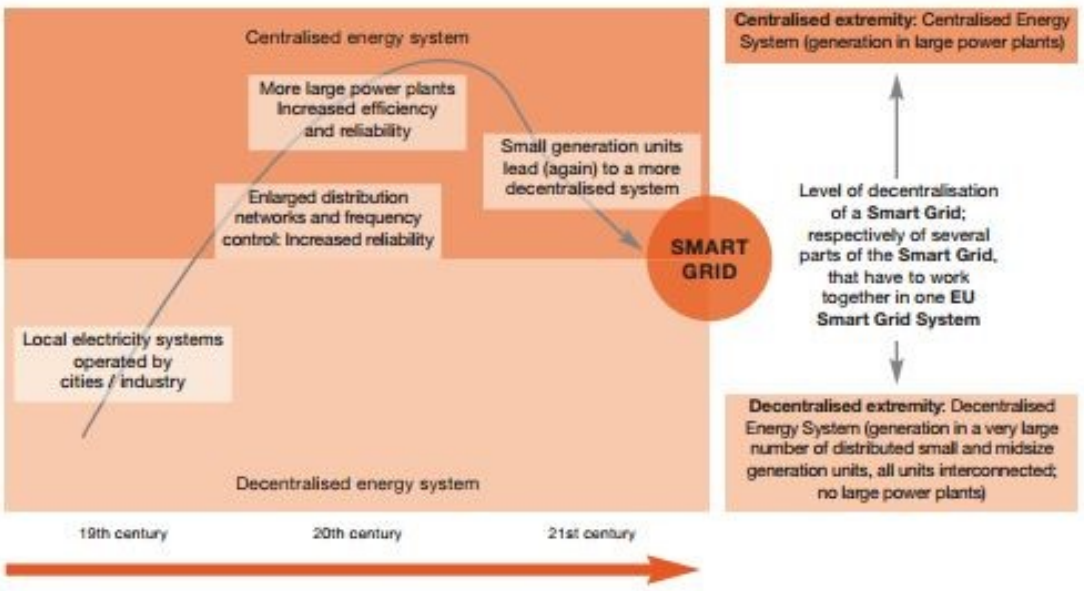

Figure 1-1 - Historical evolution of the electricity system in Europe (EPIA - based on Siemens Analysis)

Figure 1-1 shows the European Photovoltaic Industry Association plotting of the evolution of the power grid due to increases in renewable energy resources. This shows the emergence of a “Prosumer” who both produces and consumes their own electricity. Small scale renewable energy generation provides the ability for consumers to cover a portion or the entirety of their electrical needs. In the future this decentralized electricity generation will require integration strategies including a communications component [8]. Certainly, small amounts of dispersed renewable generation on the current power grid can be smoothly integrated. However, accommodating more than approximately thirty per cent electricity generation from these renewables is currently outside the scope of operation of the current power grid. Both Ummels [5] and the APS [27] have presented reports on the integration of renewable sources of energy on the electrical power grid. Together, they promote the idea that the current power grid must be extended in order to provide support for the expected increase in distributed generation. Ummels [5] has specifically looked at both local and system-wide impacts of integration of wind power in the Netherlands. This ultimately produced findings that the variability and limited predictability of weather patterns can cause renewable energy sources to produce power and voltage fluctuations and harmonics in the distribution and transmission lines [27].

1.2.3 Case Study: European Blackout in November 2006

On 4 November 2006 at approximately 22:00, the Europe Interconnected Power Grid experienced its most severe disturbance in the history of the Union for the Co-ordination of Transmission of Electricity (UCTE). The UCTE is the association of Transmission System Operators (TSOs) in continental Europe and supplies electricity to 23 countries and approximately 450 million customers [35]. The disturbance originated from the disconnection of a 380kV transmission line in the North German transmission grid [6,7,35,8] and affected 15 million customers in more than 10 countries.

At approximately 22:05, the load flow situation unexpectedly changed with an extra 100MW of load occurring on the Landesbergen-Wehrendorf line (Northern Germany, south-west of Hamburg). This caused the current to exceed the 1900A operating limit on the transmission line, and ultimately the line was tripped by an automatic protective device due to overload. This caused further transmission lines to overload in a cascading manner throughout northern Germany. At 22:10, the UCTE system was split into three different areas due to the tripping of interconnection lines (see Figure 1-2).

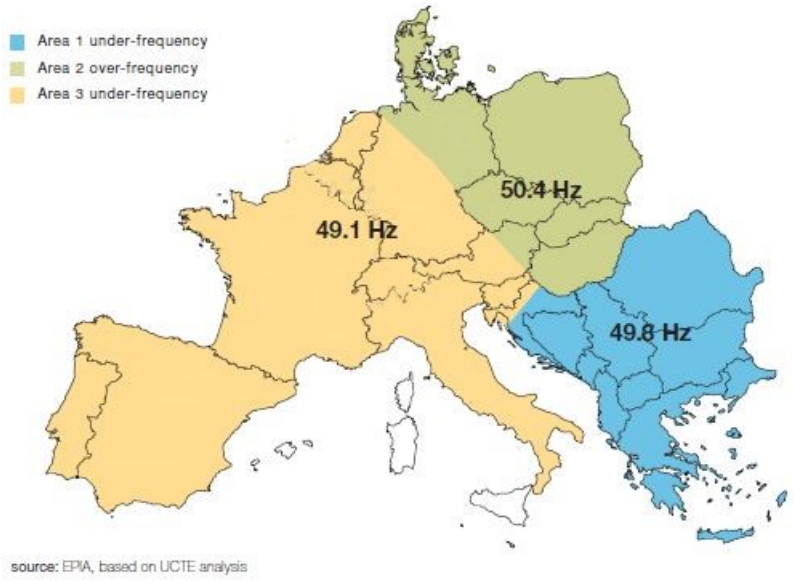

Figure 1-2 - Desynchronization in Europe on 4 November 2006

It is commonly agreed that human error in the original decision to cut the 380kV transmission line based on empirical rather than load flow analysis led to the blackout occurring. However, studies [6,7,8] suggest that recent rapid development in renewable, intermittent generation, namely wind generation, were a contributing factor to its cascading effect. The balance between the restarting of a considerable amount of wind generation in northern Germany and the decreased generation of thermal/hydro was not adequately timed. This created a large surplus of generating capacity in Germany and due to generating deficit in nearby Poland and the Czech Republic caused transmission lines to overload. Renewable energy is most certainly a solution to the increasing demand for power. However, it also creates power grid compatibility issues that must be addressed for successful and widespread integration.

1.2.3.1 Electrical System Inertia

Electrical System Inertia is an inherent characteristic of electrical power system and is created by the rotation of turbines most used in base-load power generation such as gas, coal, hydro and nuclear. These generators are generally very heavy and consequently store a large amount of kinetic energy when rotating at nominal frequencies. If a large generator with a heavy rotor is suddenly cut off from the grid, other generators connected to the grid will slow and release more power as they release their stored energy or inertia. This inertia resists the decline in frequency thereby allowing control systems some time to automatically apply more power to the remaining connected generators [6,24].

The increasing prevalence of Distributed Renewable Energy Resources has had some widespread effects on the current power grid. By increasing the number of Distributed Generators operating on the Distribution Grid, the inherent intermittency of Renewable Energy Resources can cause the grid to quickly go into generation surplus or deficit. When the grid load and generation are not synchronised, under or over frequency events can occur which reduce power quality and can harm some electrical devices. During an under or over frequency event, the power grid will try to restore nominal frequency by either shutting off generators or turning on loads. In some cases, the power grid will isolate an area that contains the fault. This will most likely results in loss of power in the isolated, disconnected area. To allow for the increased

penetration of renewable energy resources on the distribution grid further monitoring and control will be required to ensure such grid events do not occur.

By rushing towards a future of Renewable Energy Resources we are depriving the power grid of electrical system inertia. This reduction in electrical system inertia coupled with the variability of renewable energy resources has produced a decrease in power security in modern power grids [6,7,8]. These disadvantages of increased integration of Renewable Energy Resources can be negated by increased power grid monitoring, protection and control. However, this will require the use of a communications network to incorporate the increased number of Smart Grid IEDs required to provide such monitoring, protection and control.

It is not this thesis's objective to provide models for incorporating higher percentages of Renewable Energy Resources. However, it is expected that the proposed telecommunications resource allocation model can provide higher support for an increased amount of Smart Grid IEDs that can apply monitoring and control capabilities such that increased capacity of renewables can be realised.

1.3 WIDE AREA MONITORING PROTECTION & CONTROL

Wide Area Monitoring Protection and Control (WAMPAC) is used to communicate local information to the system, and analysed alongside system-wide information, prevents localized disturbances from spreading [36]. It is evident that an increasing number of devices are required to monitor the stability of the distribution grid, and as seen in Europe in 2006, the transmission grid also. However, with an ever increasing amount of Intelligent Electronic Devices (IEDs) to monitor and control the power grid, what existing communication network can facilitate them? The QoS requirements of Smart Grid data packets differ from regular cellular traffic due to the significance of the information they may contain. For example: a Smart Grid data packet with crucial information relating to a grid disturbance that could cause further power system imbalances or a reduction of power quality, security or reliability should be sent with higher priority than a data packet containing a webpage or a voice call. Therefore, a robust communications network that can encompass an expansive Smart Grid

network with high reliability, high throughput and low latency is required. The communications network must also be able to dynamically alter its resource allocation and scheduling to suit the needs of the Smart Grid, especially during fault conditions.

1.3.1 Communications Architecture to Support the Smart Grid

The Smart Grid is defined as a communications system overlaying the current power grid to provide increased control and monitoring abilities. As the Smart Grid is an emerging technology in its infancy, many researchers are postulating what the Smart Grid could achieve in the future [4,37]. The Smart Grid will incorporate many differing functions from grid monitoring at a transmission and distribution grid level to power meter readings at a residential or commercial level. This shows that whilst the number of data packets to be sent by the Smart Grid will be high not all packets will have the same priority, dependent on the information stored in their payload. Many researchers haven't accounted for the Smart Grid's communication requirements or the differing levels of priority and QoS that will become incumbent [37].

Information flow between the numerous devices operating on the Smart Grid will need a capable network to communicate over that can change dynamically to suit multiple QoS requirements simultaneously. Therefore the communication must be of high bandwidth to accommodate these devices, low latency with high throughput, and with low bit error levels to ensure efficient and timely transmission of data that could affect the availability of the power grid.

1.3.2 Wireless Communications Environment

The Smart Grid is well suited to a communications environment based on wireless access due to the enormity of its scale. Smart Grid IED distribution is widely agreed to envelop an extensive area with higher density in the distribution grid, especially at lower voltages [38]. It is apparent that a wireless communications medium is required to connect the numerous Smart Grid IEDs, especially in the distribution grid where physical connection would not be cost effective [39]. Next generation telecommunication networks utilizing Orthogonal Frequency Division Multiplexing

(OFDM) technology for downlink and Single Carrier Frequency Division Multiplexing (SC-FDMA) for the uplink hold much promise in the support of a large scale Smart Grid network.

1.3.3 Long Term Evolution Communications

Long Term Evolution (LTE) is the next revolutionary step beyond 3G for wireless communications [9]. The growth in high-bandwidth internet applications has driven the need for higher throughput and lower latency communication networks. The proliferation of smart phones and tablets in the last few years, with consistent growth of both has pushed for a network able to handle an ever increasing number of users. According to Cisco Visual Networking Index (VNI) Forecast [40], Asia-Pacific Mobile traffic grew at a rate of eighty-six per-cent in 2013 and is set to increase at a compounded annual growth of sixty-seven percent from 2013 to 2018. Fixed/Wired traffic only grew at a rate of twenty-three percent in 2013 and is set to increase at a compounded annual growth of thirteen per-cent from 2013 to 2018. This shows that whilst the internet is still expanding with new applications emerging every day, most users are opting for a wireless connection to such media [40].

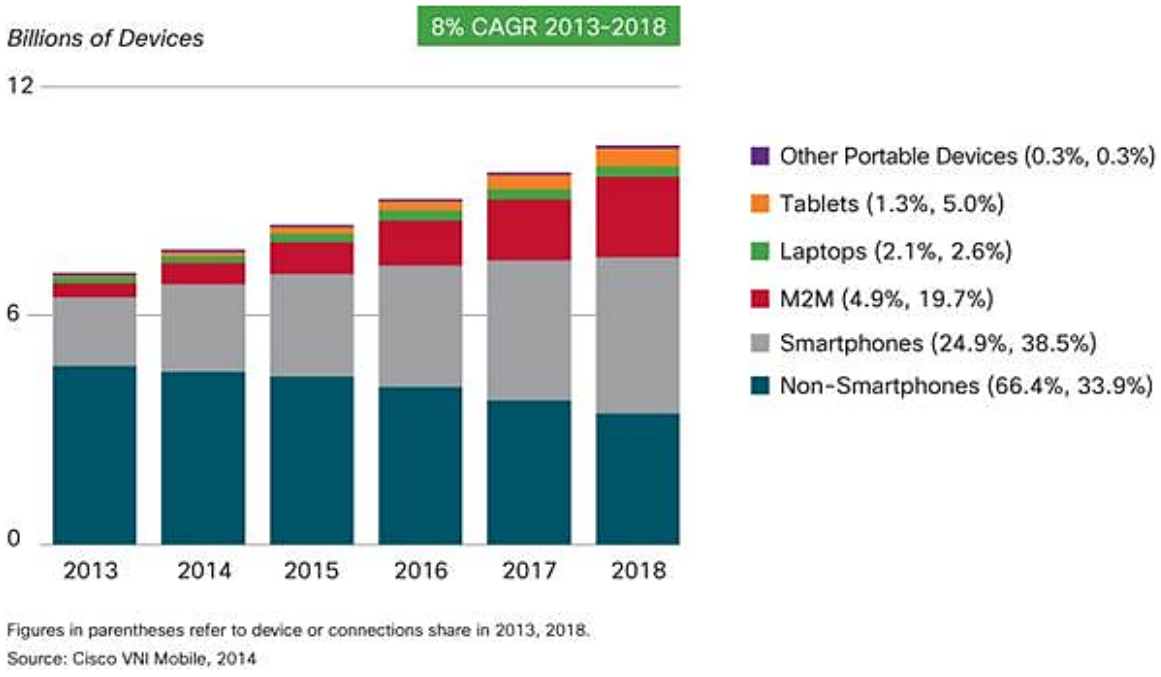

Figure 1-3 - Global Mobile Devices and Connections Growth

Machine to Machine (M2M) are becoming more pervasive. As shown in Figure *1-3*, the growth from 2013 to 2018 is approximately four-hundred percent. This growth rate is larger than any other class of device and will consist of four times the amount of tablet devices operating worldwide. A subset of the M2M category will be Smart Metering Infrastructure, Phasor Measurement Units and other Utilities which will be components of the Smart Grid Data Network. The network share for these M2M devices will need to increase at a time when all other sectors including Smart Phones, Tablets, Laptops, etc. are also increasing.

LTE is a mobile broadband standard developed by the 3rd Generation Partnership Project (3GPP). During development, its main requirements were that the network have high spectral efficiency, high peak data rates, short round trip time and flexibility in frequency and bandwidth [41]. Orthogonal Frequency Division Multiplexing communications is the basis of the Evolved Packet System, which provides LTE Downlink telecommunications with such high data rates and robustness against multipath fading [42]. Combined with higher order modulation schemes, including up to 64QAM (Quadrature Amplitude Modulation), large bandwidths up to 20MHz and spatial multiplexing allowing the use of 4x4 MIMO (Multiple Input Multiple Output), LTE is capable of achieving peak data rates as high as 300Mbps. Due to these factors many countries are endorsing LTE communications technologies and is becoming the de-facto standard for mobile broadband networks. LTE is well suited as the telecommunications network for the Smart Grid due to its low latency, high throughput and dynamic resource allocation capabilities.

1.3.3.1 Radio Resource Management & Opportunistic Scheduling

The Orthogonal Frequency Division Multiple Access scheme used in LTE provides WSO's the ability to allocate channel resources with great flexibility. The LTE standard does not specify resource allocation algorithms to take advantage of Multi-User Diversity so each LTE developer has the ability to create their own. Multi-User Diversity also provides the ability for WNOs to opportunistically schedule users based on channel conditions to ensure low levels of destructive interference and fading to ensure high Signal to Noise Ratios [9].

OFDM technology allows scheduling in both time and frequency domains by using a multi-carrier approach and spreading users over differing subcarriers. Figure *1-4* provides an illustration of the difference between OFDMA used in LTE downlink and SC-FDMA used in LTE uplink. The bandwidth of the system in the OFDMA downlink scenario is shared over a number of differing subcarriers. In the uplink scenario, each user uses a single carrier frequency with all data transmitted over that frequency.

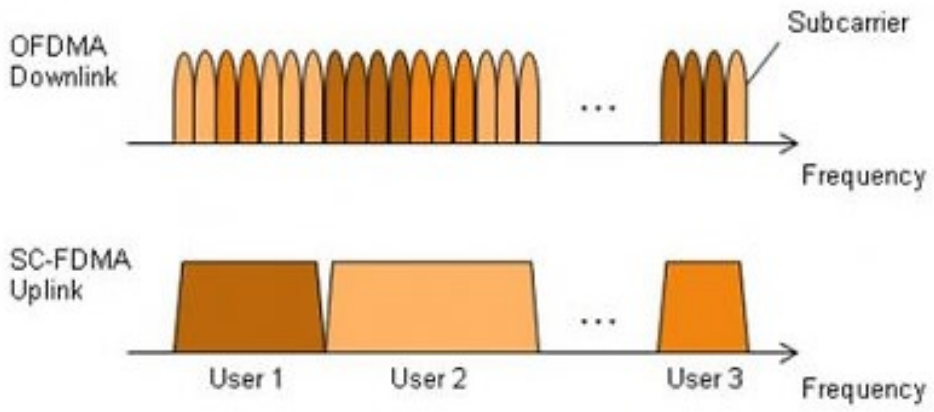

Figure 1-4 - OFDMA and SC-FDMA

OFDMA requires a large amount of power and expensive, high precision power amplifiers leading to high Peak-To-Average-Power Ratios (PAPR). For this reason, OFDMA is not suitable for the uplink channel where mobile users would need increasingly larger batteries and very expensive amplifiers. The opportunistic allocation of the subcarriers can yield substantial Multi-User gain, much higher than if random allocation of resources is used. Optimal allocation will yield the greatest results, thus allowing the inclusion of Smart Grid data packets in a broadband mobile network already saturated by tablets, smartphones, laptops, fixed broadband etc.

1.4 APPROACH OF THIS THESIS

Never before has the power grid undergone such a transformation. With the inclusion of distributed generation including renewables set to increase over the next few years, the power grid must be able to predict and control these intermittent and variable

power supplies, without doing so, a re-occurrence of the 2006 European Blackout could be possible. Once heralded as the greatest tool against climate change and global warming, Distributed Renewable Resources have become a headache for Grid Operators due to their volatility and complexity in scheduling. The Smart Grid is the solution to this problem, providing higher monitoring, control and protection against system wide and localized faults and events. However, there are still inconsistencies in the approach of researchers to both harvest and control these intermittent sources of renewable energy. There is even less research on the communication network requirements to monitor and control the distribution grid with higher penetration of renewable energy resources in real time.

This thesis is dedicated to solution of the Smart Grid's communication network requirements by using Radio Resource Management controlled by Lotka-Volterra population dynamics equations. The Lotka-Volterra inspired RRM scheme is borne from competitive ecological environments where differing species compete against each other and amongst themselves to survive. By analysing the stability of the model, an equilibrium or stable operating limit can be found allowing co-existence of all classes of communication data operating on a wireless network, whilst also incorporating the inherent randomness exhibited by communications traffic.

1.5 CONTRIBUTION OF THIS THESIS

This thesis essentially argues that Radio Resource Management and Opportunistic Scheduling has the capability to include the Smart Grid data class whilst minimising its effect on current wireless communications that already dominate much of the wireless medium.

This research primarily involves an investigation into how an existing wireless communications network will be affected by the advent of increased distributed generation and Smart Metering Infrastructure operating on the Smart Grid and how best to minimize this effect whilst upholding QoS requirements for all classes of information operating on the network. This work is a novel solution utilizing to the Resource Allocation problem plaguing high traffic networks. Lotka-Volterra population

dynamics equations have never before been utilized in a wireless telecommunication environment, and yet they are well suited due to the competitive nature of a wireless telecommunication network.

The major contributions of this thesis are listed as follows:

- Design of a periodic and sporadic traffic model used to suit a wireless communications network.
- Integration of Smart Grid traffic in a pre-existing OFDM based communications network.
- Class differentiation between three classes, Smart Grid, Voice, and Data. Service differentiation between Smart Grid applications: Distribution Automation, and Smart Metering Infrastructure.
- Development of a novel Resource Allocation and Scheduling based on Lotka-Volterra Population Dynamics equations.
- Increased performance of proposed Resource Allocation and Scheduling scheme over common opportunistic schedulers.
- Opportunistic Scheduler capable of handling periodic and sporadic traffic, and allocating future resources based on expected periodic traffic.
- Reduced queue latency for periodic Smart Grid traffic.
- Smart Grid Reliability, Latency & Throughput Requirements satisfied by proposed Resource Allocation and Scheduling scheme.
- High degree of fairness in proposed Resource Allocation and Scheduler scheme.
- Optimization of Smart Grid packets to ensure expedient delivery.

1.6 OUTLINE OF THESIS

This first chapter has introduced the Smart Grid as an evolution of the power grid. The integration of renewable energy resources is set to alter the power grid from a completely centralized to de-centralized power production model. Such a decentralized model was developed and explored further in [43]. A wireless access

medium such as provided by LTE is the solution to connecting the numerous Smart Grid IEDs.

Chapter Two contains a thorough analysis of the contributions that others have made to this research area to date. The literature survey is based around Radio Resource Management techniques, with particular focus on current algorithms used by researchers to allocate subcarriers to users. Firstly it introduces the Smart Grid network components and applications with specific QoS requirements for different Smart Grid applications. This is followed by a study of the formulation of Smart Grid traffic requirements, most notably bandwidth, latency and throughput. This is then followed by analysis of current research in resource allocation in high traffic environments. Finally, Chapter Two concludes with my argument for the need for a Lotka-Volterra inspired Resource Allocation scheme.

Chapter Three details the traffic and channel models used to test the Lotka-Volterra based Resource Allocation & Scheduler scheme defined in Chapter Four. The simulation model was built in Matlab and utilized the Simulink simulation environment.

Chapter Five consists of analysing the reliability of utilizing a high traffic OFDM (LTE) network for applying Smart Grid applications. Chapter Six contains the results and analysis for the investigation into latency analysis of the proposed Radio Resource Management scheme. The results and methodology contained in Chapter Six were used in part in [44]. In Chapter Seven, the results for the investigation into throughput analysis are set out and critically analysed. The results and methodology contained in Chapter Seven were used in part in [45]. Chapter Eight introduces the metric of fairness and measures the proposed Radio Resource Management scheme against common, popular Opportunistic Schedulers.

Chapter Nine analyses the results contained in Chapters Five to Eight and concluding remarks are provided. A final analysis of the effectiveness of the proposed Radio Resource Management & Scheduler scheme is also provided. Chapter Nine also contains a description of any possible sources of error and limitations of the research. This is followed by a summary of future potential work in the research field.

Chapter 2.
Smart Grid Communications: Traffic Requirements & Radio Resource Management

This chapter provides a detailed background into the state of the art research of Smart Grid communications, gaps in current research, and proposed solutions. There are three relevant research areas driving the proposed Resource Allocation Scheme presented in this thesis. These are:

- Smart Grid Communications Traffic and QoS Requirements
- LTE Communications Architecture including Radio Resource Management
- Comparison between common Opportunistic Schedulers and their limitations

In this thesis, these three research areas provide the framework upon which the Lotka-Volterra Resource Allocation and Scheduler Scheme is based. Initially, this Chapter will introduce the two types of Smart Grid applications researched in this thesis: Distribution Automation and Smart Metering Infrastructure. The traffic requirements for each Smart Grid application will be determined. This is followed by an in-depth

analysis of state of the art Smart Grid Communications literature, with gaps in research identified. Finally, the chapter concludes with a summary of the proposed solution to the Smart Grid resource allocation problem, in the form of the proposed Lotka-Volterra Resource Allocation and Scheduler scheme.

2.1 DISTRIBUTION AUTOMATION (DA)

Bu et al defines the integration of distributed renewable energy generators as a main driver in the development of the Smart Grid and all the entailed infrastructure modernisation [46]. Distribution Automation is widely regarded as the automation of services provided by the distribution power grid, and is characterised by its ability to operate the power system more reliably and efficiently whilst taking into account the variability imposed by the recent insurgence in distributed generation [47,48,49]. The Distribution Automation Network (DAN) is able to provide Wide-Area Situational Awareness [49] by the implementation of a Wireless Sensor Network that is able to collect information relating to the state of the power grid and provide protection and control [50]. This scheme is more formally known as WAMPAC – Wide-Area Monitoring, Protection and Control.

Network topologies within the distribution grid become increasingly mesh-like as the distances between nodes decreases. This mesh network has posed significant difficulties to grid operators as the number of interconnections increase [4]. Additionally, the increase of intermittent renewable energy resources on the distribution power grid has created instability issues, with extra busses required to provide a higher resolution image of the distribution grid to operators. This requires an increased amount of Phasor Measurement Units (PMU) to provide information relating to the state of each bus within the power system.

2.1.1 Phasor Measurement Units

Digital computer based measurement, protection, and control systems have become common features of electric power systems. These measurement, protection, and

control systems use sampled data to compute various quantities such as voltage and current phasors. Phasors are used in many protection and data acquisition functions, and their utility is increased further by referencing them to a common time base. This can be accomplished by synchronizing the phasor estimate to a precise time source that is common to the various measuring sites. Phasor estimates synchronized to a common time source and referenced to a common nominal frequency are defined as synchrophasors. Simultaneous measurement sets derived from synchronized phasors provide a vastly improved method for tracking power system dynamic phenomena for improved power system monitoring, protection, operation, and control [51].

2.2 SMART METERING INFRASTRUCTURE (SMI)

Smart Metering Infrastructure will be required to send data every few minutes. However, it will also be required to receive data relating to time and scheduling of Renewable Energy Resources attached to the dwelling if they exist. Current literature states message intervals can be of the order of seconds to multiple minutes. This research has opted for a realistic message interval of every two minutes, not including sporadic messages which occur randomly [52]. As Smart Meter Infrastructure is rolled out nationally, the number of devices will increase to a limit of one per dwelling. In urban scenarios, this can account for hundreds in a single telecommunications cell. It is assumed in this thesis that Smart Metering Infrastructure will communicate directly to the eNB without use of a data concentrator or storage module.

SMI is expected to periodically send updates to the Smart Grid regarding power consumption and production. SMI is also expected to receive data periodically to perform time synchronization, load balancing/scheduling and generator scheduling [52]. The time synchronization packets are assumed to flash across the whole network at once introducing a spike in traffic on the communications network [2]. Without proper planning and allocation of resources, the SMI traffic may saturate the network, decreasing network availability and increasing communications latency.

2.3 TRAFFIC REQUIREMENTS

The data transmitted by the Smart Grid is vital to the security and reliability of the most important piece of national infrastructure: the power grid. As such, the Smart Grid data should be transmitted with highest priority to decrease latency and with high accuracy.

Many researchers have modelled and simulated the Smart Grid data flow over a telecommunications network. There still remains inconsistency between the agreed upon medium on which to transmit the data. Zaballos et al, & Levorato et al all propose Broadband over Power Lines (BPL) as part of the communications infrastructure [49,53]. As the telecommunications network serves to provide the power grid with higher reliability, efficiency and security it seems a novel approach to use the power line cables for communication too. However, this approach limits the "plug and play" approach to modern Wireless Sensor Networks (WSN) by imposing a wired medium.

Levorato et al applies an approach in which applications are forwarded to the input queues of differing networks based on their QoS requirements and the abilities of the communication networks [53]. Using this approach allows the use of existing wired networks such as BPL and fibre which can increase the utility of specific Smart Grid applications without adversely affecting those with high bandwidth and low latency requirements [53].

2.3.1 Synchrophasor (PMU) Data

The IEEE Standard for Synchrophasor Data Transfer defines the method for exchange of synchronized Phasor measurement data between power system equipment. It goes on to specify messaging including types, use, contents and data formats for real-time communication between Phasor measurement units, Phasor data concentrators (PDCs), and other applications [51].

The frame size of PMU data is defined in IEEE Std C37.118.2-2011 Table 8 [51], *'Configuration frame 1 and 2 organization'* and is of the order:

$$Frame_{Size} = 24bytes + NUM\_PMU \times 58bytes \quad (2\text{-}1)$$

$$NUM\_PMU = The\ number\ of\ PMUs\ included\ in\ the\ data\ frame \quad (2\text{-}2)$$

The IEEE Standard for Synchrophasor Measurement for Power Systems (IEEE Std C37.118.1 – 2011) defines the data collected by PMUs and the manner in which they attain this data [54]. Apart from the expected metrics such as voltage, phase, frequency etc IEEE Std C37.118.1 also defines the of Rate of Change of Frequency (ROCOF) as an important quantity for the measurement of system accuracy [54]. The North American SynchroPhasor Initiative (NASPI) also defines the data used for Wide Area Situational Awareness and the differing applications for which PMUs are suitable now and in the future [55].

The reporting rate of PMUs in a synchrophasor network are defined in IEEE Standard C37.118.2 – 2011, page 7 [51]. The PMU shall support data reporting at sub-multiples of the nominal power line frequency. The required reporting rates are displayed in Table 2-1, however, the actual rate to be used shall be user selectable, with support for higher and lower rates available.

Table 2-1 - Required PMU Reporting Rates

System Frequency	**50 Hz**			**60 Hz**					
Reporting Rates (F_s – frames per second)	10	25	50	10	12	15	20	30	60

With an increasingly complicated distribution grid (due to increased integration of renewables), and even when choosing the minimum reporting rate of 10 frames per PMU per second, the telecommunications traffic imposed by a synchrophasor network will be large. No such dedicated network exists for PMU data, and many researchers point towards a network such as 4G LTE due to its omnipresence, which enables future expansion of the network with no capital expenditure on transmission mediums [49,50]. However, the large amount of traffic imposed on a LTE network could, like SMI, saturate the network and decrease its availability, whilst increasing latency.

2.3.1.1 PMU Network Topology

A simplified structure for a PMU network is shown below in Figure 2-1 which consists of PMUs and Phasor Data Concentrators along with other data storage devices [56]. The Phasor Data Concentrator is used a communications link between PMUs within that locality and the eNode-B which is connected to the wider Smart Grid communications environment [50].

A PDC works as a node in a communication network where synchrophasor data from a number of PMUs or PDCs is correlated and fed out as a single stream to the higher level PDCs and/or applications. The PDC correlates synchrophasor data by time tag to create a system wide measurement set whilst also providing other analysis and detection services [51].

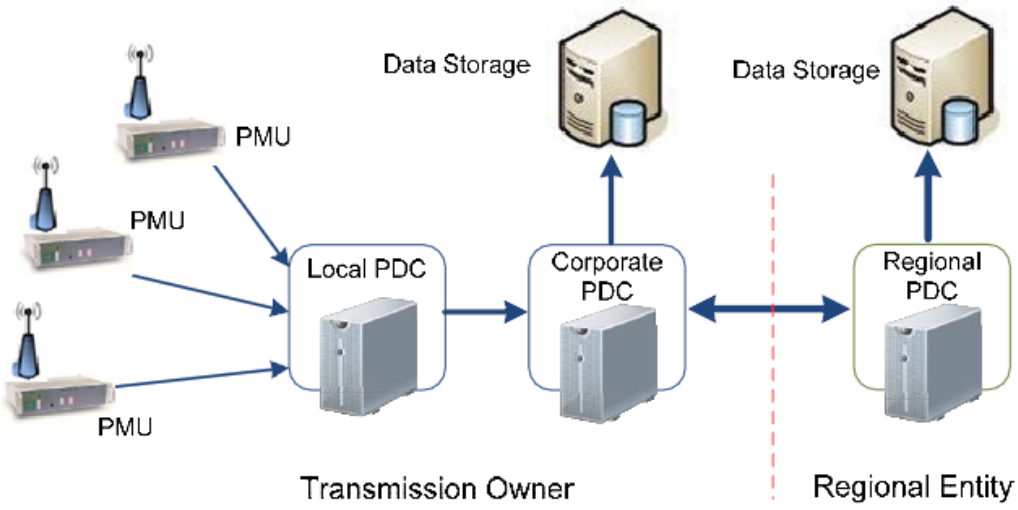

Figure 2-1 - Synchrophasor Data Collection Network

2.3.2 Bandwidth and Latency Requirements

While most researchers in the area of Smart Grid telecommunications development have postulated that the Smart Grid will be a data rich, but information poor environment [37,49], not many have actually researched the actual bandwidth and latency requirements of proposed Smart Grid applications. Most researchers [2,38,39,52,57,58] have instead provided detail from such publications as the United States Department of Energy (DOE) requirements of Smart Grid traffic for differing applications as fact, without modelling specific traffic interdependencies within their

proposed model [59]. However, there is ample research in the effect of data traffic on the Bandwidth and Latency requirements imposed by such bodies as the IEEE but there lacks a consensus on the optimal method to alleviate increased latency and optimal allocation of bandwidth to Smart Grid services.

Latency, as defined by the IEEE, is a measurement of the time delay from when an event occurs on the power system to the time that it is reported in data [54]. Communication latency is commonly considered as a stochastic quantity due to many random factors such as distance, repeater malfunction, density of the medium, Electro-Magnetic Interference (EMI), ambient temperature and much more. Therefore, Nguyen et al (2011) provides a good model of potential Smart Grid latency by modelling a discrete probability density function of a communication path from agent *i* to agent *j* [60]. Nguyen's model is different to those proposed in [27,47] as it is composed of a Multi-Agent System (MAS) that can interact with each other, whilst [27,47] provides an analysis of LTE-FDD/TDD uplink latency, where agents communicate directly with the Evolved-Node-B (eNB) [60]. Whilst these models are important in the realisation of a Smart Grid specific latency requirement, the Smart Grid is not a single technology. Rather, it is a collection of applications; each with differing QoS requirements. As such, each application within the Smart Grid will belong to one of four different classes characterised by their QoS requirements, as defined by Cherukuri et al (2011) [57].

Table 2-2 - Smart Grid Application Classes

	Class A	Class B	Class C	Class D
Low Latency	Critical	Fairly Critical	Somewhat Critical	Not Critical
Reliability / Availability	Critical	Somewhat Critical	Not Critical	Fairly Critical
Data Accuracy	Critical	Somewhat Critical	Not Critical	Critical
Time Synchronisation	Critical	Critical	Somewhat Critical	Not Critical
Message Rate	Critical	Somewhat Critical	Somewhat Critical	Critical

Distribution Automation, which is a Smart Grid application provided by Phasor Measurement Units belongs to Class A in Table 2-2, and is defined by critical requirements placed on its QoS [61]. The United States Department of Energy report contains the following table in Appendix A:

Table 2-3 - Smart Grid Functionalities and Communication Needs

Application	Throughput	Latency	Reliability	Security	Backup Power
Wide Area Situational Awareness	600-1500 kbps	20 ms – 200 ms	99.999 – 99.9999%	High	24 hour supply

Wide Area Situational Awareness, as defined by the DOE, is a set of applications (such as Distribution Automation) that draw their data from sensors such as PMUs. As Table 2-3 shows, the throughput, latency and reliability requirements are very stringent, and supports Cherukuri et al's analysis of Smart Grid traffic requirements [57].

2.3.3 Quality-of-Service Scheduling for Smart Grid

Whilst most researchers see communication resource allocation as a QoS problem, many researchers [48,53,52,57,62,63,64,65,66,67,68,69] did not include service differentiation between Smart Grid applications and other communication applications using the wireless medium. Those who did differentiate between Smart Grid and non-Smart Grid services, did not provide further separation between differing Smart Grid applications [52,57]. Cherukuri et al & Rengaraju et al provide different QoS requirements for Smart Grid applications, and thus differentiate between services [52,57] . Rengaraju et al's model is based on 4G (WiMAX & LTE-A) technology whilst Cherukuri does not define the medium used in the model [52,57]. Whilst this provides a good base measurement of bandwidth and latency requirements of Smart Grid data, the research does not take into account the idiosyncrasies of different communication standards and mediums.

A common trend in the literature involves the use of QoS queuing. This involves the use of different queues for data of similar requirements. For example, Sun et al, utilises two queues to provide priority to emergency data [68]. The scope of QoS queuing far exceeds the use by Sun et al in [53] where packets are assigned to output network queues as a function of the performance profile of the output networks and the QoS of the Smart Grid data packets [68]. Whilst the model used in [53] utilises multiple networks, the use of a Lyapunov algorithm to perform scheduling provides an optimal utilisation of the bandwidth of the networks, and as such achieves a very low latency for Smart Grid data packets.

Multi-dimensional queuing algorithms are difficult to model and also find a convergent solution. Müller achieves a lower system dimensionality by reducing different applications of similar QoS requirements into service classes. This provides a framework for class differentiation, but is not quantified as in Table 2-2 by Cherukuri et al [57]. [46,68,69,70] all use a Markovian chain to model Smart Grid data traffic, which is characterised by differing resource requirements. Le et al [69] proposes a star network. However, data communications outside of the Smart Grid are disregarded, which is a major flaw in Le et al's model. On the other hand, Bose disagrees that the use of a Star Topology for a Smart Grid communications network is viable as the eNB will be overwhelmed with the voluminous data [47]. Markov chains can only be utilised when the traffic is distributed according to a Poisson process, which is good for modelling continuous-time stochastic events such as Smart Grid data packets [58]. Utilising this method prioritised Smart Grid data traffic over the medium which lowered communication latency, a requirement of services provided by Distribution Automation.

As opposed to the Markovian queue model characterised previously, some researchers pose a graph theory-based approach to ensure the optimal allocation of communications resources is given to time critical data packets with high QoS requirements, such as those produced by a Distribution Automation Network. This approach is novel in nature, and is well served by the mesh topology present in current day distribution power grids. Bose, whilst theorising the requirements for a communications infrastructure capable of handling ubiquitous and heterogeneous phasor measurements, concluded that a state estimator is required for the

communications network [47]. State estimation is a tool used to estimate the current status of the power grid [71].

Graph theory provides the use of Shortest Path Algorithms which optimises the distance between source and destination in a packet switched network, such as the models used in [65,71,72]. Utilising a state estimator, a network graph can be produced that is composed of nodes (in this research PMUs) and edges which have specified weights as defined by certain metrics. For the Smart Grid, the weights are used to represent such real world metrics as delay, bandwidth, power consumption and reliability [67]. Ting et al [65] computes one or more Label Switched Paths (LSPs) for each class of traffic and optimally configures these LSPs to make full use of the network and effectively avoid network congestion. This is a very novel, multi-hop architecture and ensures efficient use of bandwidth incurring minimal errors. Packets are successfully transmitted hop-to-hop from source to destination without requiring re-transmissions due to error. However, the overall latency is much larger due to the sum of processing times required at each hop to determine next destination. This discredits a multi-hop network for Smart Grid applications requiring low latency. Li et al utilises a similar method but takes into account the impact of outage, and the delay this can cause. This is an important metric in terms of Smart Grid applications, which are high priority and should be used in future edge-weighted graph models [67].

The literature explored above idealised the Smart Grid communications network environment, with low or no bandwidth allocated to other sectors such as mobile communications from smart phones or tablets etc. Also, localised data analysis required at the PMU is often neglected or trivialised. Hoag et al provides a model involving local analysis by the Phasor Measurement Units [50]. This involves the use of Fast Fourier Transforms (FFT), of which the accuracy is dependent on the sampling period. With use of the IEEE Standard for Measurements for Power Systems [54], Hoag determines that utilising a sampling rate of 900 Hertz (Hz) a response time of 33 ms – 65 ms can be expected [50]. Combined with Analog to Digital Conversion (ADC), Hoag et al predicts the end-to-end latency of 125 ms – 205ms. This differs significantly from the lower bounds of the DOE and IEEE Smart Grid application requirements [50,59].

2.4 LTE RESOURCE ALLOCATION FOR SMART GRID DATA PACKETS

Allocation of communication resources on the Smart Grid has recently become a topic of major research. As defined by [37] this is mainly due to application vendors requiring more and more bandwidth to provide the theorised services to be provided by the Smart Grid. However, as Zaballos et al states, there is currently an inefficient use of data within the Smart Grid with inherent redundancies in services and acquired data [49].

2.4.1 Optimisation of LTE Resource Allocation

Radio Resource Allocation of Orthogonal Frequency Division Multiplexing systems such as LTE rely on the scheduling of subcarriers to transmit data The bulk of research uses utility theory to optimise these communication resources for Smart Grid data transfer.

Al-Anbagi et al (2012) [62] proposed a Delay Responsive Cross Layer (DRX) protocol to address delay and service differentiation requirements of the Smart Grid. Whilst the proposed protocol reduced the delay of high priority data while preserving acceptable packet loss values it doesn't take into account multi-hop scenarios and the effect of interfering nodes. The DRX scheme performs a delay estimation using a probabilistic model. If the model predicts that the data will not meet the delay requirements of the Smart Grid application the DRX scheme fast-tracks this data for transmission. This approach is very good at prioritising Smart Grid data that needs faster allocation of resources however it is over-complicated. As the Smart Grid Wireless Sensor Network will most be composed of stationary sensors, there will be little or no change in latency during normal network conditions. Therefore, the requirement to estimate the delay for each packet is in itself a time-consuming process and can be minimised by determining the estimated delay at set time intervals and storing the result.

Prukner et al (2012) [73] aimed to find a real time balance between electricity supply and demand effects on the Smart Grid data communication network taking into account latency and packet loss requirements. Whilst this model serves a distributed generation intensive scenario, which suits real world trends (which motivates the increased requirement of Distribution Automation and number of PMU sensors), the utility function utilised is flawed. This is due to the its market operated nature, which increases the monetary gain of individuals, which either reduces the reliability of the Smart Grid or increases computational complexity to ensure reliability is achieved. However, in respect to future Smart Grid applications, the matching between supply and demand, maximising the utility of distributed generators will become a major participant in lowering greenhouse gas emissions.

Like many researchers, Zhang et al [63] utilises the Utility Proportional Fairness (UPF) algorithm to maximise the sum of utilities of users, of which are based on variety of utility functions with differing restrictions. Whilst this approach produces lower computation complexity and fulfils QoS requirements of multiple applications, the use of average data rates instead of instantaneous data rates reduces its effective use for Smart Grid applications, where real-time data is required. Joseph et al [74] provided further detail to the UPF algorithm by incorporating the detrimental impact of temporal variability in users' allocated resources. In further research, Zhang et al [66] compares the following algorithms: Utility Proportional Fairness (UPF); Rate Proportional Fairness (RPF); Nash Bargaining Solution (NBS); Utility Sum Maximization (USM). RPF maximised throughput when load is low. However utility fairness amongst different applications was greater for NBS, which converged towards utility fairness and QoS guarantees faster than all other algorithms. These authors point to a Nash Bargaining Solution to providing fairness between communication applications when allocating resources. However, only [75] provides a framework that takes into account transmission power, which is an important metric for Wireless Sensor Networks, and provides a multi-hop environment, which combines well with Ting et al's [65] which uses Labelled Switch Paths to maximise bandwidth efficiency. An optimal power allocation policy is also proposed by Biggelaar et al [76], in which a decentralised Q-Learning algorithm is used. This is applied to secondary users under the constraint that secondary user interference on primary users is negligible. The Q-Learning algorithm outlined in the paper is efficient in applications where reinforcement

information is provided after an action is performed in an environment. This provides the basis for further research, whereby utility function allocated communications resources could perform further optimisation upon receipt of UE perceived QoS.

Xu et al [77] provides a tool for determining which packets are Smart Grid packets. This is done by examining a UEs' data updating rates, equivalent packet sizes and invariant channel qualities. These metrics are then defined by a Smart Grid 'weight' which is integrated into the modelled Utility Function. This weight function allows the scheduler to allocate more resources for Smart Grid sensors thereby increasing Smart Grid application utility. The inclusion and determination of a Smart Grid weight is an intelligent method of prioritising Smart Grid data packets without imposing further computational complexity.

People typically view temporal variability negatively and too easily reach the conclusion that it is a sign of an unreliable service [74]. For problems involving resource allocation in networks, providing a consistent QoS by intentionally lowering the quality delivered to the user can sometimes lead to a greater Quality-of-Experience. This mantra leads to the production of a utility function, that when required, can reduce user communication utility. This reduction of utility can provide higher bandwidth for Smart Grid applications, which in turn will lower the latency of these applications.

2.5 COMMON OPPORTUNISTIC SCHEDULERS

The Multi-User Diverse Environment introduced in Chapter 1 has provided the ability for LTE System Operators to apply algorithms to maximize the Multi-User Gain. Multi-User Gain is achieved by allocating a common channel resource to the user that is best able to exploit it [9,14] . By doing so, the system can maximize the total throughput. However, the throughput of the system is not the only metric that measures the performance of a communication link. There are many other factors that must be taken into account to ensure fair and equitable distribution of resources between all users.

The Long Term Evolution Standard does not specify any algorithms to exploit the diversity of users, nor does it specify the quantity to maximize or optimize. It is for this reason that many Opportunistic Schedulers have been developed by many researchers [9,14,13,15,78,16]. This work will critique the most common algorithms that exploit the Multi-User Diversity.

2.5.1 Maximum Sum Rate

The Maximum Sum Rate (MSR) scheduler seeks to maximize the sum rate of all users within a limiting power constraint. When scheduling users, MSR will always allocate resources to the user with the largest Signal to Noise Ratio (SNR), and therefore users with poor channel conditions are unlikely to be scheduled at all [9]. MSR yields higher throughput than any other scheduler at the cost of fairness. Users subjected to fluctuating channel conditions, such as in wireless environments, are worst served by an MSR type algorithm. The MSR algorithm maximizes the sum rate of user throughput (although a different metric can be used) by the following expression:

$$\max_{P_{k,l}} \sum_{k=1}^{K} \sum_{l=1}^{L} \frac{B}{L} \log\left(1 + SINR_{k,l}\right) \tag{2-3}$$

With a total power constraint:

$$\sum_{k=1}^{K} \sum_{l=1}^{L} P_{k,l} \leq P_{total} \tag{2-4}$$

Where:

- $P_{k,l}$ denotes the transmit power of user k using subcarrier l
- $SINR_{k,l}$ is the Signal-To-Interference-Plus-Noise (SINR) ratio for user k using subcarrier l.

Utilizing this algorithm will maximize the throughput for each subcarrier by only allowing the user with the highest SINR to utilize that subcarrier. Whilst the MSR

produces maximized system total throughput, if a Smart Grid UE is located near the cell boundary or has poor channel conditions it will be under-served by the MSR scheduler. This is contrary to the requirements set in Table 2-3 therefore MSR use in a wireless environment incorporating Smart Grid UEs cannot be endorsed.

2.5.2 Maximum Fairness Scheduler

As the name suggests, the Maximum Fairness Scheduler (MFS) aims to allocate subcarriers fairly between the users. It does so by maximizing the data rate for the user with the lowest SNR. The algorithm essentially equalizes the data rate of all UEs operating within the cell, however, this means that data rates are constrained to comparable data rates achieved by the UE with the poorest performance.

The MFS can be referred to as a max-min problem since the goal is to maximize the minimum data rate [13]. The max-min problem for MFS can be formulated as follows:

$$\max_{P_{k,l},S_k} \min_{k} \sum_{n \subset S_k} \frac{B}{L} \log\left(1 + SINR_{k,l}\right) \tag{2-5}$$

Subject to:

- $\sum_{l=1}^{L} \sum_{k=1}^{K} P_{k,l} \leq P_{total}$ (2-6)
- $S_1, S_2, \ldots, \boldsymbol{S_K}$ are disjoint sets (2-7)
- $S_1 \cup S_2 \cup \ldots \cup S_k \subset \{1,2,\ldots,K\}$ (2-8)

Where S_k is the set of indices of subchannels assigned to user k. The max-min problem posed by the MFS is NP-Hard therefore forcing separate, sub-optimal algorithms for the subcarrier allocation and the power allocation [9]. The MFS addresses the issue of under-serving UEs by the MSR in a wireless environment due to their channel conditions, intensified by fading, path loss and shadowing effects. By doing so, the MFS produces poor throughput performance and the lowest Multi-User Gain [16].

2.5.3 Proportional Rates Constraints

Whilst the Maximum Fairness Scheduler ensures equitable distribution of resources between UEs it is inflexible in its rate distribution. In a Multi-User diverse environment, many UEs have different, application-specific QoS requirements. The Proportional Rates Constraints (PRC) Scheduler addresses these specific QoS requirements by providing a proportionality parameter $\{\beta\}_{k=1}^{K}$ that ensures data rates are proportional [14,15,78]:

$$\frac{R_1}{\beta_1} = \frac{R_2}{\beta_2} = \cdots = \frac{R_K}{\beta_K} \tag{2-9}$$

By setting $\beta_k = 1$ the PRC reverts to the Maximum Fairness Scheduler. The PRC scheduler seeks to maximize the sum throughput of the system (within the constraint above) and the $k\ th$ user data rate is expressed by:

$$R_k = \sum_{l=1}^{L} C_{k,l} \frac{B}{L} log\left(1 + SINR_{k,l}\right) \tag{2-10}$$

Where

$$\boldsymbol{C} = \left[C_{k,l}\right] \tag{2-11}$$

is a subcarrier allocation matrix that stores which subcarriers are allocated to each user such that:

$$\sum_{k=1}^{K} C_{k,l} = \{0,1\}; l = 1,2,\dots,L \tag{2-12}$$

Where $C_{k,l}$ is equal to one when the subcarrier has been allocated, and equal to zero when the subcarrier is available to be allocated.

The PRC scheduler is similar to the max-min problem described in Section 2.5.2 with the embedded rate proportionality constraint. Due to this, the optimization problem is difficult to solve and just as with the MSF, the power allocation and subcarrier

allocation must be separated. The PRC scheduler provides optimal allocation of resources for a diverse range of UEs, thereby improving throughput performance.

2.5.4 Proportional Fairness

So far, the MSR, MFS & PRC have attempted to instantaneously achieve an objective with regards to throughput. Due to their time-independent solutions they lack the ability to account for latency constraints. The Proportional Fairness Scheduler balances the combined UE objectives of low latency and high throughput [17]. It does this by allocating subcarriers to the user k^* with the highest ratio between attainable data rate and average throughput. Or mathematically, users that maximize

$$\frac{R_k(t)}{T_k(t)} \tag{2-13}$$

Where

- $R_k(t)$ is the instantaneous data rate of user k attainable at time slot t
- $T_k(t)$ is the average throughput of user k up to time slot t

Over time, this equates to the PFS allocating resources to the user with the highest instantaneous data rate relative to its mean throughput.

Average throughput T_k must be updated periodically to ensure accuracy

$$T_k(t+1) = \begin{cases} \left(1 - \frac{1}{t_c}\right) T_k(t) + \frac{1}{t_c} R_k(t), & k = k^* \\ \left(1 - \frac{1}{t_c}\right) T_k(t), & k \neq k^* \end{cases} \tag{2-14}$$

The parameter t_c controls the latency of the system. Lower values of t_c relates to a decrease in the latency of the system at the expense of total system throughput. The PFS allows for both latency and throughput requirements to be achieved and more fully exploits the Multi-User Diversity. However, it provides no support for class differentiation which could result in the QoS requirements in Table 2-3 for Smart Grid applications to not be attained.

2.5.5 Opportunistic Scheduler Comparison

The four common Opportunistic Schedulers presented all provide differing levels of performance based on the metrics of throughput, fairness and algorithm complexity. The schedulers are summarised in Table 2-4 below:

Table 2-4 - Comparison of Common OFDMA Opportunistic Schedulers

Opportunistic Scheduler	Throughput	Fairness	Algorithm Complexity
Maximum Sum Rate	Highest	Lowest and inflexible	Lowest
Maximum Fairness	Lowest	Highest and inflexible	Moderate
Proportional Rate Constraints	Moderate	Moderate and most flexible	Highest
Proportional Fairness	Moderate	Moderate and moderately flexible	Low

Individually, the four Opportunistic Schedulers examined are suitable for specific objectives, such as maximizing throughput, fairness, minimizing latency. However, sometimes there is a need for a combinatorial approach that not only fully embraces Multi-User Diversity but also accounts for fluctuating traffic conditions.

2.6 A DYNAMIC, ENVIRONMENT-AWARE RESOURCE ALLOCATION SCHEDULER

Whilst the Smart Grid is in its infancy, its effect on the wireless communications environment will be huge. Due to the critical nature of the information stored in Smart Grid packets it is imperative they be delivered with low latency and free from error. In some cases, this may mean that allocation of Radio Resources cannot and should not be fair or proportional. Therefore, this research proposes the design and implementation of a Dynamic, Environment-Aware Resource Allocation Scheduler capable of adapting to current and future traffic conditions and allocating resources accordingly.

2.7 SUMMARY

So far, this thesis has introduced the Smart Grid as the solution for facilitating, monitoring and controlling an ever rapid ascent of intermittent renewable energy resources operating on the distribution grid. In order to do so, the Smart Grid requires a capable, efficient and accurate communications network. The current literature, as prescribed in this chapter, has determined that there is no class-based opportunistic scheduling algorithm to incorporate the inclusion of a Smart Grid class. As is the case for most wireless sensor networks, the data sent by individual UEs is low in usefulness and precision. Collection of a large amount of data produces information useful to the system and can be acted upon. However, this increases the communication traffic in an environment where communication traffic is already high.

Radio Resource Management and allocation has developed to the point where it can compensate for changing channel conditions and individual UE constraints but doesn't account for changing traffic conditions that can affect the QoS of users communicating within the system. This research introduces an Environment-Aware opportunistic scheduler based on population dynamic algorithms and class differentiation. Radio Resources are allocated to classes based on class growth rates (future communicating requirements) and queue sizes (current communicating requirements). Furthermore, it will be shown that a Dynamic, Environment-Aware based algorithm ensures Smart Grid applications QoS requirements are met by optimising the relationship between user communication QoE and Smart Grid QoS.

In conclusion this work proposes a reactionary distributed automation model for the Smart Grid, which aims to decrease the communication requirement imposed by the Smart Grid on an LTE wireless network. This differs to other research in this area as its basis is that the LTE network should not be stymied by the burden of a Smart Grid. This may appear to be counterintuitive as the reliability of the Smart Grid is paramount; however, this research aims to find an optimal operating point in which both Smart Grid and pre-existing data and voice communications can be achieved with satisfactory Quality of Service for all.

Chapter 3 will provide a model for the traffic and communication channel used in this research. A brief background into the LTE frame and Resource Block will be provided to better contextualize the application of the resource allocation model proposed in this research.

Chapter 3.
Channel & Traffic Modelling

Thus far, this thesis has introduced the concept of Radio Resource Management and Scheduling in the context of the Smart Grid operating in a wireless communications environment. In doing so, it has become increasingly apparent that there is a need for RRM algorithm that can fully integrate Smart Grid communications without greatly affecting pre-existing customers currently using the wireless channel. This chapter examines the channel and traffic models used for the data collection and sets out the experimental method so as to better contextualize the results in the following chapters. The channel and traffic models detailed in this chapter are used to determine the results in Chapters 5 – 8.

The first section of this chapter focuses on the traffic model presented in this research. The importance of a complete and realistic traffic model sets the precision and accuracy of the results. The LTE network is explored and a channel model is applied to the OFDM downlink channel.

The data modelled is divided into two areas. Firstly, traffic requirements, packet sizing and class differentiations for the types of data prevalent in modern wireless communications. The traffic profile of a singular LTE-A cell, with packets as defined

in section 1 of this chapter. Finally, a channel model for the LTE OFDM downlink channel is presented thus realising our complete network.

The apparatus used in this research was a traffic model that was built using Matlab's Simulink modelling software. The LTE-Advanced eNodeB model was designed and built in the Matlab programming environment. The traffic model was directly inputted into the LTE-A eNodeB system. The resource allocation and scheduling was then applied to each packet simulated in the system. This provided the framework for applying the Radio Resource Management protocol proposed in this thesis.

3.1 SOFTWARE AND HARDWARE

The only apparatus used in this experiment was a Personal Computer (PC) operating Matlab R2013a with Simulink. Table 3.1 shows the configuration of the PC used.

Table 3-1 - Hardware/Software Details

Hardware/Software	Description
Operating System	Windows 8.1 Pro (64bit)
Processor	Intel Core i7 Q820, 1.73 – 3.06 GHz
RAM	8Gb DDR3 1066MHz
Matlab	R2013a including Simulink

It was on this PC that the following Simulink model and Matlab programming was developed and built. However, it should be noted that any computer that satisfies the basic Matlab operating requirements could have been used. Matlab is a cross-platform program, which means that its use is not constrained to a computer with a Windows based operating system. A computer using an Apple or Linux based operating system could have been used just as successfully.

3.2 DATA COLLECTION

This section details the method of data collection and the type of data collected, and explains why the data was required. It begins with the modelling of a teletraffic model

with heterogeneous, packet switched traffic. This is followed by the creation of a wireless communication channel based on LTE-OFDM architecture.

3.2.1 Teletraffic Model

Important metrics in teletraffic theory based on specific types of random processes include the following: average connection duration; average number of users in the system; busy time; service time; and call arrival process.

The heterogeneous traffic produced by the UEs within the cell was modeled as an M/M/N markov chain, with inter-arrival time Poisson distributed, exponentially distributed service time, and with N servers. Upon arrival, the class of the user is assigned randomly to ensure generality. The queue size over time of each class $\{Smart\ Grid, Data, Voice\}$ is shown in Figure 3-1. An arrival is selected for service if any channel $n \epsilon 1, \dots, N$ is idle. When the utilization of the channels is low, the allocation of a user $u \epsilon 1, \dots . U$ can be optimized. However, once all channels are allocated, the next user that arrives is best served by accepting the next available channel, whether it is optimal or not. This reduces the wait time in the queue, but can increase the transmission delay due to higher bit error rates. By allocating channels to set classes based on the population dynamics of the environment, it is possible to increase the overall throughput and decrease the latency of users. To map the dynamical properties of the populated environment, it must be possible to measure how the population is changing.

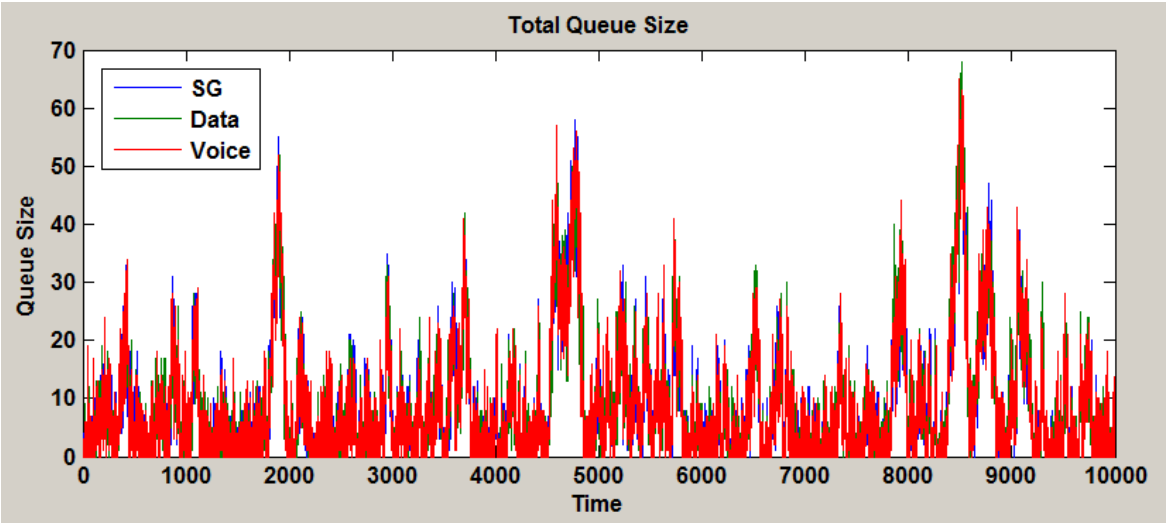

Figure 3-1 - Total Queue Size with Class Magnitude (Time in ms)

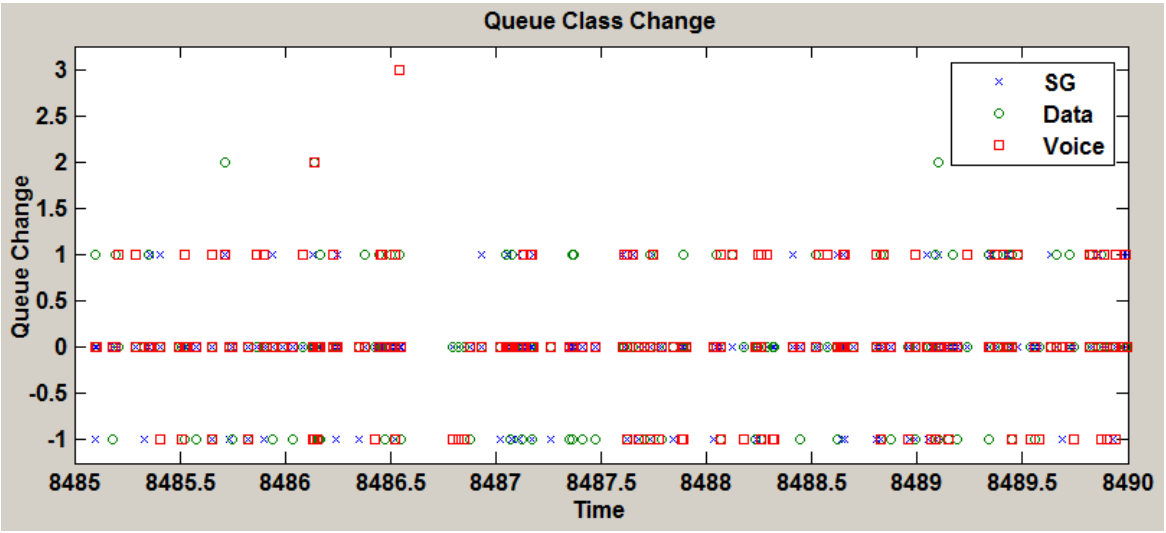

Figure 3-2 - Change in Class Queue Magnitude (Time in ms)

The change in arrival and departure of UEs over a small time frame δt is shown in Figure 3-2. At any one time, it is most likely that only a single arrival occurs. However, as can be seen in Figure 3-2, this is not always the case. Equally, the number of instantaneous allocations of channels is also one. This provides a framework for mapping the change in population to a differential equation interaction matrix. In the case that not all channels are allocated, a user u is allocated a channel upon arrival to the queue, thus increasing the magnitude of $class_u$ by one. When all channels are allocated, the user must wait until another user v relinquishes its channel. Therefore,

at this time, $class_v$ is reduced by one and $class_u$ is increased by one. The magnitudes of all other classes in the system remain unchanged. So:

$$\Delta(class_u) = \Delta(class_v) \tag{3-1}$$

This research defines two different types of traffic, which can belong to any of the three defined classes of information. Sporadic Traffic is used to define traffic of a random or bursty nature that is not scheduled. The other is Periodic Traffic which defines scheduled traffic such as status updates or synchronization messages. The Smart Grid, as a Machine-To-Machine network will be composed of traffic that is both Sporadic and also Periodic. The data class will also have a certain subset of Periodic Traffic but will mostly be composed of Sporadic Traffic. In voice traffic, the voice packets are periodic in nature with a randomized inter-packet arrival rate. Therefore, the voice traffic was modelled with a call arrival time relationship following an Erlang Distribution with call burst times Poisson distributed. Although voice data rates (~16kbps) are low compared to data traffic, being real time, transmission of voice data is highly sensitive to loss of packets and even low levels of transmission latency [79]. Silent periods consume half the duration of the talk burst (or voice call) making it possible to schedule resources during every voice spurt and then de-allocating the resources at the end of the spurt.

3.3 LONG TERM EVOLUTION COMMUNICATIONS

Long Term Evolution or the Evolved Universal Terrestrial Access Network (E-UTRAN) was developed by The 3rd Generation Partnership Project, a collaboration between six telecommunications standard development organizations [80]. LTE is based on Orthogonal Frequency Division Multiple Access in combination with higher order modulation schemes (up to 64QAM) providing better access the purely IP based Evolved Packet System. OFDM, is a multi-carrier technology based on the breaking the spectrum into a set of orthogonal narrowband subcarriers which can be shared between multiple users [81]. Orthogonal subcarriers have the added benefit of reducing Co-Channel-Interference (CCI) thus eliminating the requirement for guard bands. Inter-Symbol-Interference (ISI) is also improved due to low-symbol rates which

are less affected by multipath propagation. The LTE access network is a collection of interconnected evolved Node-Bs with no central controller and connected via the X2 interface.

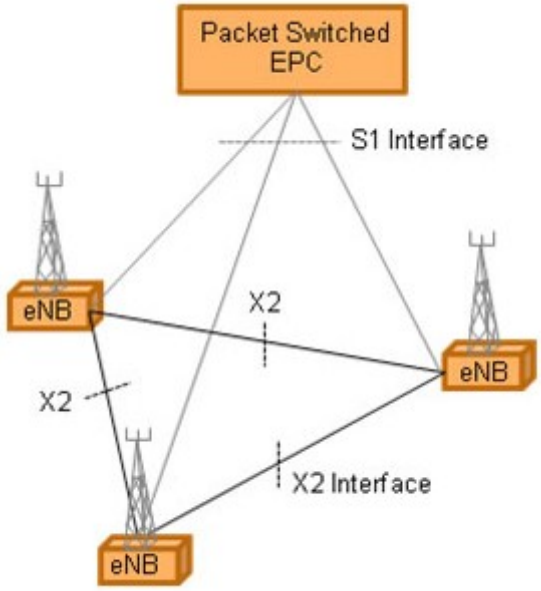

Figure 3-3 – LTE Core Network

LTE also provides support for higher bandwidths (up to 20MHz) and spatial multiplexing producing high data rates up to 300Mbps in the downlink. LTE-Advanced (LTE-A) builds upon the LTE network and provides carrier aggregation, higher order Spatial Multiplexing (8x8 MIMO in the downlink and 4x4 in the uplink) and supports the use of relay nodes to increase coverage [82]. Whilst LTE-A is the most up to date form of the LTE standard, the extra inclusions of higher order MIMO and carrier aggregation are outside the scope of this research.

3.3.1 LTE Frame Structure & Resource Block

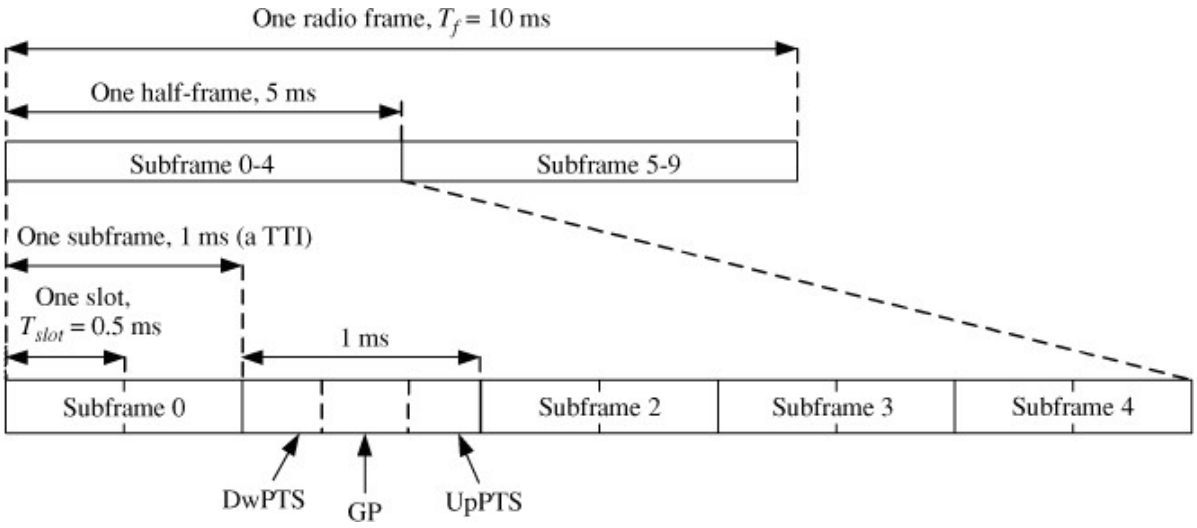

Figure 3-4 – Long Term Evolution Frame

As shown in the above Figure 3-4 [9], the LTE frame is broken into 10 subframes. Each subframe is then also divided into two slots, each of which is of length 0.5ms. This combines to provide an overall frame size of 10ms. There are also special subframes, which consist of three fields:

The Downlink Pilot TimeSlot (DwPTS), the guard period (GP) and the Uplink Pilot TimeSlot (UpPTS). These fields provide sufficiently large guard periods for the equipment to switch between transmission and reception of data. LTE supports a guard period ranging from two to ten OFDM symbols, sufficient for a cell size up to and beyond 100km in size. The figure shows the structure of the first half of the frame, however, the second half of the frame has similar structure.

The structure of the LTE resource grid is shown in Figure 3-5 [9] below. This is the structure of the downlink resource grid, however, the structure of the uplink resource grid is very similar. For both downlink and uplink, the eNode-B schedulare dynamically controls which time-frequency resources are allocated to a certain UE. The resource assignments, including the assigned time/frequency resources and respective transmission formats, are conveyed through downlink control signalling. The minimum size of radio resource that can be allocated to a UE corresponds to two resource blocks, which is 1ms in duration in the time domain and 180kHz in the frequency

domain. Both downlink and uplink employ orthogonal transmission, so each resource block is allocated to a single UE.

The resource grid is characterised by three parameters:

N_{DL}^{RB} – Number of downlink resource blocks: this number is dependent on the transmission bandwidth

N_{SC}^{RB} – Number of subcarriers in each resource block: this depends on the subcarrier spacing. With each resource block 180kHz wide in the frequency domain. When configured to normal cyclic prefix, the number of subcarriers is 12, with each of 15kHz width provides the 180kHz band of each resource block.

N_{Symb}^{DL} – Number of OFDM symbols in each block: this depends on the cyclic prefix length and the subcarrier spacing. For a normal cyclic prefix length, which provides the number of subcarriers as 12, the number of OFDM symbols is 7.

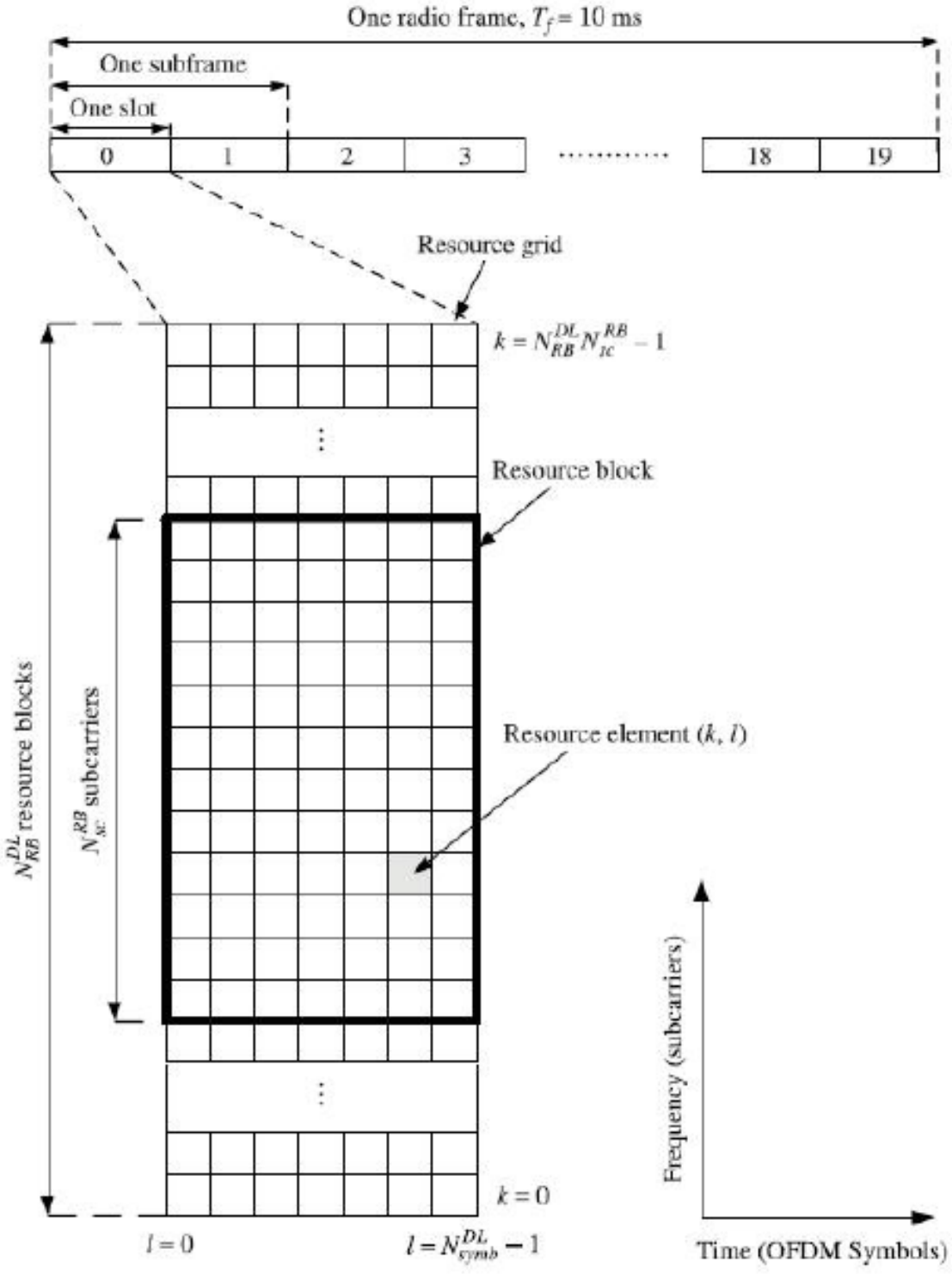

Figure 3-5 – Long Term Evolution Resource Grid Structure

Therefore it is now easy to calculate that the number of resource elements in the downlink resource grid is 4200. This number does not take into account Multiple Input – Multiple Output technology, of which it would be an integer multiple of this number.

When these resource blocks are optimally allocated, the latency requirements of the Smart Grid Distribution Automation Network can be achieved.

3.3.2 Broadband Wireless Channel

The Broadband Wireless Channel is affected by multiple factors, including: path loss, shadowing, Doppler spread, delay, multipath propagation etc. This phenomenon is named 'fading' and produces variations in signal amplitude over time and frequency [83]. Path loss is due to the signal dissipation over an expanding spherical wavefront. This is represented as an inverse relationship between the received signal power and sphere surface area at distance d. Directional antennae can provide a scalar gain and are denoted as G_t and G_r for the received and transmitted gains respectively in the equation below, which determines the received signal power:

$$P_r = P_t \frac{\lambda G_t G_r}{(4\pi d)^2} \tag{3-2}$$

So far, we have accounted for the signal dissipation due to the distance between the receiver and transmitter. However, in a typical wireless environment, there are also many obstacles such as trees, buildings etc that cause temporary degradation in the received signal strength. Shadowing accounts for these variations in signal strength by introducing a random stochastic quantity. The equation for the received signal power including shadowing loss is:

$$P_r = P_t P_0 \chi \left(\frac{d_o}{d}\right)^{\alpha} \tag{3-3}$$

The shadowing value χ is typically modelled as a lognormal random variable:

$$\chi = 10^{\frac{x}{10}} \tag{3-4}$$

where x is a normal distribution with mean 0 and variance σ^2:

$$x \sim N(0, \sigma^2) \tag{3-5}$$

Essentially, this allows the receiver at the same distance d to have different path losses.

So far, this thesis has introduced the Large Scale Fading effects of Path Loss and Shadowing, which are generally categorized as slow fading processes and mainly affected by distance from the transmitter. On the other hand, Small Scale Fading refers to the rapid variation of signal qualities due to the constructive and destructive interference of multiple signal paths. The reception of multiple signals due to signal reflections is known as multi-path fading and can cause phase differences and signal delays.

Rayleigh Fading is characterized by a large number of scatterers and no dominant path, such as Line-of-Sight (LOS) path between the transmitter and receiver being available [9]. This suits a built-up urban scenario well where there are many obstacles.

The Rayleigh Fading envelope amplitude is characterized by the following formula:

$$f_{|r|}(x) = \frac{2x}{P_r} e^{\frac{-x^2}{P_r}} \quad , \quad x \geq 0 \tag{3-6}$$

and the received signal power is then defined as:

$$f_{|r|^2}(x) = \frac{1}{P_r} e^{\frac{-x}{P_r}} \quad , \quad x \geq 0 \tag{3-7}$$

Where P_r is the average received power due to shadowing and path loss. Empirical models for LTE fading channels are available but added extra complexity without adding further precision. The inclusion of MIMO in such models was deemed outside the scope of this research and the Rayleigh Fading channel modelled provided close resemblance to actual channel conditions.

The path loss and shadowing determine the mean received signal power with the total received power fluctuating around this mean due to Rayleigh Channel fading. This is presented in Figure 3-6 with path loss, shadowing and fading characteristics easily differentiated.

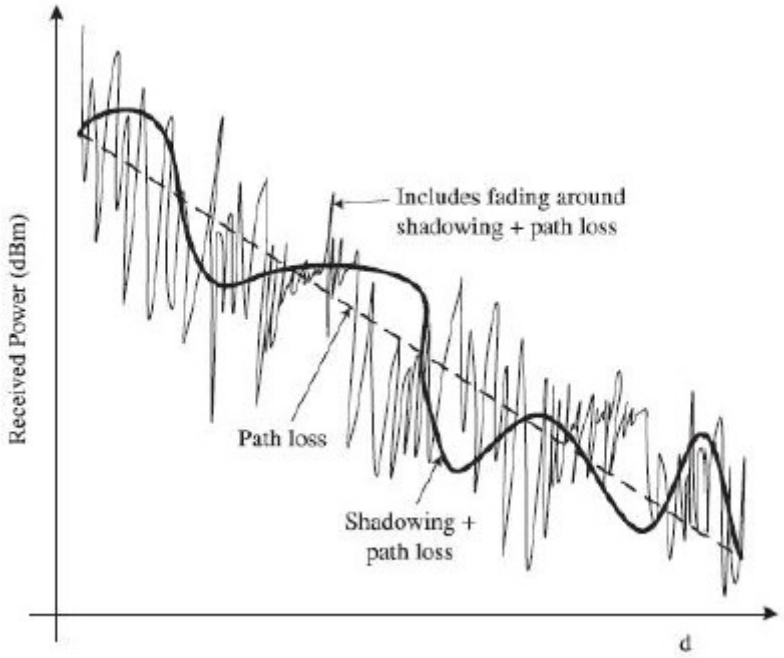

Figure 3-6 - Path Loss, Shadowing & Multi-Path Fading Attenuation Factors Affecting Channel Quality

Using the statistical model for a Rayleigh Fading Channel the channel gain of selected users was modelled in Matlab and is shown in Figure 3-7. The distances of the users in Figure 3-7 were ordered to show the effect of path loss on the overall channel gain, however, in the simulation the users are randomly distributed within the cell.

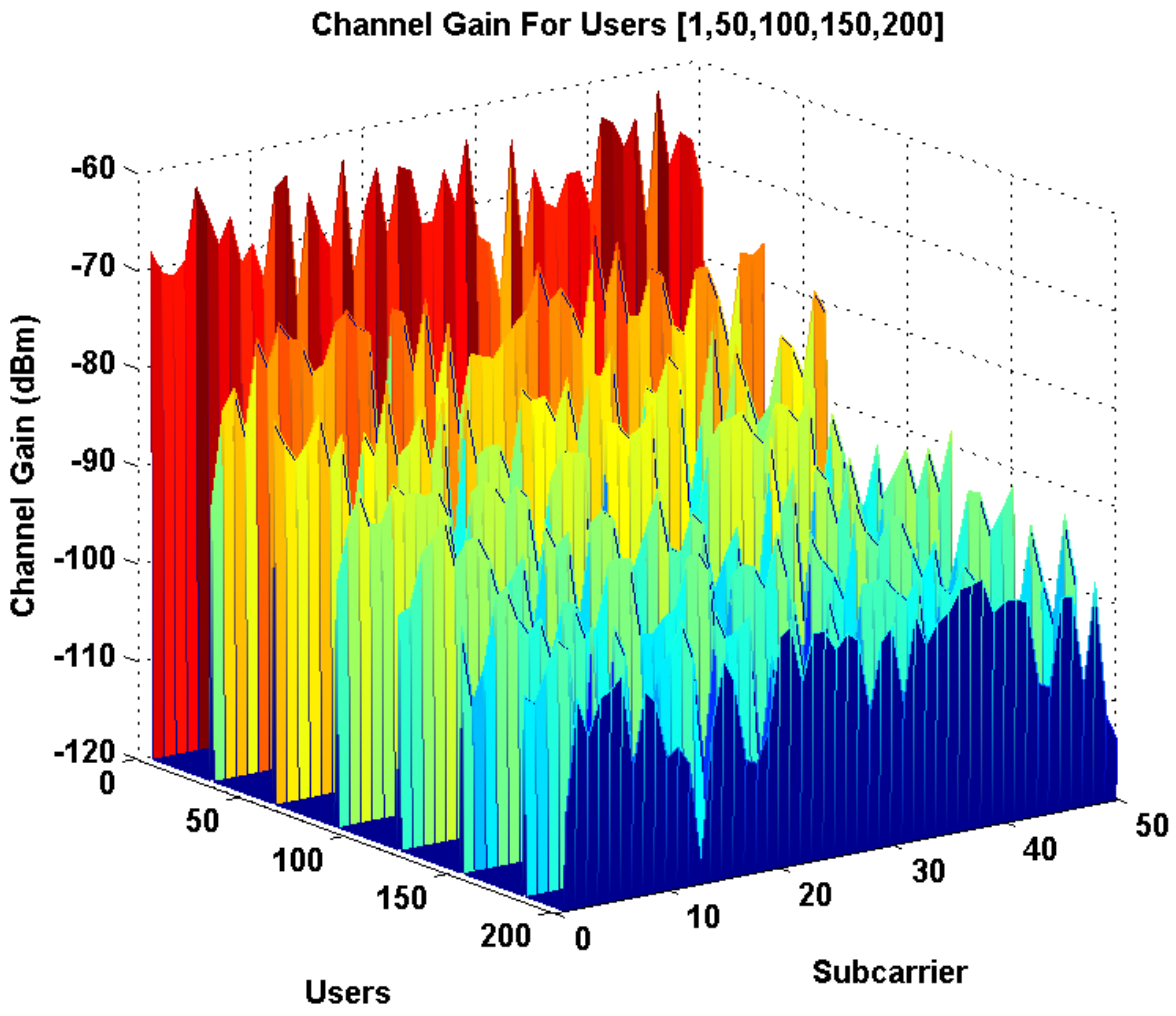

Figure 3-7 - Example Channel Gains for Selected Users. User 1 is closest the BS and User 200 is the farthest

The channel gain for each user u over each subcarrier n is stored in the matrix $\boldsymbol{G} = [G_{u,n}]$ with no temporal variation. The channel capacity provided by the subchannel of the nth subcarrier is given by the Shannon-Hartley channel capacity formula [84]:

$$C_n = \Delta_n \, log_2\left(1 + |G_n|^2 \frac{P_n}{N_0}\right) \tag{3-8}$$

where Δ_n, P_n, N_0 is the subcarrier spacing (in Hz), transmission power, and the noise variance, respectively, of the nth subcarrier.

3.4 SUMMARY

This chapter has introduced the channel and traffic model utilized by this research. The traffic model is presented with two types of traffic identified: Sporadic and Periodic. The communications traffic is also segregated into three different classes: Smart Grid, Data, & Voice.

The Long Term Evolution core network, Frame and Resource Grid Structure was explained. Such a communications is required to carry the traffic formulated above. A detailed description of the Rayleigh Fading Channel is then applied as the communication channel for the LTE network to carry the Smart Grid, Data & Voice traffic. A channel gain model is then calculated using the channel gain for each individual subcarrier.

The question remains, how do we allocate the subcarriers to the users to maximize our goals of high throughput, low latency and fairness between the classes? In order to solve this quintessential problem Chapter 4 will first provide a background into Lotka-Volterra Population Dynamic Equations that are utilized to schedule and allocate resources for UEs in the LTE OFDM communications channel.

Chapter 4.
Lotka Volterra Population Dynamics

This chapter explores the Lotka-Volterra Differential Equations used to schedule traffic and allocate LTE resources defined in Chapter 3. Initially, a small introduction to Lotka-Volterra Population Dynamic Equations will be provided. The derivation of the Lotka-Volterra model will be accompanied by definitions of the mathematical tools used such as Smales' Construction (Section 4.3.1), the Poincaré-Bendixson Theorem & Limit Cycles (Section 4.3.2) and Hamiltonian Representation of Dynamic Systems (Section 4.3.3). Finally, the development of the Lotka-Volterra Resource Allocation & Scheduler will be defined.

4.1 GENERALIZED LOTKA-VOLTERRA EQUATION

Differential equations are powerful tools for modelling processes that change with time $\left(\frac{d}{dt}, \frac{\partial}{\partial t}\right)$ or some other variable. Ordinary Differential Equations (ODEs) model many dynamical systems, for example: weather patterns, physiological processes, ecology, electrical circuits, epidemiology, chemical reactions, economics etc. The telecommunications environment can be expressed as a Lotka-Volterra N species

competition system. In this research we choose the species to be data communications, voice communications and Smart-Grid communications, where the Smart Grid is a new service of which will become more and more present in wireless telecommunications data as the Smart Grid evolves with time. Each of these three species is competing over one resource, the subcarriers of the LTE eNodeB within the local environment.

The generalized Lotka-Volterra equation is:

$$\frac{dx_i}{dt} = x_i\left(b_i \times \left(1 - \frac{1}{N_i}\right) + \sum a_{ij}x_j\right) \tag{4-1}$$

Here b_i is the intrinsic growth (or decay) rate for the i-th species, N_i is the limiting (or carrying) population of the i-th species, and the a_{ij} represents the effect of the j-th species upon the i-th one. The matrix $A = (a_{ij})$ is called the interaction matrix:

$$A = \begin{bmatrix} a_{ii} & \cdots & a_{ij} \\ \vdots & \ddots & \vdots \\ a_{ji} & \cdots & a_{jj} \end{bmatrix} \tag{4-2}$$

By choosing all $a_{ij} > 0$ the system becomes competition based, of which there is inter and intra species competition.

4.1.1 Two Species Lotka-Volterra Equations

I used the two species Lotka-Volterra equations for a simplistic exercise for proving the functionality of the proposed model.

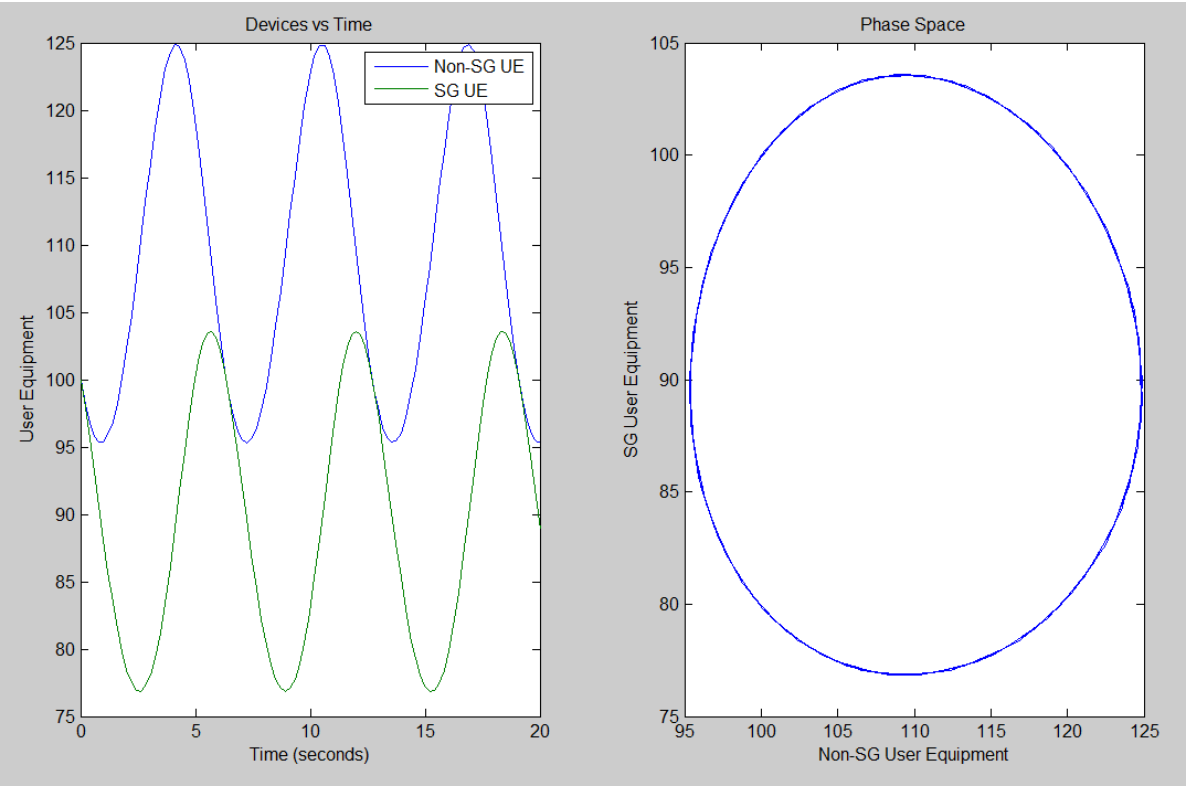

Figure 4-1: (a) - Population of SG and non-SG User Equipment as a function of time;
(b) - Phase Space of Population

In Figure 4-1(a) the periodic nature of the Two Species Lotka-Volterra equation is shown. This typifies a sharing of a single resource, of which the requirements of each on the resource is different. As the Smart Grid will be sending and receiving small data packets containing state information, its resource requirements will be lower than data services and applications already existing in the communications network. Also, the modelled number of Smart Grid User Equipment is smaller which is based on the choice of an urban scenario with more people than critical grid infrastructure requiring constant monitoring. The periodic nature of the relationship between the species causes the phase space of the species to be a limit cycle, as shown in Figure 4-1(b). It should be noted that this limit cycle only represents a singular solution to the Lotka-Volterra equations, with each solution dependent on the initial conditions and growth rates of each species.

4.1.2 Allocation of LTE Resource Blocks

By applying the magnitudes of the individual service population as a percentage of the total population it is possible to allocate the resource elements of an LTE resource grid. Using Figure 4-1(a) as a reference in Figure 4-2 it is possible to see the difference in the allocation of LTE resource elements between Smart Grid and non-Smart Grid user equipment.

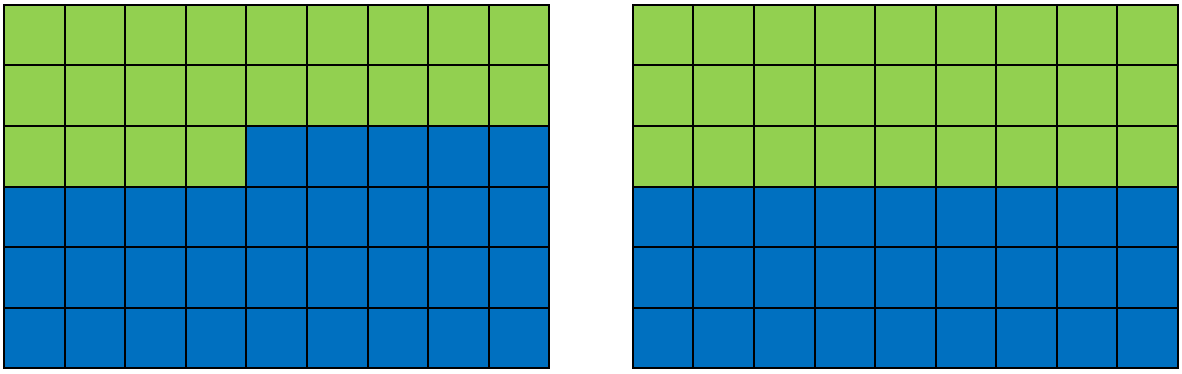

Figure 4-2: (a) – LTE Resource Block Allocation when SG UE Bandwidth Requirements are low;
(b) – LTE Resource Block Allocation when SG UE Bandwidth Requirements are high

In Figure 4-2(a), the resource requirements for the Smart Grid are lower; therefore the number of resource elements allocated for its use is also lower. When the Smart Grid reacts to outside operating conditions, such as when a fault occurs, the Phasor Measurement Units and/or other critical diagnostic infrastructure will require bandwidth to send and receive data. During this time, the number of resource elements allocated to the Smart Grid UEs will need to increase, at the expense of non-Smart Grid UEs, as is shown in Figure 4-2(b).

Figure 4-3 shows the phase plane of two species Lotka-Volterra equation with no-intra species competition. The multiple plots represent the effect on the equations by changing the initial conditions, which for this case were the starting populations of the two species, namely Smart Grid User Equipment and Non-Smart Grid User Equipment. The periodic nature of Figure 4-1(a) is shown by each phase plane for each initial condition is a limit cycle (closed orbit solution). In this way, the resource allocation of LTE bandwidth can also be periodic.

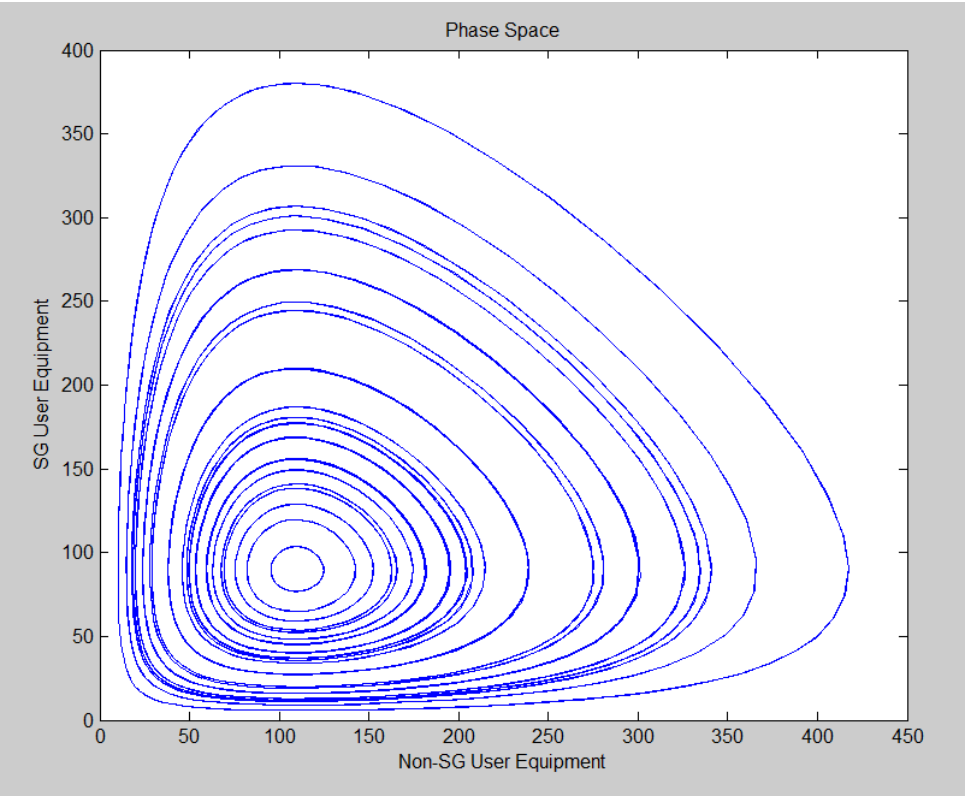

Figure 4-3 - Phase Plane of Populations with Changing Initial Conditions

4.2 LOTKA-VOLTERRA PURE COMPETITIVE MODEL

The Lotka-Volterra Population Dynamic Equations allow for a multitude of differing environmental scenarios. One such scenario is a purely competitive model where each species competes with every other species, and also members of its own species for resources. This translates well to a telecommunications network, where the channel (the resource) is fought over by UEs wishing to communicate. By choosing all items in the interaction matrix to be greater than zero, the model is constrained to a competitive scenario.

4.2.1 Two Species Competition

The two species, pure competition phase portraits are shown in Figure 4-4 below. The black lines overlaying the individual plots are the nullclines. From left to right, top to bottom:

- Case 1 - $\alpha = 0.75$, $\beta = 0.75$
- Case 2 - $\alpha = 1.25$, $\beta = 1.25$
- Case 3 - $\alpha = 0.75$, $\beta = 1.25$
- Case 4 - $\alpha = 1.25$, $\beta = 0.75$

Where α and β are the Non-Smart Grid User Equipment growth and Smart Grid User Equipment growth respectively.

Nullclines are an incredibly useful tool for analysing nonlinear systems of differential equations. Nullclines usually separate $\mathbb{R}^n$ into a collection of regions in which the trajectories of the vector field point in either the positive or negative direction.

To calculate the nullclines we use the following methodology. The nullclines are simply where $\dot{x_\iota} = 0$. Therefore we have:

- $x_1 = 0$ or $1 - x_1 - \alpha x_2 = 0$
- $x_2 = 0$ or $1 - x_2 - \beta x_1 = 0$

Therefore, we find the steady states at:

$$(x_1^*, x_2^*) = (0,0), (1,0), (0,1), P = \left(\frac{1-\alpha}{1-\alpha\beta}, \frac{1-\beta}{1-\alpha\beta}\right) \quad (4\text{-}3)$$

However, this last steady state is only feasible when either:

- $\alpha > 1$ and $\beta > 1$, since then also $1 - \alpha\beta < 0$
- $\alpha < 1$ and $\beta < 1$, since then also $1 - \alpha\beta > 0$

P is known as the interior steady state as it lies within the axes of our phase portraits, and as such also our region of evaluation. Hence, we have either three or four steady states. All four of the cases are shown in Figure 4-4:

Case 1: $\boldsymbol{\alpha < 1, \beta < 1}$

The steady state *P* attracts all of the interior of $\mathbb{R}^2_{>0}$. The remaining three steady states are unstable, with $(1,0)$ and $(0,1)$ being saddle-type nodes.

Case 2: $\boldsymbol{\alpha > 1, \beta > 1}$

Both $(1,0)$ and $(0,1)$ are stable nodes. There is a line called a sepatrix of which, if the Lotka-Volterra equations have initial conditions on the left side of the sepatrix the solutions are attracted to the stable node $(0,1)$. On the right side of the sepatrix the solutions are attracted to the stable node $(1,0)$. All other steady states are unstable.

Case 3: $\boldsymbol{\alpha < 1, \beta > 1}$

Only one steady state is stable $(1,0)$ with all solutions attracted to this node. All other steady states are unstable and steady state P does not exist.

Case 4: $\boldsymbol{\alpha > 1, \beta < 1}$

Only one steady state is stable $(0,1)$ with all solutions attracted to this node. All other steady states are unstable and steady state P does not exist.

The fundamental results of each case clarify the four possible scenarios are two-species competitive Lotka-Volterra equation can undergo. Case 1 shows that the two populations can coexist stably, only if the inter-species competition is not too strong. However, there is a price for stable coexistence with both species populations limited to less than their individual carrying capacity (upper bound population). In Case 2 the inter-species competition is aggressive, with one population eradicating the other depending on the initial population. In Cases 3 & 4, the inter-species competition of one species is dominant with the other species eradicated regardless of the initial populations.

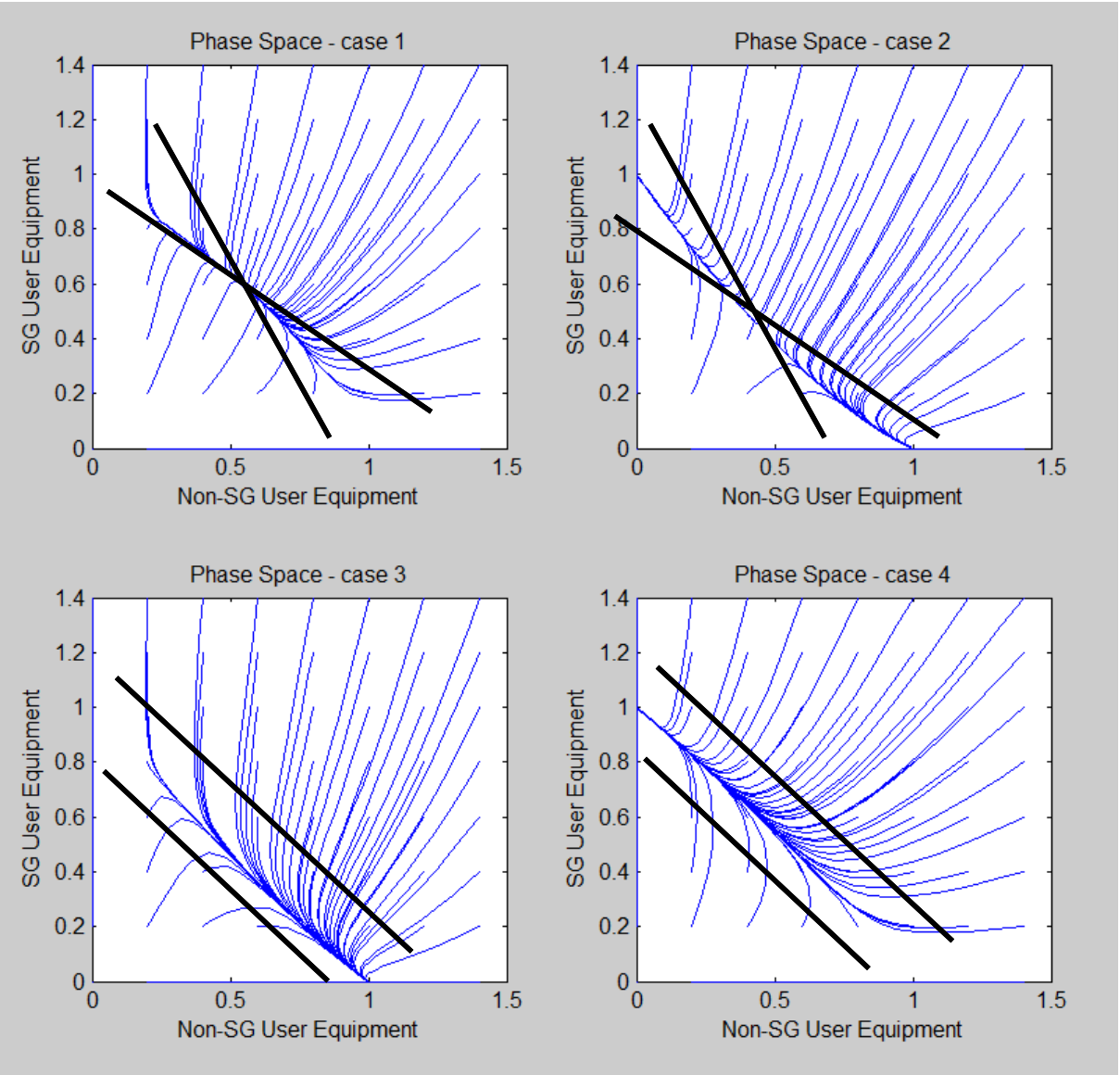

Figure 4-4 – Possible Phase Portraits for Two Species Lotka-Volterra Pure Competition Model with Changing Growth Constants

All four of the above cases can be useful for allocation of LTE resources as they define differing periods of use by either of the competing species. Case 1 typifies the scenario when both Smart Grid (SG) UEs and other Non-SG UEs must both be communicating. Case 3 and 4 defines a scenario when either SG UEs or Non-SG UEs must assume all of the bandwidth (Non-SG UEs only being able to do so when the SG UEs relinquish any bandwidth requirements). Case 2 is an intermediate state between Cases 3 and 4, where depending on the initial populations (i.e. the initial bandwidth requirements) either the SG UEs will relinquish the bandwidth or seek to

gain it all. SG UEs will be given priority over the Bandwidth usage when a major fault has occurred which must be alerted to grid operators.

4.2.2 Three Species Competition

It is very hard to show the specific dynamical properties of the below graphs including the nullclines, which was why two dimensional analysis was provided in Section 4.1.1 and Section 4.2.1 above.

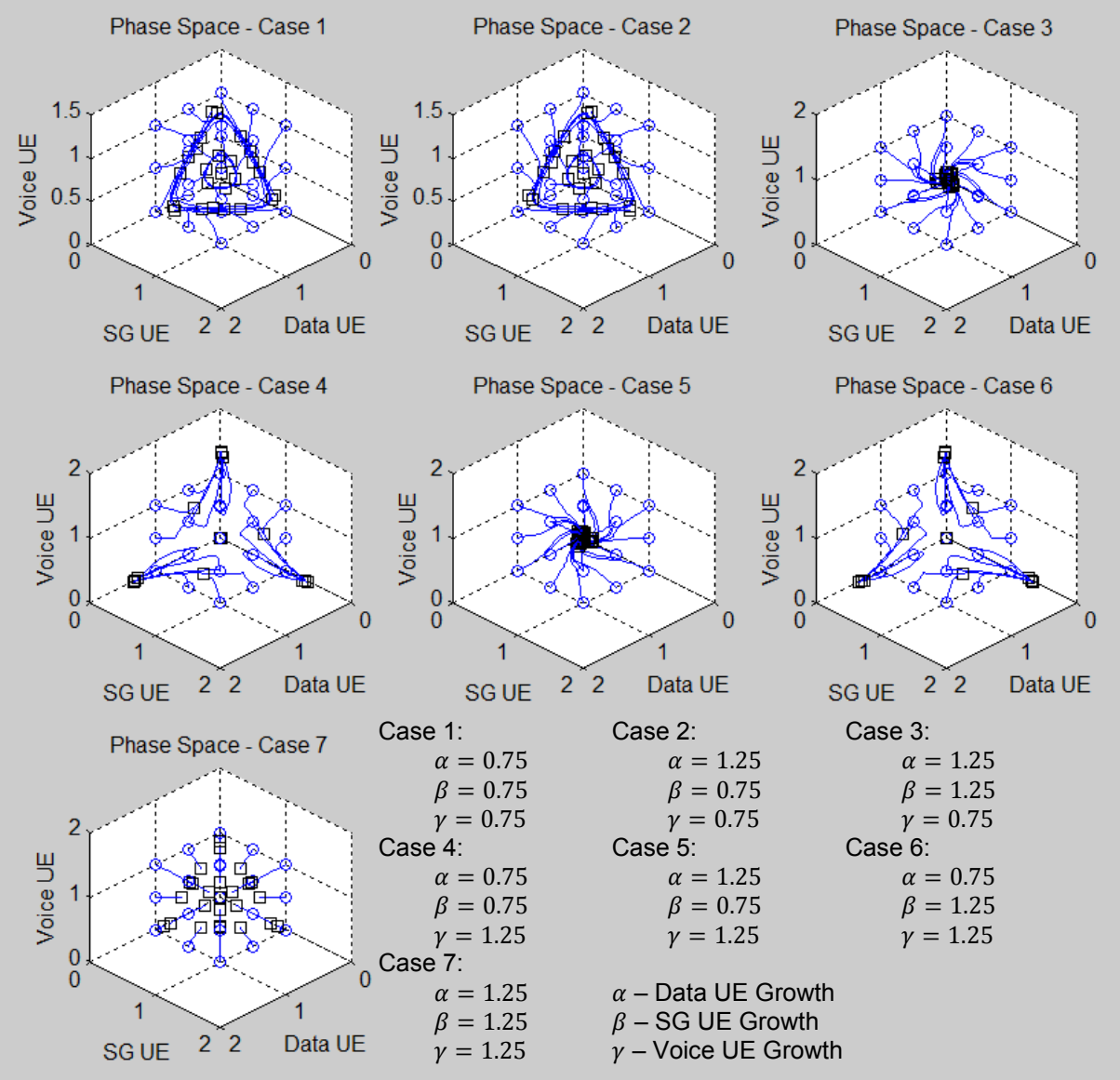

Figure 4-5 – Possible Phase Portraits for Three Species Lotka-Volterra Pure Competition Model with Changing Growth Constants

As for the three-species model above, it is possible to clarify what each state represents, however, this will be, for the most part, a re-iteration of what has been stated previously. The extra states occur for when two species co-exist by eradicating one other, or when one species is purely dominant and the others are eradicated. The coexistence of all species is also a possible and desired outcome.

4.3 THREE SPECIES EQUILIBRIUM ANALYSIS

It is often impossible to explicitly calculate solutions to non-linear systems of differential equations. The one exception occurs when an equilibrium point can be found, in which the equilibria can be stated explicitly [85]. Solutions of non-linear systems near equilibrium points resemble those of their linear parts. This is the case when the linearized system is hyperbolic, that is, when none of the eigenvalues of the system has a zero real part.

An equilibrium point is said to be stable if a minor perturbation in the system yields a solution that remains close to the original solution. Asymptotic Stability is similar but after the perturbation solutions will converge to a given orbit. A sink is asymptotically stable and therefore stable however, a saddle or source are unstable equilibria.

Solving for Equilibria states and proving their stability allows for the system to ensure that the subcarrier allocation over time doesn't revert to a single or two classes and that it remains shared and also embodies the same dynamic characteristics of the environment it is modelling. The periodicity of traffic patterns can also be mapped into the frequency of limit cycles thereby removing the need to explicitly solve the system during every change of the population.

4.3.1 Smales' Construction

A construction on the dynamics of multi-species competitive growth by Stephen Smale in 1976 disproved that the competition always diverges to a stable state or a periodic orbit [86]. Smale showed examples of systems containing totally competitive species of which their long term dynamics lie on a simplex. This proved that simplex is an

attractor for which arbitrary dynamics can be specified. By being able to arbitrarily define system dynamics that diverge to a stable simplex we can map the fluctuating properties of a telecommunication environment to the Lotka-Volterra multi-species, totally competitive equations.

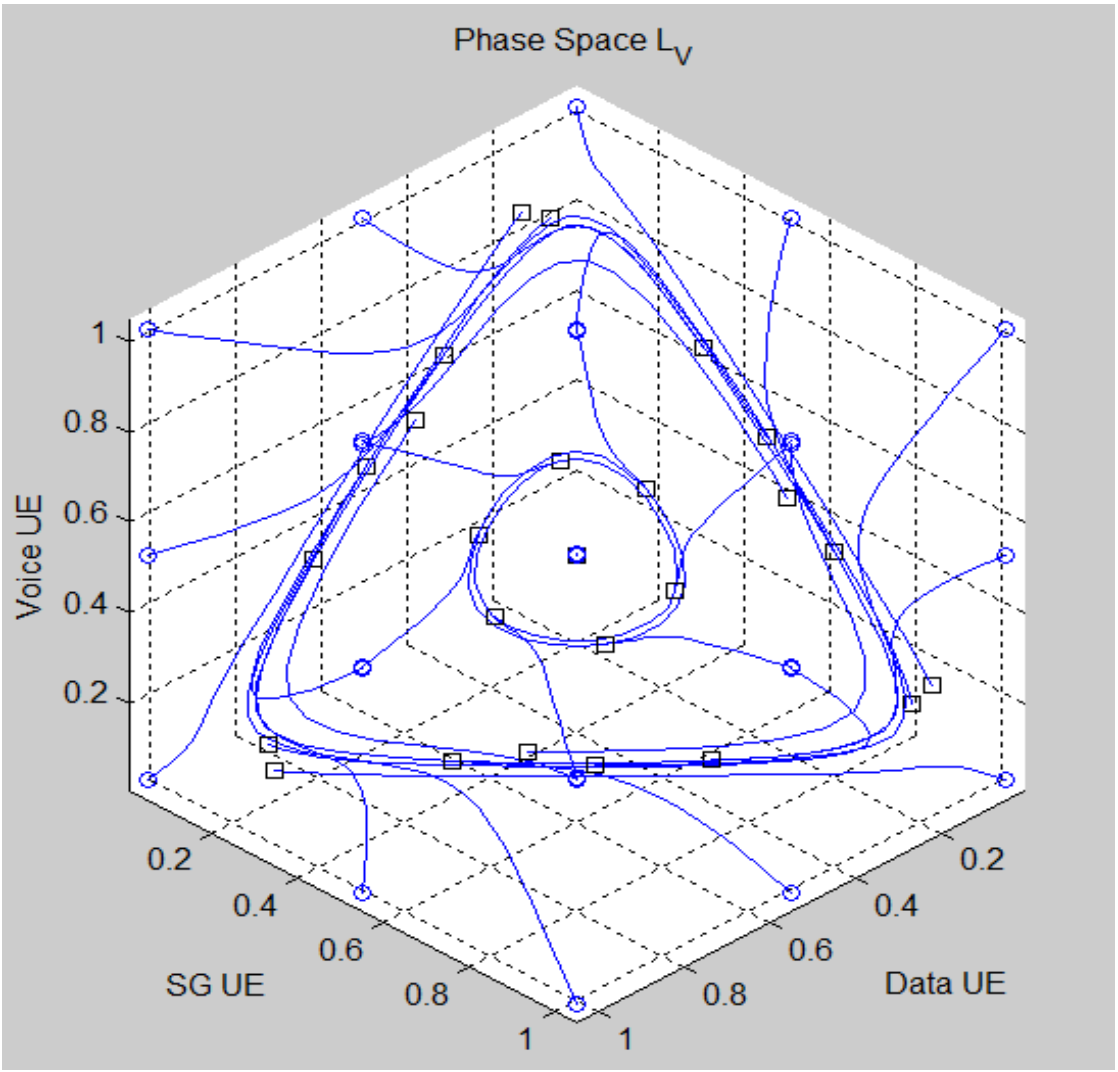

Figure 4-6 - Phase Space of 3 Species Competitive Lotka-Volterra Equations Using Smales' Construction

By incorporating Smales' Construction in the 3 Species Competitive Lotka-Volterra equations, periodic orbits occur, as seen in Figure 4-6. The carrying simplex is attracting all orbits apart from the origin, which is found to be an unstable steady state. This result provides the basis for further research, where an oscillatory relationship between the services can serve to provide a sharing of resources capability. The dynamic nature of Lotka-Volterra equations means that we can also apply this result

to differing initial conditions, and by controlling the specific growth rates, share bandwidth to the services requiring it.

4.3.2 Limit Cycles

Finding limit cycles in dynamical systems can be very complex. The Poincaré-Bendixson Theorem determines all possible limiting behaviours of a planar flow [85,87]. It states that if some Ω is a nonempty, close and bounded limit set of a planar system of differential equations that contains no equilibrium point, then Ω is a limit cycle. A limit cycle is a closed trajectory in phase space having the property that at least on other trajectory spirals into it, either as time approaches infinity or as time approaches negative infinity. Figure 4-7 shows an example of a two species Lotka-Volterra phase portrait. The phase portrait geometrically represents the trajectories of the dynamic system. Figure 4-8 shows an example of a three species Lotka-Volterra phase portrait. The limit cycles present are due to the use of Smales' Construction which has mapped the dynamics onto a simplex.

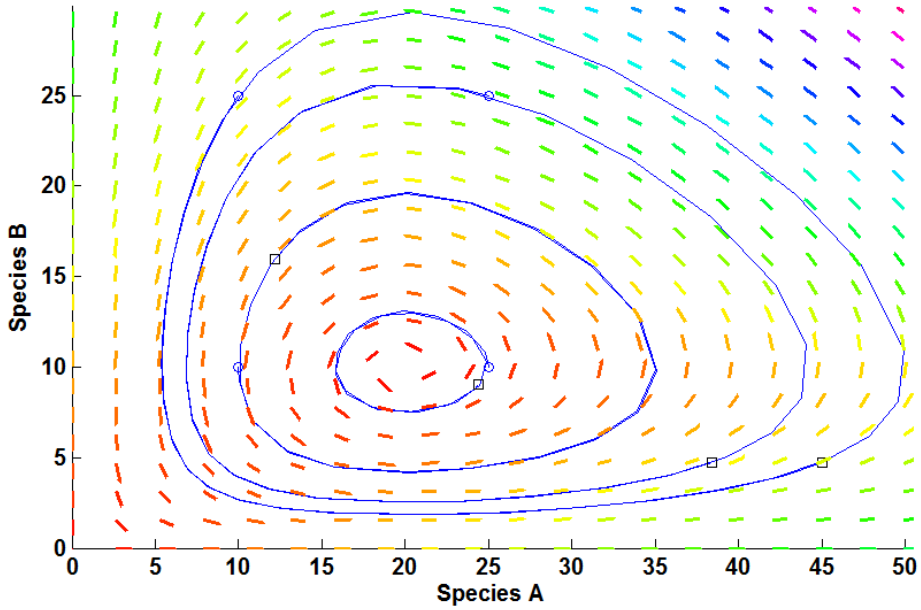

Figure 4-7 - Two Dimensional Lotka-Volterra Phase Portrait

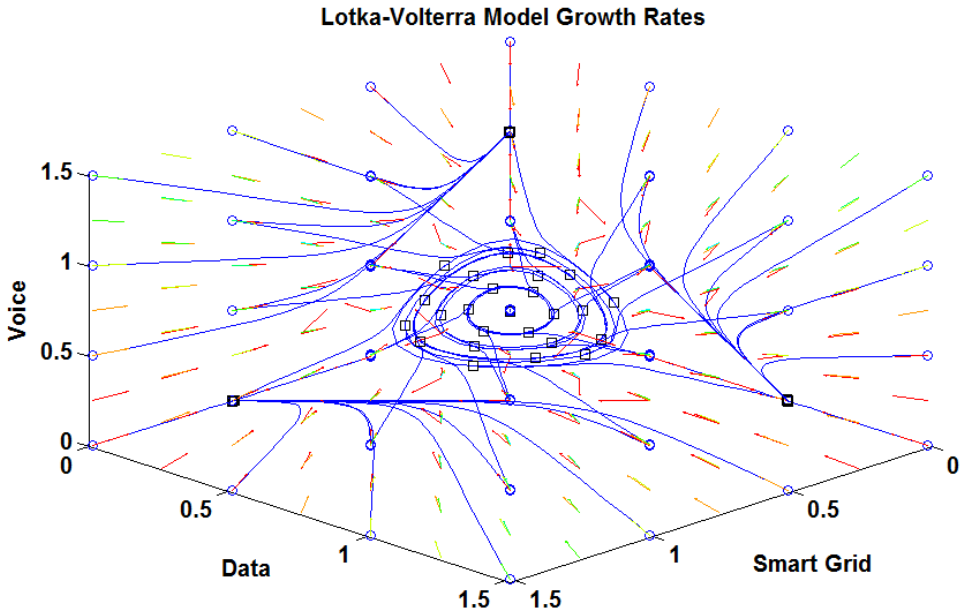

Figure 4-8 - Three Dimensional Lotka-Volterra Phase Portrait

In a physical system, a limit cycle represents periodic sharing of resources. This is good for a telecommunications environment where differing classes of traffic compete for access to the wireless channel.

4.3.3 Derivation of the Lotka-Volterra Hamiltonian Function

By applying Smales' Construction and reducing the system onto the simplex Σ, we reduce the complexity and can derive the Hamiltonian Function of the Lotka Volterra 3 species equation. The Hamiltonian Function, H, essentially represents the total power, or total bandwidth in this case, of the system. This allows straight forward calculations to growth rates, populations now and in the future.

A Hamiltonian system is a system of the form:

$$\frac{dx}{dt} = \frac{\partial H}{\partial y}(x, y) \tag{4-4}$$

$$\frac{dy}{dt} = -\frac{\partial H}{\partial x}(x, y) \tag{4-5}$$

Where $H : \mathbb{R}^2 \rightarrow \mathbb{R}$ is a smooth function. The above equations tell us how to draw the solution curves in the phase plane without solving the system. The derivation of

the Lotka-Volterra Hamiltonian Function is found below. Firstly, consider a three species competitive Lotka-Volterra model:

$$\dot{x} = x(1 - x - \alpha y - \beta z) \tag{4-6}$$

$$\dot{y} = y(1 - \beta x - y - \alpha z) \tag{4-7}$$

$$\dot{z} = z(1 - \alpha x - \beta y - z) \tag{4-8}$$

Where $\alpha + \beta = 2$. Let

$$V(x, y, z) = xyz \tag{4-9}$$

Then

$$\begin{aligned} \frac{dV}{dt} &= xyz\left(\frac{\dot{x}}{x} + \frac{\dot{y}}{y} + \frac{\dot{z}}{z}\right) \\ &= V[(1 - x - \alpha y - \beta z) + (1 - \beta x - y - \alpha z) \\ &\qquad + (1 - \alpha x - \beta y - z)] \\ &= V[3 - (x + y + z) - (\alpha + \beta)(x + y + z)] \\ &= 3V[1 - (x + y + z)] \end{aligned} \tag{4-10}$$

Moreover,

$$\begin{aligned} \frac{d}{dt}(x + y + z) \\ &= (x + y + z) - x^2 - y^2 - z^2 \\ &\quad - (\alpha + \beta)(xy + xz + yz) \\ &= (x + y + z)[1 - (xy + xz + yz)] \end{aligned} \tag{4-11}$$

Therefore, if $(x_0, y_0, z_0) \in \mathbb{R}^3 \setminus (0,0,0)$ we have $x(t) + y(t) + z(t) \to 1$ as $t \to \infty$. That is all orbits eventually end up on the simplex Δ_1 which is also the carrying simplex Σ in this case. On Δ_1 we have

$$\frac{dV}{dt} = 3V[1 - (x + y + z)] = 0 \tag{4-12}$$

That is, $V = constant$ on Δ_1.

Dynamics on the carrying simplex Σ

We may eliminate z since $z = 1 - x - y$ on the carrying simplex Σ. This gives

$$\begin{aligned}\dot{x} &= x\big(1 - x - \alpha y - \beta(1 - x - y)\big) \\ &= \frac{(\alpha - \beta)}{2} x(1 - x - 2y) \end{aligned} \tag{4-13}$$

$$\begin{aligned}\dot{y} &= y\big(1 - \beta x - y - \alpha(1 - x - y)\big) \\ &= \frac{-(\alpha - \beta)}{2} y(1 - 2x - y) \end{aligned} \tag{4-14}$$

Where $\alpha + \beta = 2$. Notice that $div(\dot{x}, \dot{y}) = 0$ and that we have a canonical Hamiltonian system with Hamiltonian function:

$$H(x, y) = \frac{(\alpha - \beta)}{2}(1 - x - y)xy \tag{4-15}$$

On the open triangle $T = \{(x, y) \in \mathbb{R}^2_{\geq 0} \ : \ 0 < x + y < 1\}$ we get closed contours, that is, the solutions are periodic. This is the projection of the dynamics on Σ onto the xy plane.

The importance of knowing that a given system is Hamiltonian is the fact that we can essentially draw the phase portrait without solving the system. Assuming that H is not constant on any open set, we simply plot the level curves $H(x, y) = constant$. The solutions of the system lie on these level sets; all we need to do is figure out the directions of the solution curves on these level sets. But this is easy since we have the vector field. Note also that the equilibrium points for a Hamiltonian System occurs at the critical points of H, that is, at points where both partial derivatives of H vanish.

Now we can solve the population dynamics of the telecommunications environment using the Lotka-Volterra Equations. By applying Smales' Construction, we can then solve for the Lotka-Volterra Hamiltonian Function. This reduces the complexity of the solution and allows easy allocation of resources. However, this only solves for (x, y) on the plane Σ. To extract the solution for z it is as simple as applying the planar equation of Σ onto the solution (x, y).

4.4 LOTKA-VOLTERRA RESOURCE ALLOCATION SCHEME

In this work we model the wireless telecommunications environment as a Lotka-Volterra system, with each '*species*' defined by the Lotka-Volterra equations a telecommunications class in the wireless environment. That is, the species used are classified as Data (representing TCP/IP connections such as downloads, webpages, peer-to-peer etc, and UDP such as videos and skype etc); Voice & Smart Grid.

Therefore, using the generalized Lotka-Volterra equation, we define the system as:

$$\dot{x}_i = x_i\left(r_i - \sum_{j=1}^{n} a_{ij}x_j\right) = F_i(x), \;\; i = 1, \dots, n \tag{4-16}$$

- x_i: population of species i
- r_i: growth rate of species i
- a_{ij}: Interaction Matrix: how species i and j interact with each other.

By choosing a special condition, S1:

$$a_{ij} > 0 \;\; \forall \;\; 1 \leq i, j \leq n \tag{4-17}$$

we have defined the system as purely competitive where each species competes with all others and itself for the environments resources, which in the telecommunications environment is available subcarriers. It should be noted that the Lotka-Volterra Differential Equations are used to model downlink packets on the eNB side with analysis of the Lotka-Volterra model used to allocate the resources. Analysis is provided by first applying Smales' Construction to reduce the dimensionality of the problem. Then the Poincaré-Bendixson Theorem is used to find any limit cycles that can produce non-convergent resource allocation, i.e. allocation is shared between all classes. Then finally, the Hamiltonian Function is used to describe the limit cycle which provides reduced complexity in calculating bandwidth required by each class.

As shown in Section 4.3.1, the long term outcome of a number of species competing with each other in a finite habitat does not converge to a steady state or a periodic orbit [5]. However, the system has long term dynamics that lie on a simplex and obey

$\dot{x} = H(x, y)$, where H is any smooth vector field of our choice. Moreover, the dynamics on the simplex is canonically Hamiltonian and for $n \geq 3$, the orbits are all periodic [27]. Consequently, we can reflect growth and death rates, resource requirements, effect of one class on another and itself, and total population in the Lotka-Volterra equations. In doing so [5,27], we can solve the long term dynamics of the telecommunications environment, and optimise the allocation of subcarriers based on QoS requirements.

4.4.1 Simulation Parameters

The parameters of the simulation are shown in Table 4-1, of which the subcarriers and rate requirements become the finite resources and data for the interaction matrix respectively. The interaction matrix also takes on values from the queue at the eNodeB as a growth rate measure, incorporating any periodic traffic similarly.

Table 4-1 - Simulation Parameters

Parameter	Setting
Carrier Frequency	1800MHz
Bandwidth	10MHz
Modulation (n={4,16,64})	n-QAM
Subcarriers per RB (N_{SC}^{RB})	12
OFDM Symbols per RB ($N_{Symb}^{DL/UL}$)	7
RB Bandwidth	180kHz
Number of RBs (N_{RB})	50
Number of Active Users	200
Data Packet Size for Smart Grid UE	100 Bytes
Data Packet Size for Data	500 Bytes
Data Packet Size for Voice	128 Bytes

The system begins with sequential subcarrier allocation for First-In-First-Out (FIFO) queue in a waterfilling procedure. Once the subcarrier allocations have exhausted, the system will allocate subcarriers based on QoS requirements and Channel State

Information (CSI). Smart Grid UEs were biased to assume their optimal subcarriers for two reasons:

- Due to the critical nature of the Smart Grid, its data must be prioritized.
- Most Smart Grid packets are sent on set intervals allowing the system to pre-allocate subcarriers, and release them quickly thereafter.

This results in the subcarriers with the most power allocated being shared by multiple UEs over a set time interval thereby increasing network throughput.

4.4.2 Scheduler

The Resource Allocation has already been defined above, however, due to use of queue theory a Scheduler must also be defined. As shown in Figure 4-9 the scheduler first breaks the queue into three different class queues. Based on the class queue sizes and on upcoming requests, the system allocates resources accordingly.

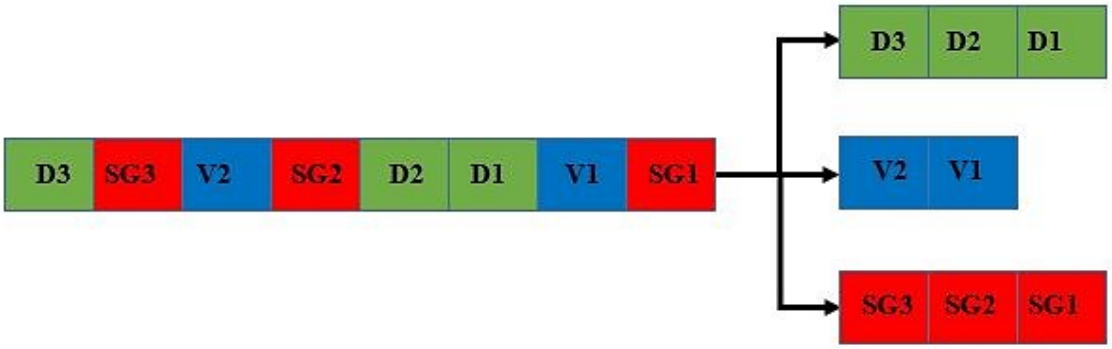

Figure 4-9 – Incoming Packets Organized by Lotka-Volterra Scheduler

In most Resource Allocation Schemes, the allocation of subcarriers occurs for the first N users in the queue, where N is the number of subcarriers that the system supports. This doesn't take into account the periodicity of some traffic or the bursty nature of some classes of communication that can easily be calculated by queue examination. The Lotka-Volterra Resource Allocation and Scheduler is able to account for these characteristics and allocate resources accordingly. Furthermore, communications traffic, whilst exhibiting many characteristics of chaos, by using the Lotka-Volterra

equations, utilizing Smales' Construction and the Poincaré-Bendixson theorem can be successfully modelled and predicted. By doing so, the traffic can be mapped to subcarriers based on QoS requirements and fairness between UEs and classes in a wireless communications environment.

4.5 SUMMARY

This research studies the effect of competition between different services on the shared communication resources they require. By altering the coefficients of the Lotka-Volterra equations based on the initial conditions present in a cell, we can allow the services to follow a periodic population change to ensure the satisfactory access to the communication resources by each user equipment device. The altering of the coefficients can also ensure, in a time of need, that a dominant population can occur. For example, due to the periodic and bursty nature of Smart Grid traffic coupled with the reactionary model of the Smart Grid used, outside of normal grid conditions many Phasor Measurement Units will be requiring to send data. This means that the PMUs will require a larger proportion of Bandwidth than other service classes operating within the wireless cell. The change in coefficients of the Lotka-Volterra equations will change the population dynamics of each service to ensure Smart Grid UEs can communicate. Careful choice of such coefficients will allow the continuation of other services albeit with lower subcarriers allocated.

The model proposed by this research is a Lotka-Volterra inspired Scheduler with flow through effects on Resource Allocation. The Lotka-Volterra limit cycle produced by current and future periodic traffic is used to map subsets of the total transmission power of the eNB to the wireless classes. Using the power allocated as bidding chips, each class can bid for subcarriers. The bidding process is controlled by the growth rate of the classes, where the class with the highest growth rate is given first choice in each bidding algorithm iteration. Once all the subcarriers have been bet on and allocated to a single class, the classes must then decide how to allocate them to individual UEs.

The UE subcarrier allocation is organized to achieve maximum average throughput for each UE. Initially, the average throughput between each classes' UE and allocated

subcarriers is calculated. The UE with the lowest SNR is then allocated the subcarrier (out of the set of non-allocated subcarriers) that afforded it the highest average throughput. This process continues until the UE with the highest SNR is allocated the last available subcarrier.

The next three chapters will provide performance analysis on the three major categories in Table 2.2: Reliability, Latency (delay), & Throughput. These three performance metrics, if satisfied, conclusively measure a Radio Resource Management and Schedulers' compatibility with Smart Grid applications.

In the next Chapter, an in depth analysis of the link reliability of the proposed channel model will be provided. The reliability results will highlight the need for such a communications network as LTE due to requirements imposed on Smart Grid applications by Table 2.1 & Table 2.2.

Chapter 5.
Link Reliability Analysis & Results

Link reliability is an important measure of a channels' ability to send information over it with low errors. Errors in a wireless communications channel can be caused by noise, signal attenuation or interference. All three can diminish signal quality and produce higher bit error rates at the receiver.

The latency or throughput of a network are directly related to the received signal quality and measured bit error rates. If the bit error rate is high, re-transmission or significant redundant bits is required to ensure reliable transmission of data. This causes latency and throughput to diminish due to:

- Transmission requiring redundant bits not part of original information
- Re-transmission of frame

The eNB can utilize bit error rates and Signal Strengths to determine the modulation and coding techniques required to ensure high link reliability thus providing higher QoS. Therefore, reliability is an important metric that helps measure the viability of a communications link to support applications and services. In this Chapter, this thesis will investigate the link reliability results achieved by the use of a LTE eNB and Rayleigh fading channel model proposed in Chapter 3. The performance of the model will be based on Smart Grid reliability requirements in Table 2-2 and Table 2-3 as defined as the United States of America Department of Energy.

Initially, this chapter will introduce the factors that can affect link performance and the tools utilized to correct channel errors. This includes the use of turbo codes and phase, time, and frequency offset corrections. Finally, the packet success rates for each class of UE: Smart Grid, Data, & Voice, will be presented and analysed.

5.1 ASSUMPTIONS

It is an assumption of this research that the receiver has the capability to decode the three types of modulation schemes used, i.e. QPSK, 16QAM, and 64QAM. It is also assumed that the receiver is able to selectively choose the modulation technique based on the channel conditions of the UE.

The sender and receiver must have adaptive coding rates that allow for coding and de-coding of either $1/3$ or $2/3$ turbo-coded OFDM symbols. The packet length for Smart Grid, Voice & Data remains constant, however, due to their difference can be used to measure channel quality over increasing packet lengths.

Any acknowledgments send utilizing Hybrid Automatic Repeat reQuests (H-ARQ) are assumed to be received with no error.

5.2 FACTORS AFFECTING LINK PERFORMANCE

In the proposed channel and traffic model, random Gaussian noise is added to transmitted signals. The signals are also subject to attenuation, shadowing and fading. When the additive noise and signal effects distort the signal significantly, the receiver is unable to determine the original bits. This can cause a symbol or bit error. The number of transmitted errors in a packet can increase the latency and decrease the throughput of the communications link. If the number of errors is such that the received packet is irreconcilable by error detection and correction methods then a packet retransmission is required. Packet retransmission produces very high latencies due to extra propagation delays and could be subject to the same high bit error rates

as the first packet. Re-transmission also causes further congestion of data on the network which can affect other UEs operating on the same network.

The bit error rate (BER) is a good measure of signal quality. The bit error rate is affected by the precision of the transmitting device, the channel conditions in which the data is communicated, and the precision of the receiver device. It is therefore imperative that data is transmitted with the lowest attainable bit error rate.

5.2.1 Bit Error Rate

The Bit Error Rate is a quantity that measure the number of bit errors received divided by the total number of bits transmitted. Quadrature Amplitude Multiplexing provides high data rates and spectral efficiencies and it was for this reason it is the chosen form of modulation in this research. The analysis part of this thesis analyses the throughput, latency & fairness between three QAM modulation schemes, QPSK (or 4-QAM), 16-QAM & 64-QAM. The symbols in the QAM constellation are gray-coded. This helps to ensure that symbol errors only result in single bit errors. The analytical formula for average bit error rate tor an M-ary QAM signal in a Rayleigh fading channel is:

$$P_b = \frac{M-1}{Mk}\left(1 - \sqrt{\frac{3\frac{E_b}{N_0}\left(\frac{k}{M^2-1}\right)}{3\frac{E_b}{N_0}\frac{k}{(M^2-1)}+1}}\right) \tag{5-1}$$

Where

$$k = \log_2 M \tag{5-2}$$

represents the number of bits per M-QAM symbol. The theoretical results for the un-coded Bit-Error Rate using of QPSK ($M = 4$), 16QAM ($M = 16$) and 64QAM ($M = 64$) Modulation in a Rayleigh Fading Channel are shown in Figure 5-1 & Figure 5-2 against the energy per bit noise power spectral density ratio (E_B/N_0) and SNR respectively.

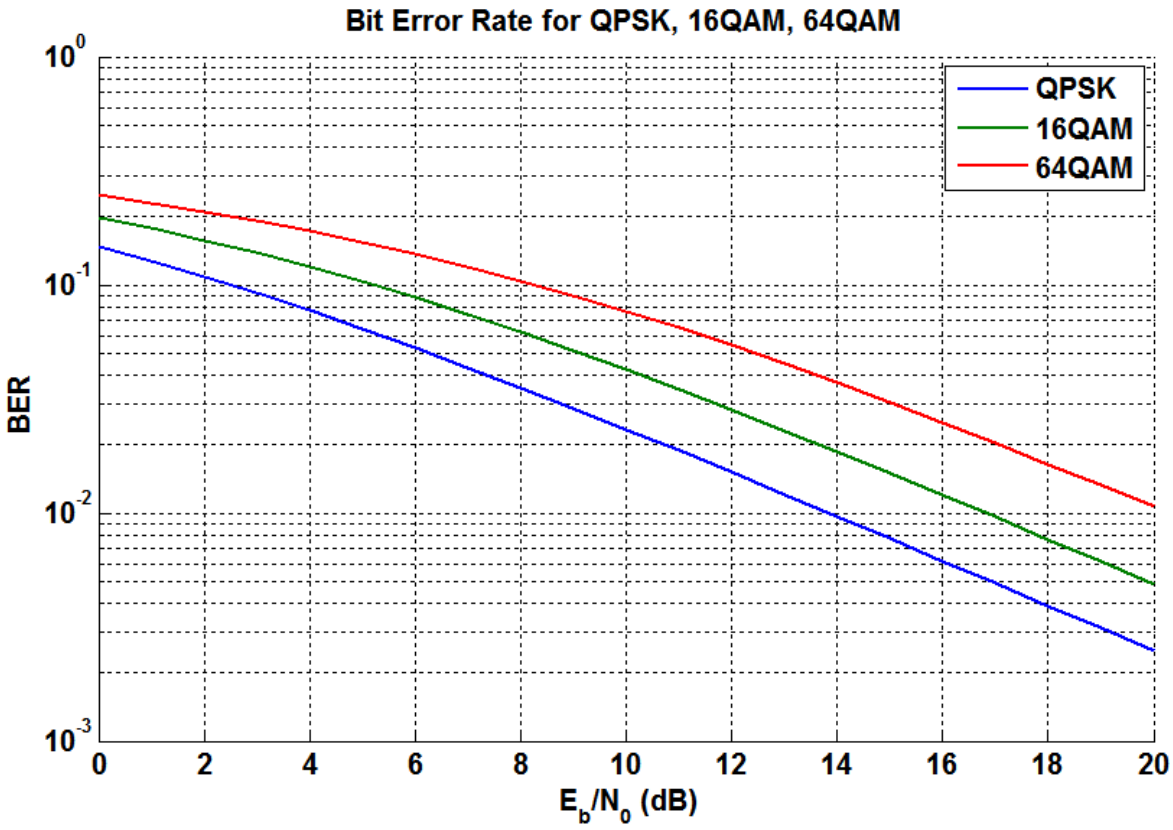

Figure 5-1 - Theoretical Bit Error Rates Against SNR per Bit (Eb/N0) (QPSK,16QAM,64QAM)

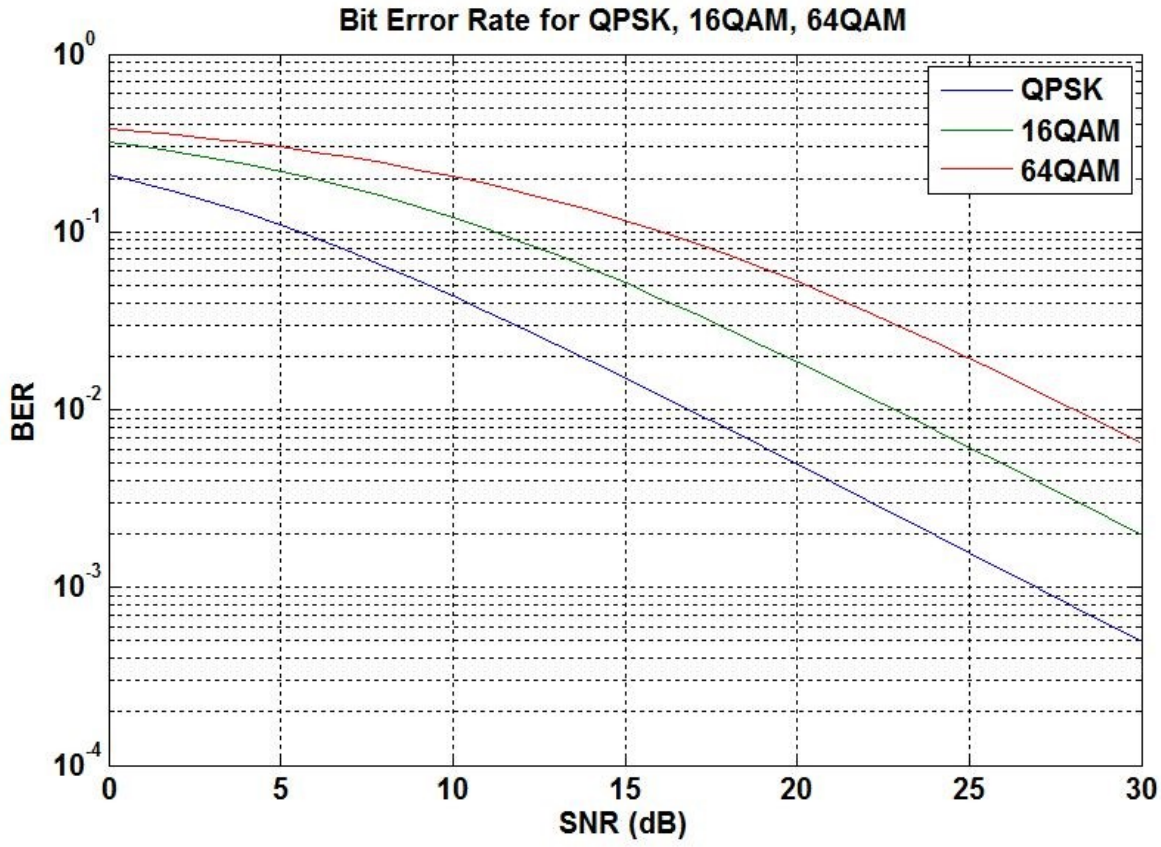

Figure 5-2 - Theoretical Bit Error Rates Against SNR (QPSK,16QAM,64QAM)

5.2.2 Packet Error Probability

The Packet Error Probability is a measure of how many packets are successfully delivered without any errors. Figure 5-3 shows the theoretical Packet Error Probability with differentiation between class type and modulation used. The theoretical differences between the classes is due to the packet length involved. The Smart Grid has the smallest packet (100 bytes) so therefore is subject to a lower BER, thus lowering the Packet Error Probability. The Data Class, with the largest packet length of 500 bytes corresponds to the higher Packet Error Probabilities as shown in Figure 5-3.

The formula for the Packet Error Rate (PER) is:

$$PER = 1 - (1 - BER)^L \quad (5\text{-}3)$$

Where L is the length of the packet. The Packet Error Probability is the expectation value of the Packet Error Rate (PER) which is the number of incorrectly transmitted data packets.

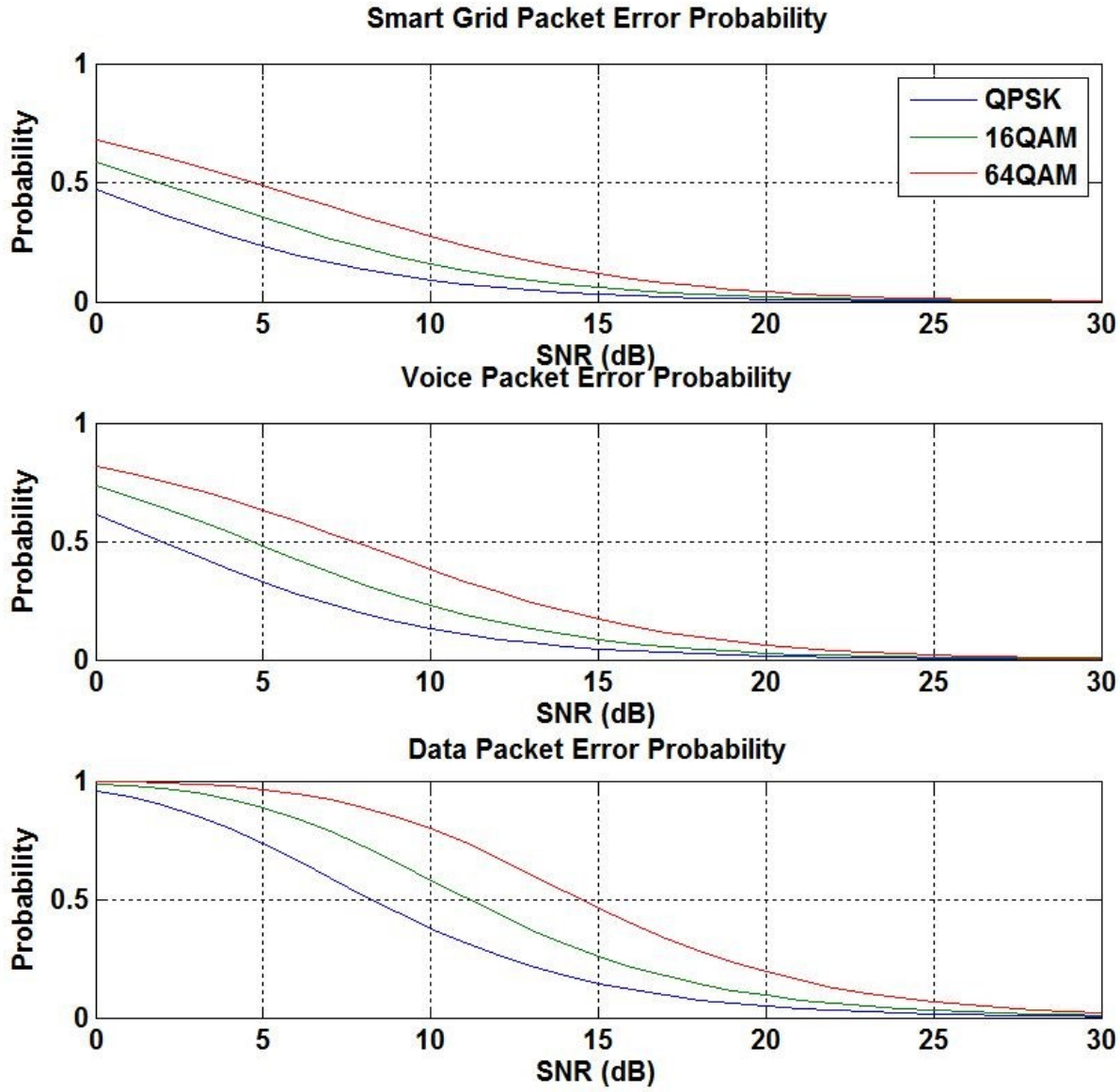

Figure 5-3 - Class Differentiated Theoretical Packet Error Probability (QPSK,16QAM,64QAM)

So far, this thesis has presented the theoretical BER, and Packet Error Probability for QPSK, 16QAM and 64QAM modulated bit streams over a Rayleigh channel. From this point on this thesis will present our experimental results using the modelled channel in Section 3.3.2 in conjunction with the proposed Lotka-Volterra Resource Allocation & Scheduler.

5.2.3 Time Offset Correction

During transmission over a wireless link, data is subjected to many forms of interference that can distort the received signal. In this research, timing and phase error correction were required to correctly extract the transmitted data after noise was added.

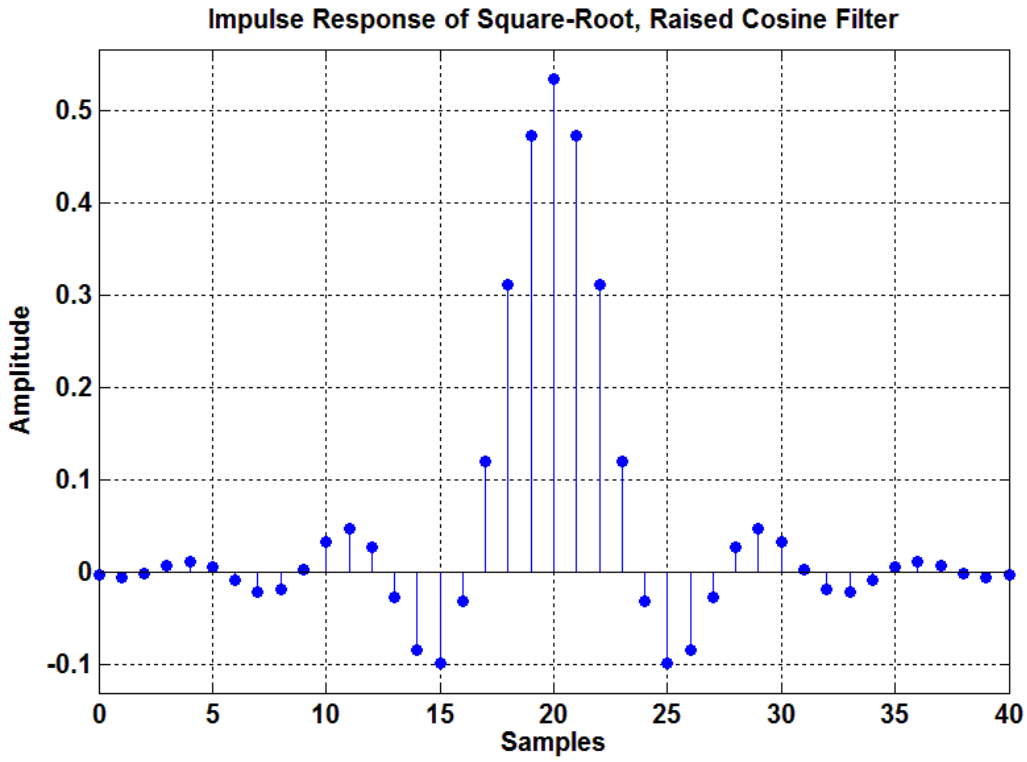

Figure 5-4 - Square Root Raised Cosine Filter Response

Conceptually, symbol timing synchronization is the process of estimating a clock signal that is aligned in both phase and frequency with the clock used to generate the data at the transmitter [89]. It is not efficient to allocate spectrum to transmit the clock signal therefore the clock signal must be extracted from the noised received waveforms that carry the data. Timing Error Detectors are used to detect the difference in phase between the data clock embedded in the matched filter output (see Figure 5-4) and a Voltage Controlled Clock at the receiver side. The timing error is then filtered and used to adjust the phase of the VCC output to align the clock edges with the symbol boundaries. This is then applied to the received filter symbol and forwarded to the de-modulator for symbol to bit de-modulation. The filtered symbols are much closer to

the real modulated symbols than their unfiltered counterparts. This is due to the removal of the time offset, which ensures optimal sampling times are used in the receiver. This corresponds to the sampling of data at times where a transition between symbols is not occurring. When sampling during transitional times (which is the case when Timing Error Detection and Correction is not used) the spread of symbols is much larger and thus will cause much higher bit error rates in the receiver.

5.2.4 Phase and Frequency Offset Correction

OFDM systems are more sensitive to frequency errors than single carrier modulation systems. Inter-Carrier Interference (ICI) is experienced in OFDM systems when an un-corrected frequency offset destroys the subcarrier orthogonality. Therefore, it is very important to detect and correct any frequency offsets that may occur in the OFDM system.

Frequency offsets in a received signal can occur from a multitude of differing factors in a wireless communications network. Most notable are Doppler shifts and frequency discrepancies between the transmitter and receiver oscillator frequencies. Doppler shifts occur when there is relative motion between the transmitter and receiver [89]. In this case, the Doppler shift is measured by:

$$\Delta f = \frac{v}{c} f_c \tag{5-4}$$

where v is the relative velocity, c is the speed of light, and f_c is the carrier frequency. In terms of carrier phase and frequency errors, the Doppler shift observed in wireless OFDM symbols is minimal. A carrier phase error causes a rotation in the signal space causes a rotation in the signal space projections [89]. If the rotation is large enough, it can cause each symbol to lie in the wrong position with no visible sign on error. Therefore, large symbol error rates can still be observed even when symbol timing is synchronized. Carrier phase offset is corrected by synchronization of transmitter and receiver oscillators in both phase and frequency. This is achieved by using a Phase-Locked-Loop (PLL). The PLL detects differences between the Unlike the Timing Error Detector in Section 5.2.3 which provides symbol timing synchronization by aligning

transmitter and receiver data clocks, this PLL achieves synchronization between transmitter and receiver oscillators.

The Phase-Locked-Loop consists of three major components: a multiplier, a loop filter and a voltage controlled oscillator (VCO) and their arrangement is shown in Figure 5-5:

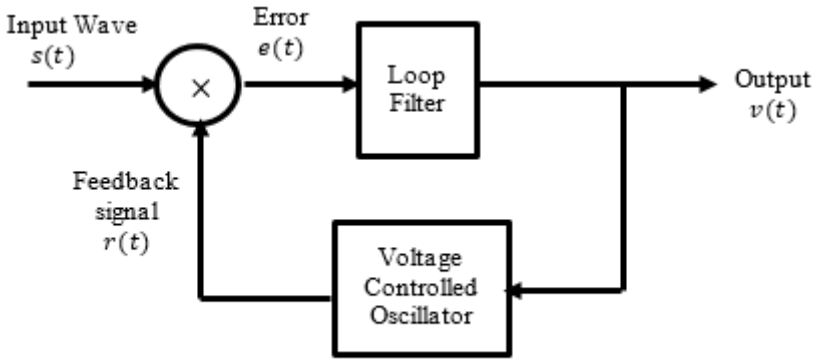

Figure 5-5 - Phase-Locked-Loop Diagram

The objective of the PLL is to generate a VCO output, $r(t)$, that has the same phase angle as the input signal $s(t)$ [84]. Supposing the input signal is a sinusoid carrier wave of the form:

$$s(t) = A_c sin[2\pi f_c t + \phi_1(t)] \tag{5-5}$$

where A_c is the amplitude of carrier wave, f_c is the frequency of the carrier wave and ϕ_1 is the phase offset of the carrier wave. When modulated by a signal $m(t)$ the phase offset is related to $m(t)$ by:

$$\phi_1(t) = 2\pi k_f \int_0^t m(\tau)\, d\tau \tag{5-6}$$

where k_f is the frequency sensitivity of the frequency modulator. The feedback signal is defined as:

$$r(t) = A_v cos[2\pi f_c t + \phi_2(t)] \tag{5-7}$$

Similarly to the carrier wave, A_v is the amplitude of output wave. With a voltage applied to the VCO input, the phase offset ϕ_2 is related to $v(t)$ by the integral:

$$\phi_2(t) = 2\pi k_v \int_0^t v(\tau)\, d\tau \tag{5-8}$$

where k_v is the frequency sensitivity (Hz/V) of the VCO. The PLL feedback loop will adjust the control voltage $v(t)$ to produce a phase estimate that drives the phase error to zero. This eradicates the frequency and phase offsets apparent in the system and allows de-modulation of the symbols to occur with a lower bit error rate. However, some errors will still be transmitted and not detected by the receiver which must be detected and then corrected. This is done by using Forward Error Correction based on convolutional coding methods.

5.3 CODED OFDM

Subcarriers are subjected to fading as described in Section 3.3.2 and sometimes the signal SNR is degraded below the required SNR level to decode the OFDM symbols. The system can either reduce the required SNR level by altering the SNR gap as denoted by Γ. In broad terms, Γ is the ratio of ideal SNR at which the system can transmit at C (channel capacity) bits/transmission to a practical SNR at which the system can transmit R bits/transmission. Altering Γ has an effect on the number of bits that can be allocated to subcarriers and thus reducing total system data rate [83]:

$$b[n] = \log_2\left(1 + \frac{SNR_n}{\Gamma}\right) \tag{5-9}$$

where:

- $b[n]$ is the number of bits subcarrier n can be allocated
- SNR_n is the received SNR for subcarrier k

5.3.1 Forward Error Correction

Forward Error Correction (FEC), sometimes known as channel coding or Error Correction Control (ECC), provides resilience to errors by way of algebraic methods. Forward Error Correction works by introducing redundancy at the transmitter thereby allowing the receiver to recover the input signal even if badly affected by interference, attenuation, noise and fading [9]. This allows the system to maintain a higher bit rate by keeping the required SNR higher.

FEC codes can be categorized by their coding rate $r \leq 1$, where r is the inverse of the redundancy added. For example, a code that provides a rate of $r = 1/3$ has introduced two redundant bits for each original information bit. In doing so it is operating at three times the original rate. Well designed FEC codes can actually increase the data rate even when $r < 1$. This is due to the reliability increase provided by such codes decreases the bit error rate at a factor greater than $1/r$, producing an overall net gain. This research is limited to the use of Turbo codes due to their close fit with the Shannon-Hartley theoretical limit on channel capacity [84], however, there are many other popular Forward Error Correction Codes.

5.3.1.1 Turbo Codes

A Turbo Code Encoder is composed of two systematic encoders joined together by use of an interleaver. A Turbo Code with rate $1/3$ is employed in Figure 5-6, which is deployed by LTE for use in shared uplink and downlink channels. The interleaver is used between two systematic convolutional encoders to provide temporal variance between the encoder outputs. The decoders, located at the receiver, pass their soft outputs (conditional probabilities) back and forth via a de-interleaver that correlates these values [9]. The Turbo Decoder proceeds to iterate back and forth between each convolutional decoder until the symbol estimates converge. That is, until the interleaver is no longer able to de-correlate the soft outputs.

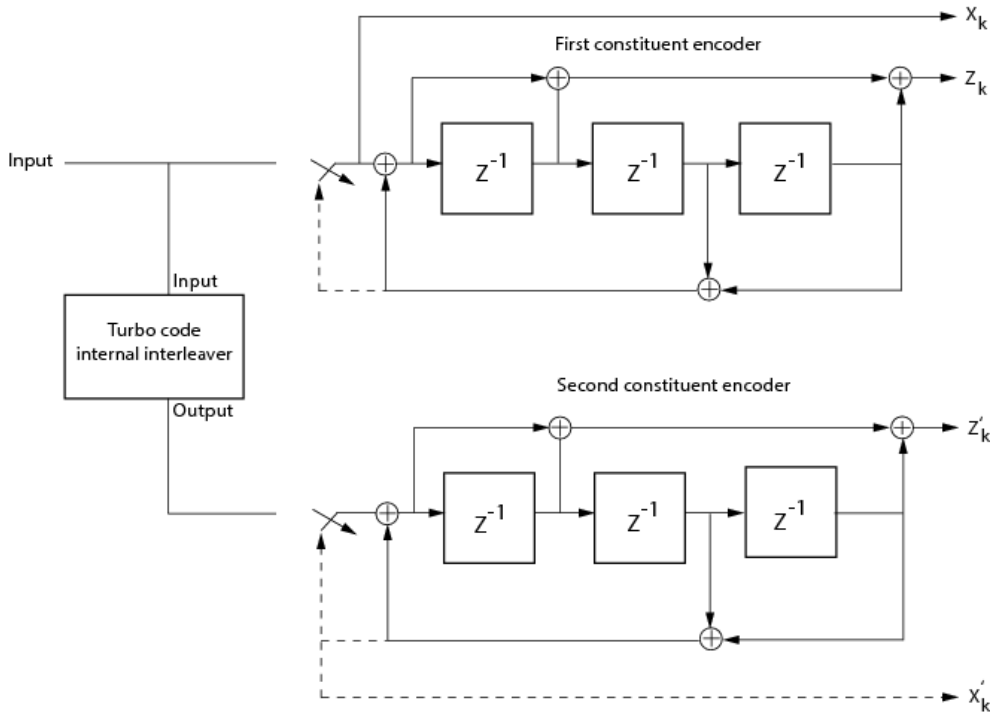

Figure 5-6 - 1/3 Rate Parallel Concatenated Turbo Encoder

To attain high levels of performance, the size of the interleaver, which equates to the block length of the Turbo Code, must be high. However, this produces long interleaving and de-interleaving delays in the encoder and decoder respectively. This is due to the serial nature of the coding, where interleaving and de-interleaving can only be performed on an entire block that has been fully populated with coded bits. This puts a constraint on the size of the coded block length used, and for simplicity, is chosen as the size of the packet.

The Turbo Coded bit error rate performance for the Rayleigh Fading channel defined in Section 3.3.2 is graphed in Figure 5-7 & Figure 5-8 against the energy per bit noise power spectral density ratio (E_B/N_0) and SNR respectively. When compared with the results in Section 5.2.1, the Turbo-Coded Bit Error Rate performs much better than the non-Turbo Coded theoretical results displayed Figure 5-1 & Figure 5-2, as expected.

When Figure 5-1 is compared with Figure 5-7, the performance for the turbo coded transmission differs significantly. At lower values of E_b/N_0 the un-coded transmission performs better with lower bit errors occurring. However, the bit error rate for turbo-

coded transmissions decrease rapidly when reaching a threshold value of E_b/N_0, which can be seen in the steep slopes of the graphs in Figure 5-7.

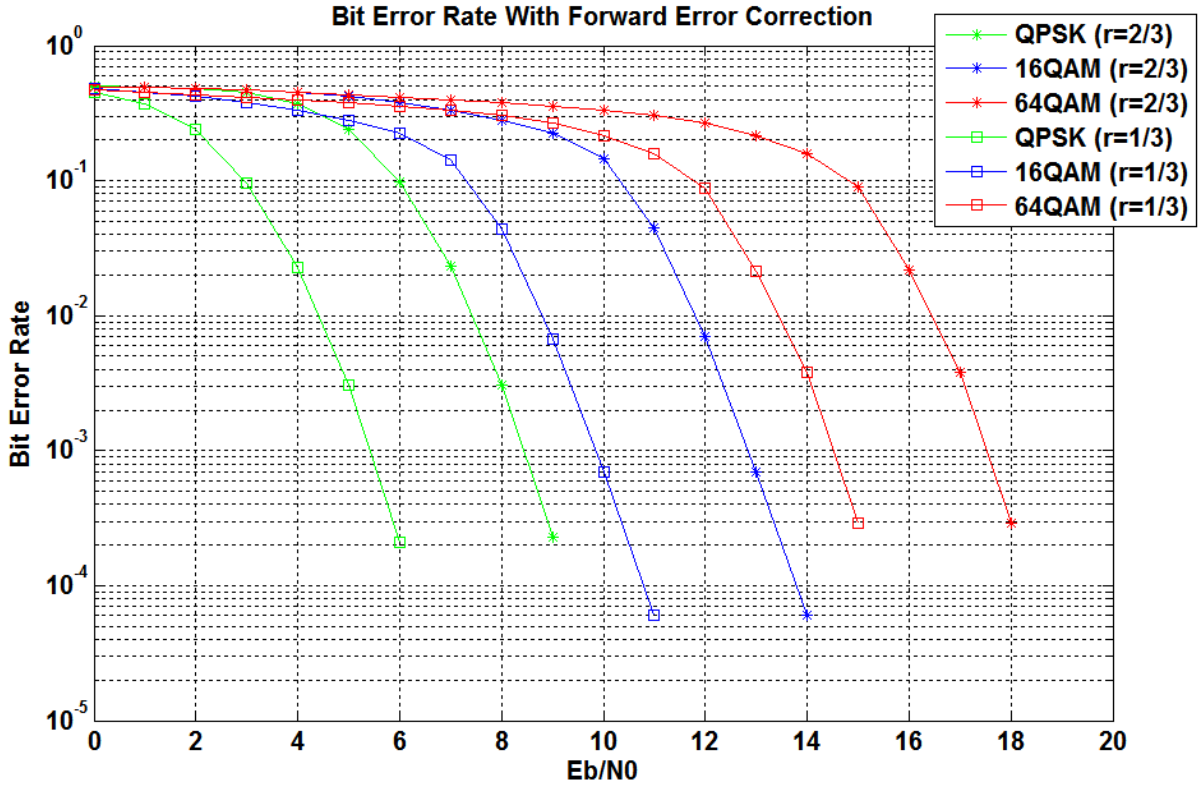

Figure 5-7 - Bit Error Rate With Forward Error Correction Against SNR Per Bit (Eb/N0)

Comparison between Figure 5-2 & Figure 5-8 yields the same results as those in the previous comparison however this time measured against SNR. The thresholds for high performance Turbo-Coding producing low bit error rates are easily noted in Figure 5-8. For QPSK, this threshold is approximately -2dB, 16QAM the threshold is approximately 5dB and for 64QAM the threshold is approximately 12dB. For SNR above these threshold values the system produces significant gains in performance due to Turbo Coding.

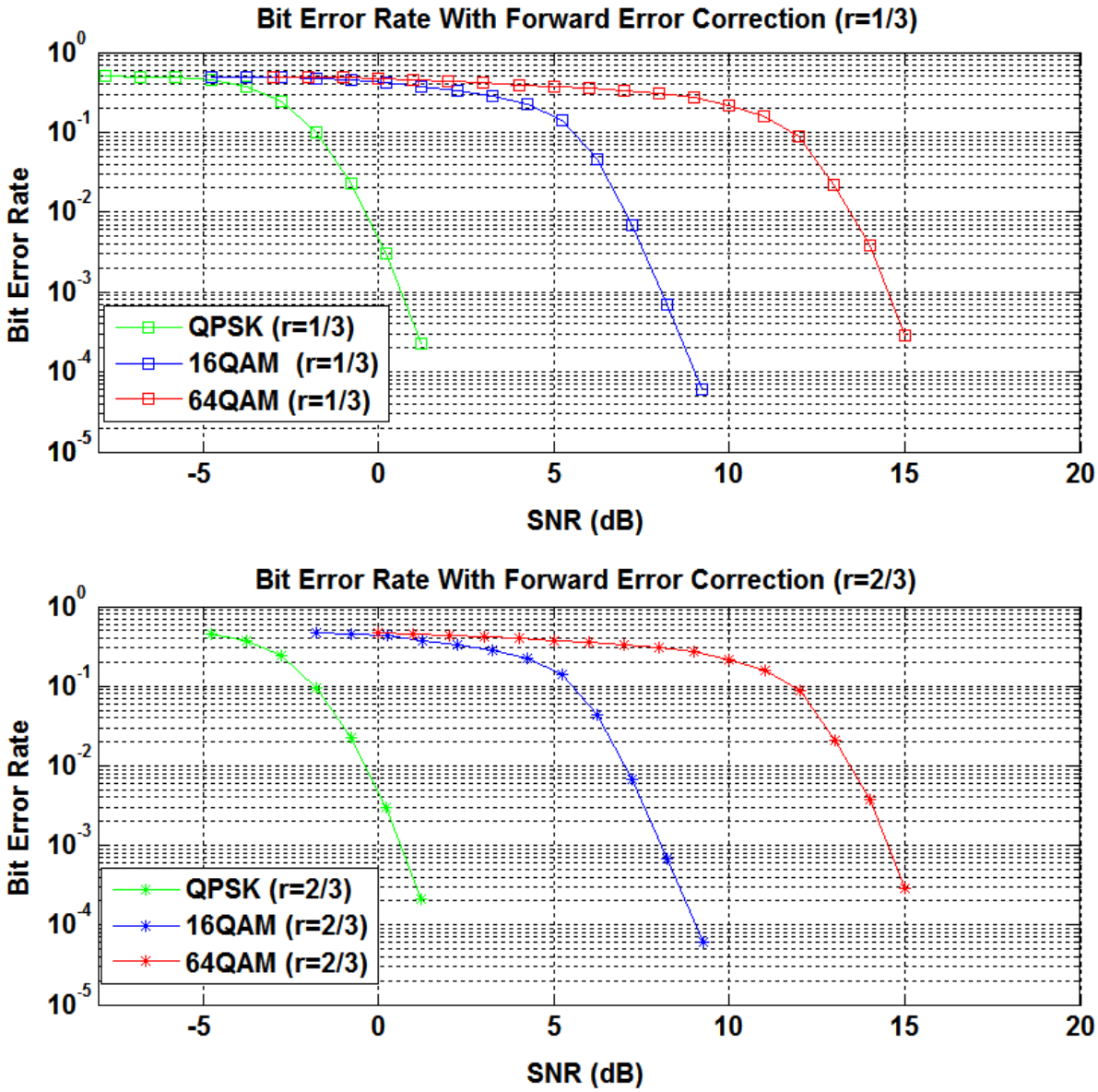

Figure 5-8 - Bit Error Rate With Forward Error Correction Against SNR

The packet success rate is determined by how many packets required retransmission due to bit errors and is calculated directly from the BER. When a bit error or many bit errors occur, sometimes the Forward Error Correction module is incapable of correcting the error. This is particularly true for larger number of bit errors in bursty transmissions. The packet success probability (P_s) is calculated using the formula:

$$P_s = \sum_{n=0}^{t} \binom{L}{n} P_e^n (1 - P_e)^{L-n} \qquad (5\text{-}10)$$

Where t is a chosen number of encoded bit errors, P_e is the bit error rate and L is the length of the packet in bits. From this equation, it is easy to note that the probability of a successful packet transmission will decrease with an increasing packet length. Therefore, we expect the data class with a packet length of 500 bytes to incur the lowest successful packet transmission. This requires the Lotka-Volterra Resource Allocation Scheme to allocate more subcarriers, or higher performance subcarriers to the data class to ensure successful, error-free transmission of packets.

The packet success rate for the three data classes: Smart Grid, Voice, & Data along with the three differing modulations: QPSK, 16QAM, & 64QAM are shown in Figure 5-9, Figure 5-10, & Figure 5-11. There is also differentiation between the two coding rates analysed in this research, specifically, $1/3$ and $2/3$. Each figure corresponds to four graphs, each of which has a differing number of error bits, $t = \{0, 20, 50, 100\}$. As expected, the Turbo-Coded data is best decoded when no encoded bit errors are present, however, it is still subject to Rayleigh Channel conditions creating non-uniform results.

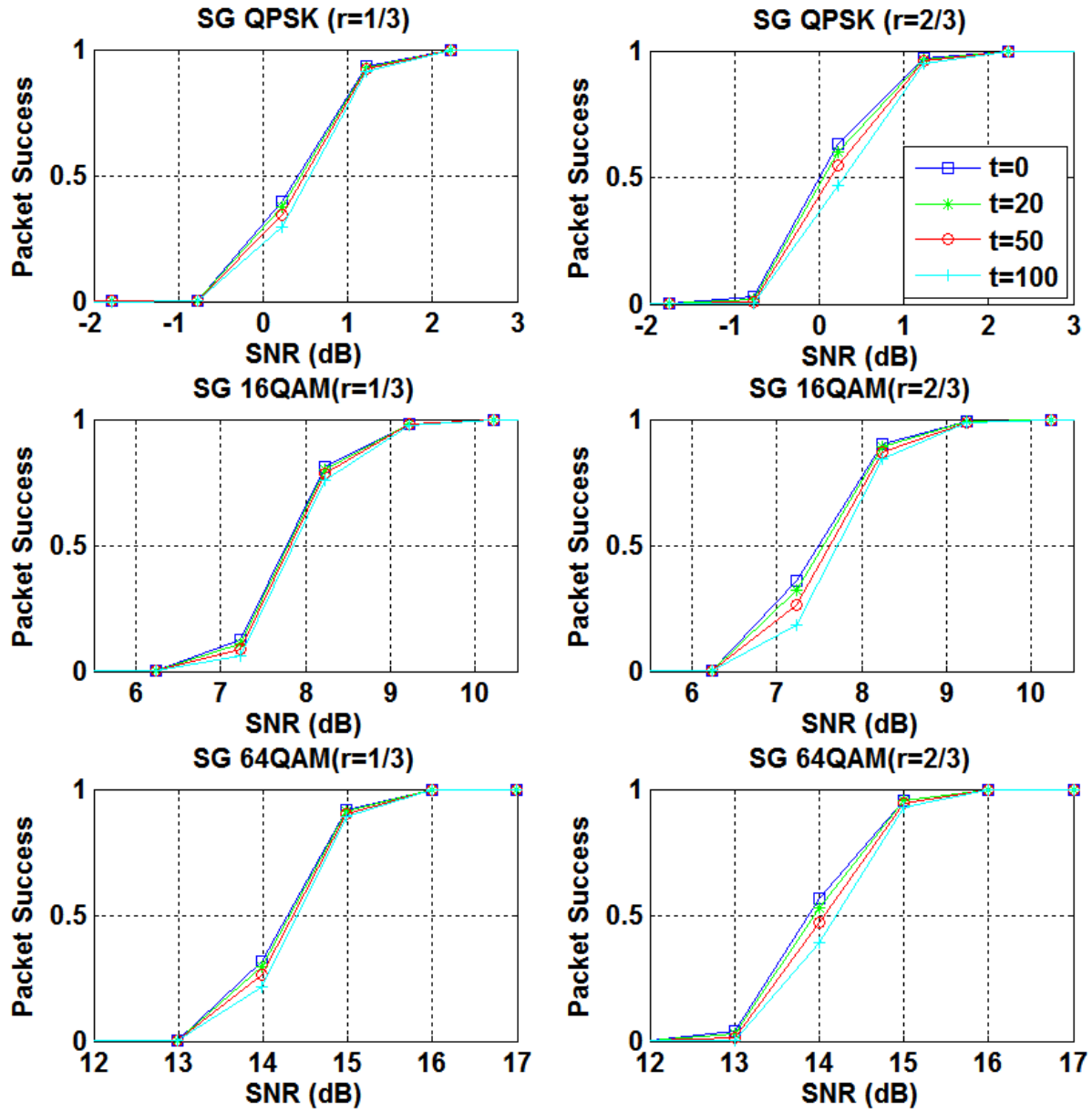

Figure 5-9 - Smart Grid Packet Success Probability With Forward Error Correction & Encoded Errors

The packet success probabilities for the Smart Grid class are presented in Figure 5-9. The threshold values for optimum Turbo-Coding are summarized as the following:

- QPSK: $SNR > 2dB$
- 16QAM: $SNR > 9dB$
- 64QAM: $SNR > 16dB$

Interestingly, the packet success probability is marginally better when the Turbo-Coding rate is $2/3$, which corresponds to less redundant bits used, than when the rate is $1/3$. This is due to the small length of the Smart Grid packet. The extra redundant bit required by $1/3$ Turbo Coding is only useful when packet lengths are large, as will be noted in the examination of Figure 5-11 below.

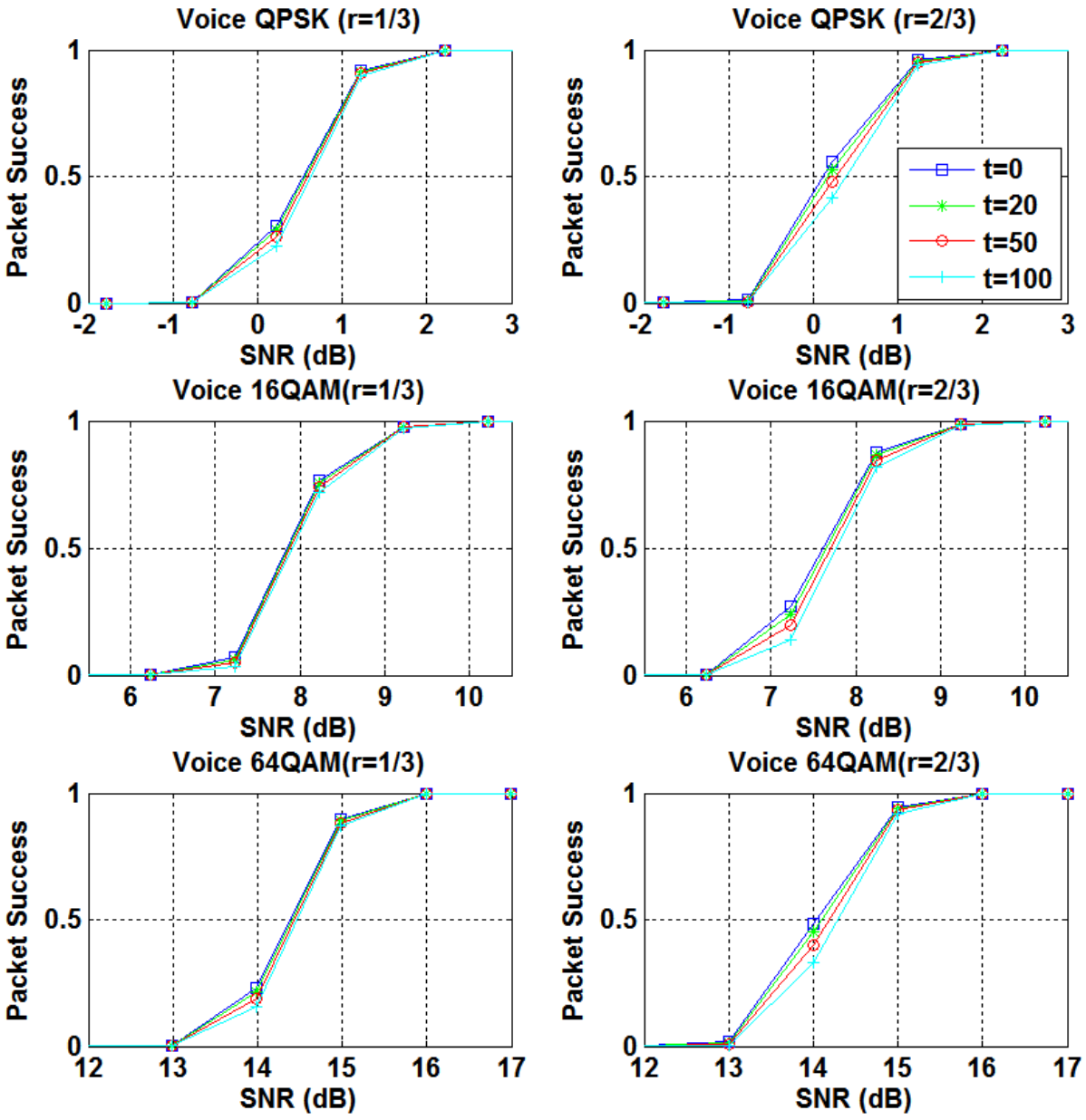

Figure 5-10 - Voice Packet Success Probability With Forward Error Correction & Encoded Errors

There is a close degree of similarity between the results displayed in Figure 5-9 & Figure 5-10 due to the difference between their respective packet lengths only being

twenty-eight bytes. Thus the Voice threshold values for optimum Turbo-Coding are identical as those for the Smart Grid. However, when compared with Figure 5-11, the differences due to packet length between the Packet Success Probabilities are easily noticed.

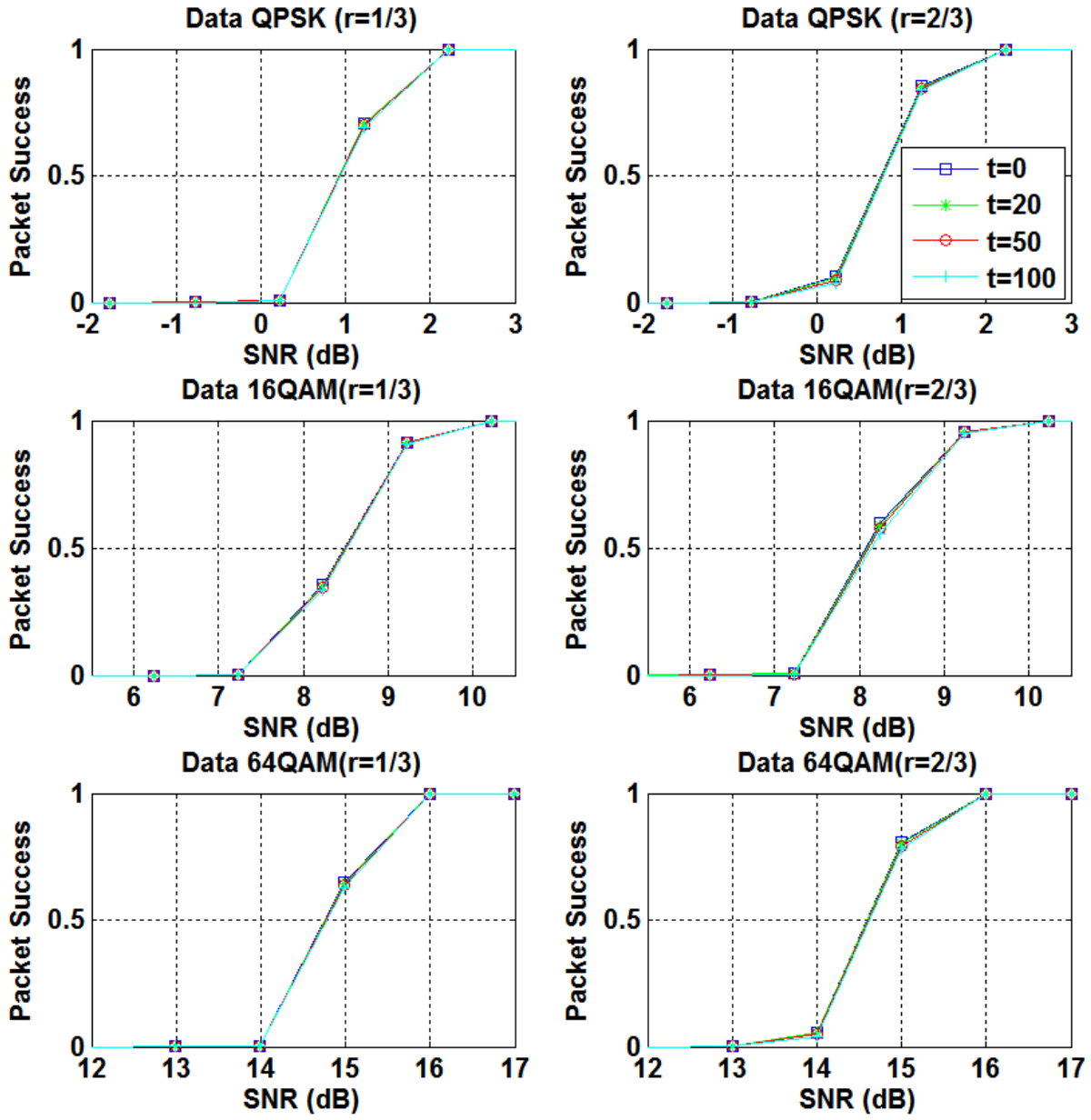

Figure 5-11 - Data Packet Success Probability With Forward Error Correction & Encoded Errors

The packet success probabilities for the Data class are presented in Figure 5-11. The threshold values for optimum Turbo-Coding are summarized as the following:

- QPSK: $SNR > 2dB$

- 16QAM: $SNR > 10dB$
- 64QAM: $SNR > 16dB$

The differences caused by overall packet length can easily be differentiated between Figure 5-9, Figure 5-10 & Figure 5-11. The larger length used by data packets causes the Turbo Decoder with rate $1/3$ to produce higher packet success probabilities which differs to the results from Smart Grid and Voice packet lengths. Also, as the packet length increases, the discernible difference between the amounts of encoded errors decreases. This is expected due to the ratio of the bit errors decoded and the total packet length decreases with increasing packet length.

5.3.1.2 Adaptive Modulation and Coding

Adaptive Modulation and Coding provides rate adaptation based on channel variation [83]. In this case, a UE chooses a modulation that best suits its channel condition. From the above results, we can conclude that QPSK modulation is best suited for UEs experiencing poor channel conditions, including deep fading, high path loss and interference noise which degrade the signal quality. However, if QPSK modulation is chosen for all UEs, the data rate gain by using higher order modulation will be lost. Therefore, QPSK is best reserved to UEs that would face higher bit error rates if using a higher order modulation such as 16QAM or 64QAM. In Figure 5-9, Figure 5-10 & Figure 5-11 it is easily determined that the QPSK operating region would be best chosen as an UE with $SNR = 0 \rightarrow 10dB$. By choosing this band of SNR as a QPSK modulation band it is possible to minimize bit errors, which in turn will maximize packet success probability, throughput. This also has the added benefits of reducing latency due to minimal re-transmission requests. Similarly, for UEs with intermediate channel conditions ($SNR = 10 \rightarrow 20dB$) 16QAM modulation is best suited. For UEs with the best channel conditions ($SNR = 20 + dB$) 64QAM can be used to maximize their throughput.

5.4 SUMMARY

The link reliability was measured and analysed using two turbo-coding rates, and for three modulation techniques. This produced packet success probability distribution against received Signal to Noise Ratios for the three differing classes of UEs: Smart Grid, Voice, and Data (ordered by increasing packet size).

With regards to packet size, smaller packet transmissions such as those involving Smart Grid packets (100 bytes) or Voice packets (128 bytes) were subject to lower bit error rates at lower SNR values. This improves the packet success probability of such packets being transmitted with little or no bit errors that cannot be corrected by use of the turbo-coding. Data packets (500 bytes) were subject to similar packet success rates, however, with packet success increasing substantially at higher SNR levels than those recorded in the Smart Grid and Voice results. The transition between high levels and low levels of packet success was much sharper in Data packets.

Information turbo-coded at a rate of $2/3$ performed better than information coded at a rate of $1/3$. This is to be expected due to the extra number of redundant bits. However, as will be shown in Chapter 6, this affects the latency observed by the packet.

The number of bit errors encoded into each packet was also examined. A range of bit errors from 0 to 100 was chosen. Whilst the actual number of bit errors did not affect the SNR threshold or cut-off levels, it did affect the spread of the transition from low probability to high probability. This was more noticeable in small packets such as Smart Grid or Voice where the ratio of bit errors to total packet length was higher. As expected, packets with zero bit errors were transmitted with a higher probability of success than those with an increasing number of bit errors.

The performance of the individual modulation schemes yields some important results. QPSK modulation achieved high levels of packet success probabilities for low values of SNR. This is to be expected due to the relative ease of de-coding 4 symbols in an equidistant symbol constellation. As the modulation index increased the SNR required to extract correct symbols free from bit errors also increased. As such, 64QAM

performs poorly at low levels of SNR, however, produces excellent results at high SNRs.

It can be concluded then, that in a model where modulation and coding can be adapted to channel conditions. Therefore, UEs with low SNRs can diminish latency and throughput performance in order to produce higher levels of successful packet transmissions. In this way, the network can successfully provide excellent levels of link reliability and reduce required re-transmissions that can cause inflated observed latencies. Higher SNR UEs can take advantage of lower turbo coding rates and higher modulation indexes to further increase their throughput and decrease their latency.

The next chapter analyses the latency of the Lotka-Volterra Resource Allocation Scheme and Scheduler and how the system performs during Periodic and Sporadic traffic conditions.

Chapter 6.
Latency Analysis & Results

Latency is a performance metric that describes the delay in a network from information being transmitted to it being received [88]. There are many types of latencies in a network, such as:

- Transmission Delay – time it takes to modulate data and send over the wireless link
- Propagation Delay – time for the signal to be received over the wireless link
- Queuing Delay – time it spends in queues awaiting transmission
- Processing Delay – time it takes to process information in the packet header

Latency is an important metric that helps measure the viability of a communications link to support applications and services. In this Chapter, this thesis will investigate the latency results achieved by the use of the Lotka-Volterra Resource Allocation & Scheduler model proposed in Chapter 4. The performance of the model will be based on Smart Grid latency requirements in Table 2-2 and Table 2-3 as defined as the United States of America Department of Energy.

Initially, this chapter will introduce the Lotka-Volterra subcarrier allocation difference between intervals of periodic and sporadic traffic. Then factors that increase latency in the proposed model are presented including an analysis into Bit-Error-Rate & Packet-Error-Rates of the proposed model. Forward Error Correction is applied to received bit streams

6.1 ASSUMPTIONS

The User Equipment processing time was not considered in the overall Latency calculations as it is the LTE network this research is analysing and its suitability in supporting the Smart Grid as its default communications network. Individual UE processing time will affect the overall Latency however it doesn't affect the latency of the communications network or the response of the Lotka-Volterra Resource Allocation Scheme used within this research.

As described in Chapter 4, Section 4.4.1, Table 4-1, the system parameters constrained packet lengths to a set number for all classes. Whilst this is no indicative of a real-world situation it provides easier analysis of the proposed Lotka-Volterra Resource Allocation & Scheduler. Of course packet lengths have effects on optimal data rates, probability of bit errors and therefore also latency, this research is concerned with the optimal allocation of resources based on class requirements. Individual allocation of resources is based on channel conditions and QoS requirements not packet lengths. Future work could require an investigation into further optimization by applying differing packet lengths and solving for optimal data rates however this is outside of the scope of this thesis.

6.2 FACTORS AFFECTING LATENCY

In the proposed model, queue delay and propagation delay are the only two factors considered when considering overall latency. This is due to non-uniform processing and transmission times between the multitude of differing devices used in the Smart

Grid and wireless telecommunication networks. However, this research does provide a good benchmark for queue and propagation delay in a Rayleigh Channel using LTE. This can be integrated with a vendors' own experimental transmission or processing delay results to provide a more complete analysis of latency in a wireless network.

6.3 LOTKA-VOLTERRA RESOURCE ALLOCATION SCHEDULER

The Lotka-Volterra Resource Allocation & Scheduler is broken into two integral components: the scheduler that determines the order of packets, and the resource allocator that aligns subcarriers with UEs. Both of these processes are important in ensuring the QoS of Smart Grid applications whilst also limiting their effect on pre-existing UEs operating in the wireless network. Figure 6-1 displays the Queue Initialization and updating process that the Lotka-Volterra Resource Allocation and Scheduler undertakes. The Scheduler takes into account both sporadic traffic that is already pre-existing in the queue and also periodic traffic that occurs at regular set time intervals. Once the system has determined the current and future queue characteristics, such as total queue length and growth rates, it sends this data to the Lotka-Volterra Algorithm for mapping to a population dynamics environment.

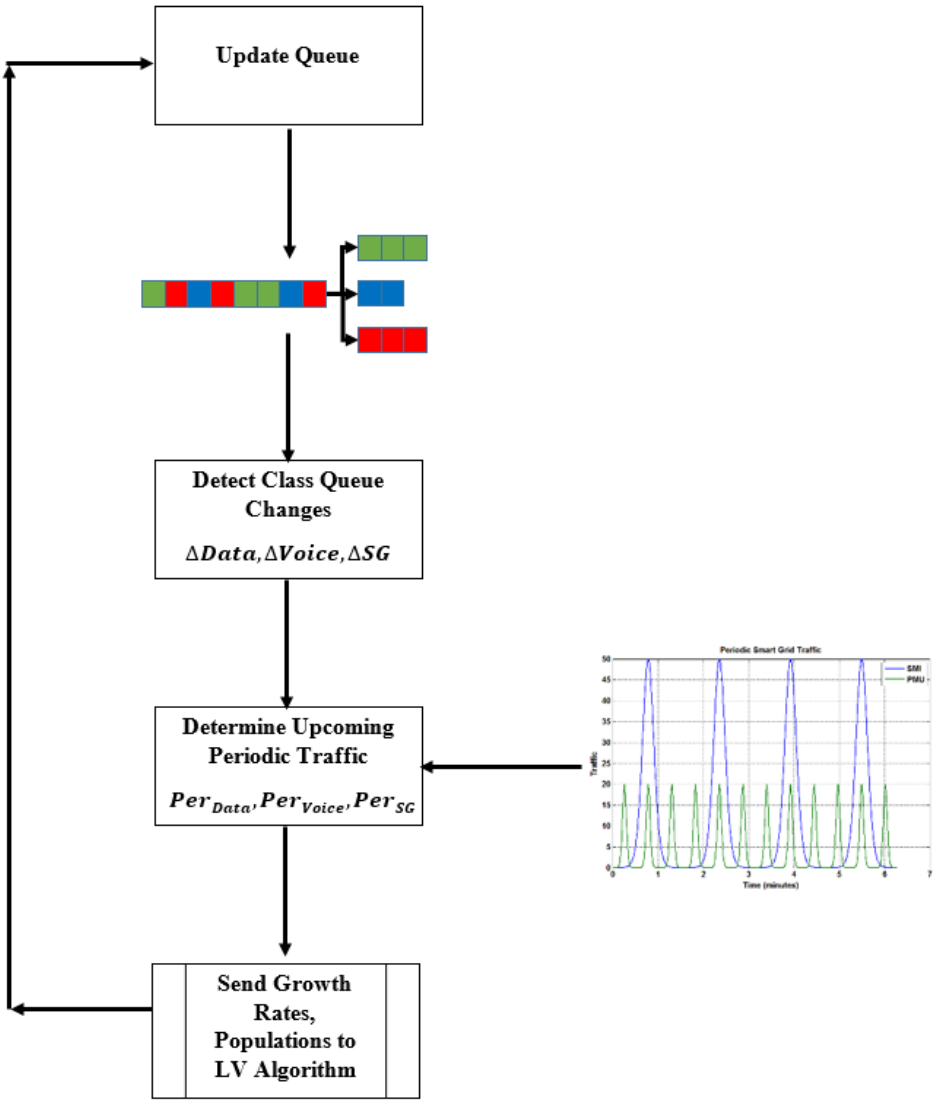

Figure 6-1 - Queue Initialization Flowchart

Figure 6-2 displays the Lotka-Volterra Resource Allocation and Scheduler Algorithm used in this research. The individual components are described in detail in Section 4.4. The growth rates and current queue lengths are passed from the scheduler to this algorithm. The initial queue lengths are used as initial conditions in the Lotka-Volterra Hamiltonian Function. The growth rates are then applied to choose the best fit Limit Cycle. This limit cycle is then normalized and mapped onto a XYZ plane to extract the third class result. The limit cycle proportions are then applied to current and future power allocations in the system.

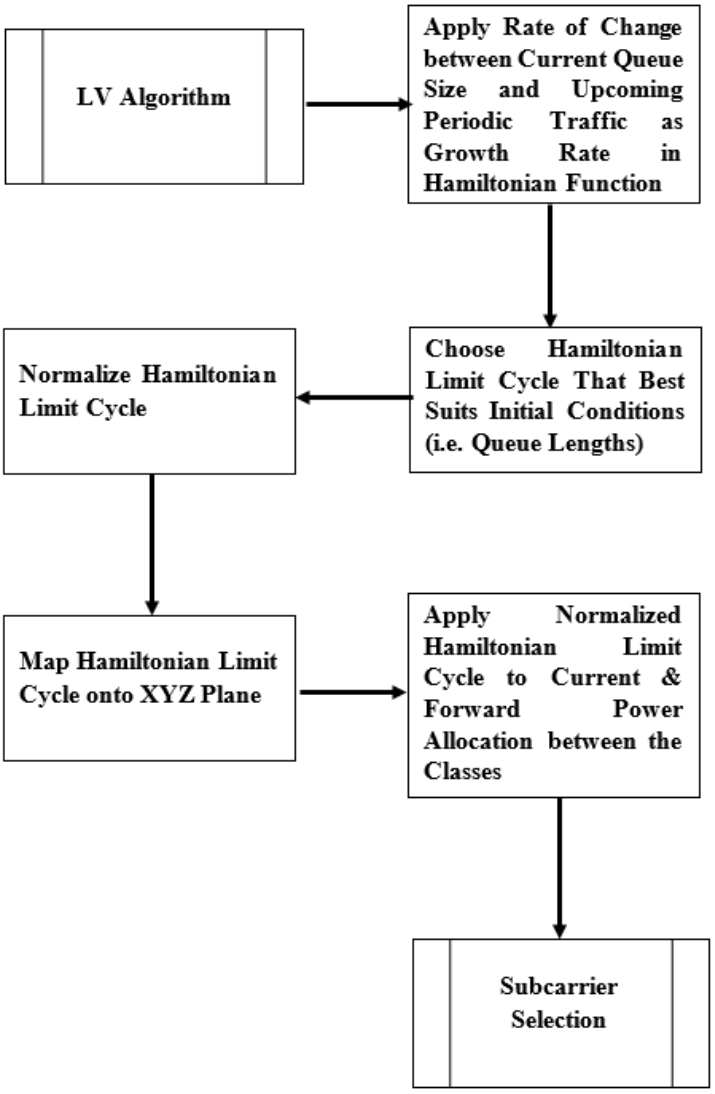

Figure 6-2 - Lotka-Volterra Algorithm Flowchart

The allocation process of subcarriers to each class is shown in Algorithm 6-3. The process to determine the growth rates of each class is shown in Algorithm 6-1. The traffic is organized into periodic and sporadic, with sporadic traffic averaged to allow for stable limit cycle mapping.

1: Algorithm for Determining Class Growth Rates
2: Determine Classes of UEs in Queue and segregate: $\{SG, Data, Voice\}$
3: if (periodic traffic will occur)
4: add blank packets into class queue $\{SG, Data, Voice\}$
to line up with periodic traffic transmission

5: Average Sporadic Traffic: $\{SG_{Sporadic_{Avg}}, Data_{Sporadic_{Avg}}, Voice_{Sporadic_{Avg}}\}$

6: Determine queue total length:

$\{SG_{Total}, Data_{Total}, Voice_{Total}\} = \{SG_{Periodic}, Data_{Periodic}, Voice_{Periodic}\} + \{SG_{Sporadic_{Avg}}, Data_{Sporadic_{Avg}}, Voice_{Sporadic_{Avg}}\}$

7: Determine Growth rates: $\frac{(Class_{Total}(t) - Class_{Total}(t-1))}{Class_{Total}(t)}$

8: Map Growth Rates and Total Queue lengths to Limit Cycle

Algorithm 6-1 - Determination of Class Growth Rates

Once the growth rates and total queue sizes are determined by Algorithm 6-1, they are directly inputted into Algorithm 6-2 to map the class populations to a stable limit cycle as determined by the Lotka-Volterra Hamiltonian Function defined in Section 4.3.3.

1: Algorithm for Mapping Class Populations to Limit Cycles

2: Map growth rates and initial conditions on simplex Σ using relation:

$Class_c = 1 - Class_B - Class_C$

3: Solve Lotka-Volterra Hamiltonian Function and determine stable limit cycles

4: Map Hamiltonian Solution from simplex Σ to individual classes

5: Normalize Hamiltonian Solution and apply to transmitted power allocated to each class for $t > 0$

Algorithm 6-2 - Mapping Class Populations to Limit Cycles on Simplex Σ

It is important that the average of the sporadic traffic is applied to the Hamiltonian Function or a closed limit cycle may not result. The Limit Cycle allows for the smooth transition between periodic and non-periodic traffic conditions. This allows for a smooth latency and throughput distribution, which can add further reliability to data transmissions.

The limit cycle is normalized and used to allocate the total power to each class for $t \geq 0$. Each class also measures the gain afforded by each subcarrier for each packet requiring transmission. The class then chooses to 'bid' on subcarriers that will increase its' average UE gain. In most circumstances this requires bidding for high power subcarriers, however, due to the variability in Rayleigh fading channels, some subcarriers provided excellent gain and others regions of high fading. The bidding

process is also subject to a maximum power constraint whereby each class can only bid for subcarriers it has power to allocate. Classes with high growth rates are given initial choice of the subcarriers. The overall bidding process is shown in the pseudocode in Algorithm 6-3.

1: Algorithm for Class Subcarrier Bidding
2: Detect Growth Rates $\{SG_{GR}, D_{GR}, V_{GR}\}$
3: Order Classes by Growth Rate $\{C_1, C_2, C_3\}$
4: Allocate Power $\{C_{N\,Power} = Class_{GR} \times P_{total}\}$
5: Order Subcarriers by Power $\{S_n | n = 1 - 50\}$
6: for $n = 1$ to 50
7: if $\left(C_{1\,Power} > S_{n\,power}\right)$
8: add subcarrier n to $\{C_{1\,subcarriers}\}$
9: $C_{1\,Power} = C_{1\,Power} - S_{n\,Power}$
10: $n = n + 1$; end;
11: if $\left(C_{2\,Power} > S_{n\,power}\right)$
12: add subcarrier n to $\{C_{2\,subcarriers}\}$
13: $C_{2\,Power} = C_{2\,Power} - S_{n\,Power}$
14: $n = n + 1$; end;
15: if $\left(C_{3\,Power} > S_{n\,power}\right)$
16: add subcarrier n to $\{C_{3\,subcarriers}\}$
17: $C_{3\,Power} = C_{3\,Power} - S_{n\,Power}$
18: $n = n + 1$; end;
19: end

Algorithm 6-3 – Class Subcarrier Selection Utilizing Bidding Algorithm

Latency is minimized by choosing modulation scheme and keeping abreast of periodic traffic profiles. Growth rate of queue signifies which class can bet for subcarriers first, second and third. By choosing growth rate, the transition between 1,2,3 is sequential, that is there is no change in growth rate that produces a class changing from category 1 to category 3 or vice versa. This helps ensure that subcarriers that are allocated by a class can be retained by that class for a number of iterations. This produces low temporal variation in the subcarriers allocated to each class. This is displayed in Figure 6-3 & Figure 6-4 where it is evident that there is not a large amount of subcarriers changing from class to class in each iteration of the Lotka-Volterra

Scheduler. This helps to retain subcarriers for UEs that require more than one time slot to transmit their complete package, or have multiple packages to transmit.

6.3.1 Scheduling During Sporadic Traffic

Sporadic traffic is scheduled in a first come first served basis. However, the allocation of subcarriers to the traffic couldn't be more different. The growth rates and queue length dependency of the Lotka-Volterra Resource Allocation and Scheduler transforms the queue from a FIFO to a class requirement based scheduler. Therefore, a queue with packets from all classes arriving at the same time doesn't necessarily mean they will all be allocated subcarriers at the same time.

The allocation of subcarriers to sporadic traffic is highlighted in Figure 6-3. The green blocks represent Smart Grid allocated subcarriers, red blocks represent Data allocated subcarriers and blue blocks represent voice allocated subcarriers. This coloring convention is retained in Figure 6-4. The power allocation profile is also evident in Figure 6-3 & Figure 6-4 where intermediate subcarriers are allocated a higher percentage of total transmitter power.

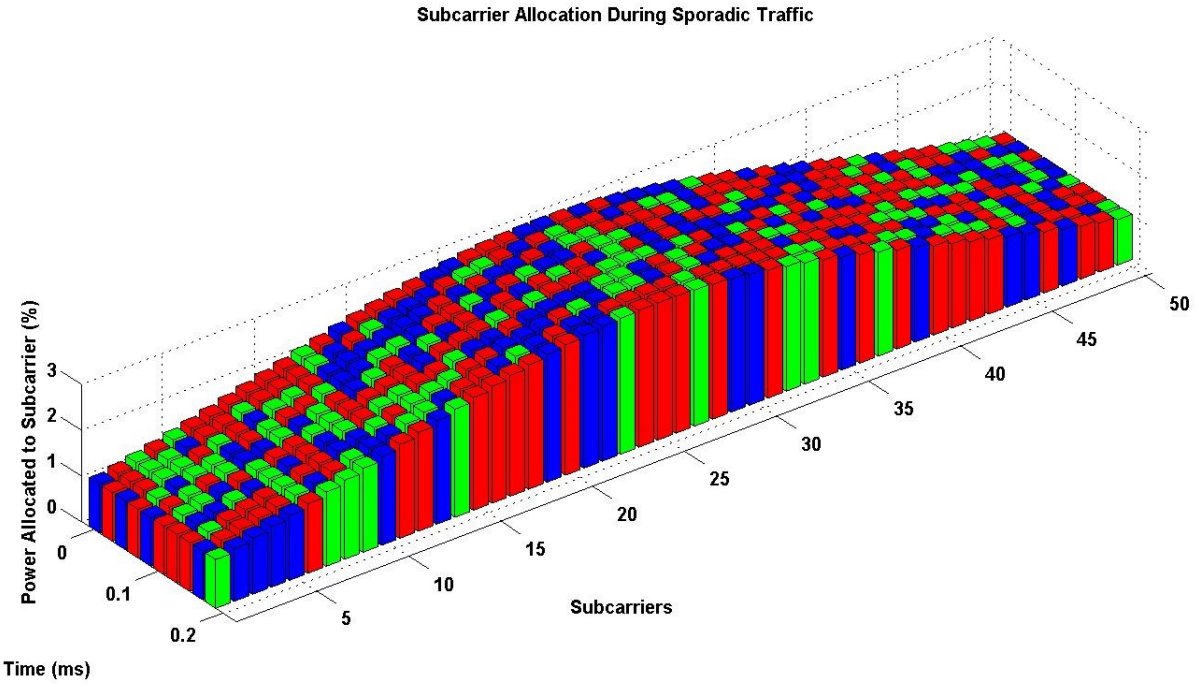

Figure 6-3 - Subcarrier Allocation During Sporadic Traffic

6.3.2 Scheduling During Periodic Traffic

The scheduling of Periodic Smart Grid Traffic is displayed in Figure 6-4. Pre-allocation of subcarriers for periodic traffic is only addressed before the periodic traffic is expected to start. The system does so by introducing empty packets into the queue with no data. When the periodic traffic is received by the eNB, the empty packets are filled with the data, thus removing their empty status. If the periodic traffic is not received by the eNB, the subcarriers are released and can be used by succeeding users in the queue. The arrival timing of the packets are of great importance as this ensures that the empty packets line up with the periodic traffic packets at the time of subcarrier allocation. By doing so, the periodic packets, with stringent latency constraints, witness near to zero queue delays which improves the overall latency of the packet.

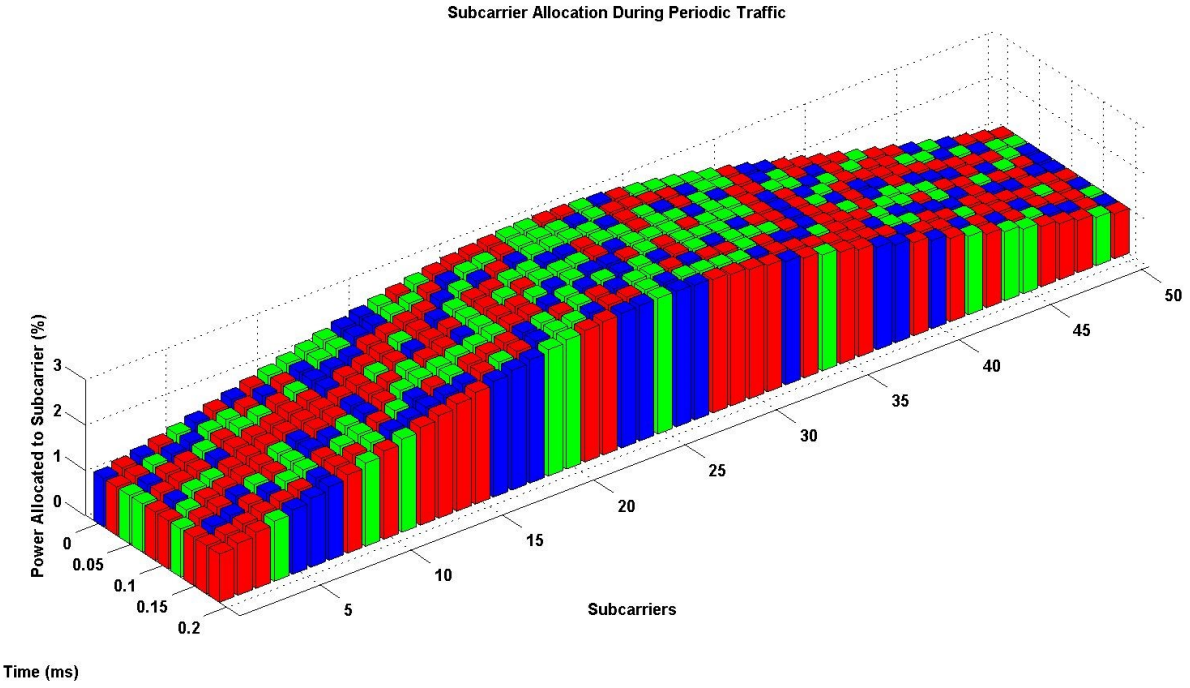

Figure 6-4 - Subcarrier Allocation During Periodic Traffic

During Periodic Smart Grid Traffic, the growth rate of the Smart Grid class is greater than that of the Data and Voice classes, or at least is at the start of the bursty traffic. This means that the Smart Grid data class has first pick in subcarriers. The queue length of the Smart Grid data class determines the size of the power allocated to it. This means if the growth rate is high and the queue length is high the Smart Grid class

can allocate the best subcarriers but also a large proportion of them. This is evident in Figure 6-4 where Smart Grid UEs have dominant subcarrier allocation in the middle (20-30) subcarriers.

In the succeeding three Sections, 6.4, 6.5 & 6.6, the latency results recorded by the simulation will be presented and analysed. The results are segregated by modulation used: QPSK, 16QAM, 64QAM and also by coding rate: $1/3, 2/3$. Each graph contains a latency probability distribution for each subcarrier over the Rayleigh Fading channel modelled in Section 3.3.2. The latency results presented are due to transmission and do not include queue wait time. The results and analysis of queue wait times are presented in Section 6.7.

6.4 QPSK RESULTS

The QPSK latency results for coding rates of $1/3$ and $2/3$ are represented by Figure 6-5 and Figure 6-6 respectively.

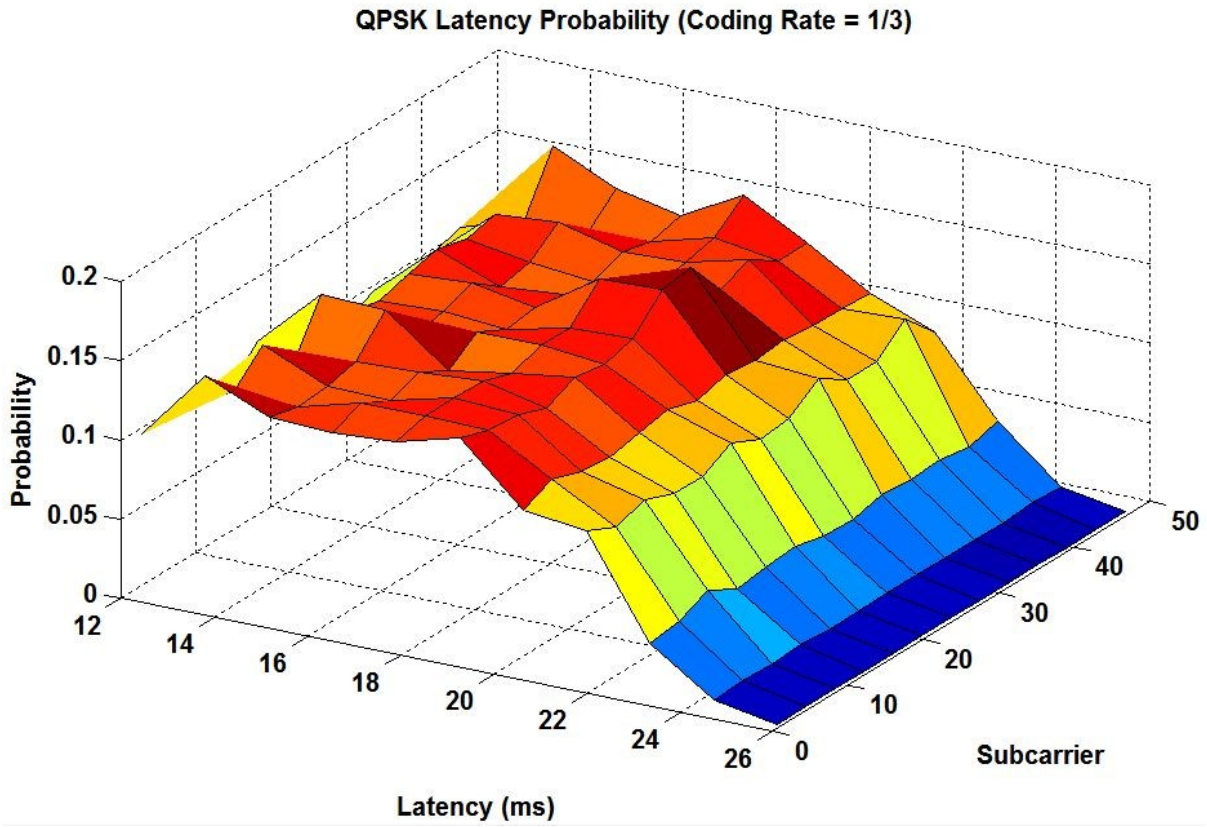

Figure 6-5 - Latency Results Using QPSK Modulation and a Coding Rate of 1/3

The latency of a QPSK modulated packet, using a $1/3$ Turbo code is most likely to face a latency of between 12 to 18ms with low probability of higher latencies occurring. The largest possible delay recorded was approximately 26ms, which is inside the latency constraints prescribed by Table 2-2 & Table 2-3.

QPSK modulated packets with $2/3$ Turbo Code are subject a lower number of bits and therefore provide lower latency than displayed Figure 6-5. This is clearly shown in Figure 6-6, where packets can expect nominal delays of between 8 to 16ms and a much lower probability for delays higher than 16ms.

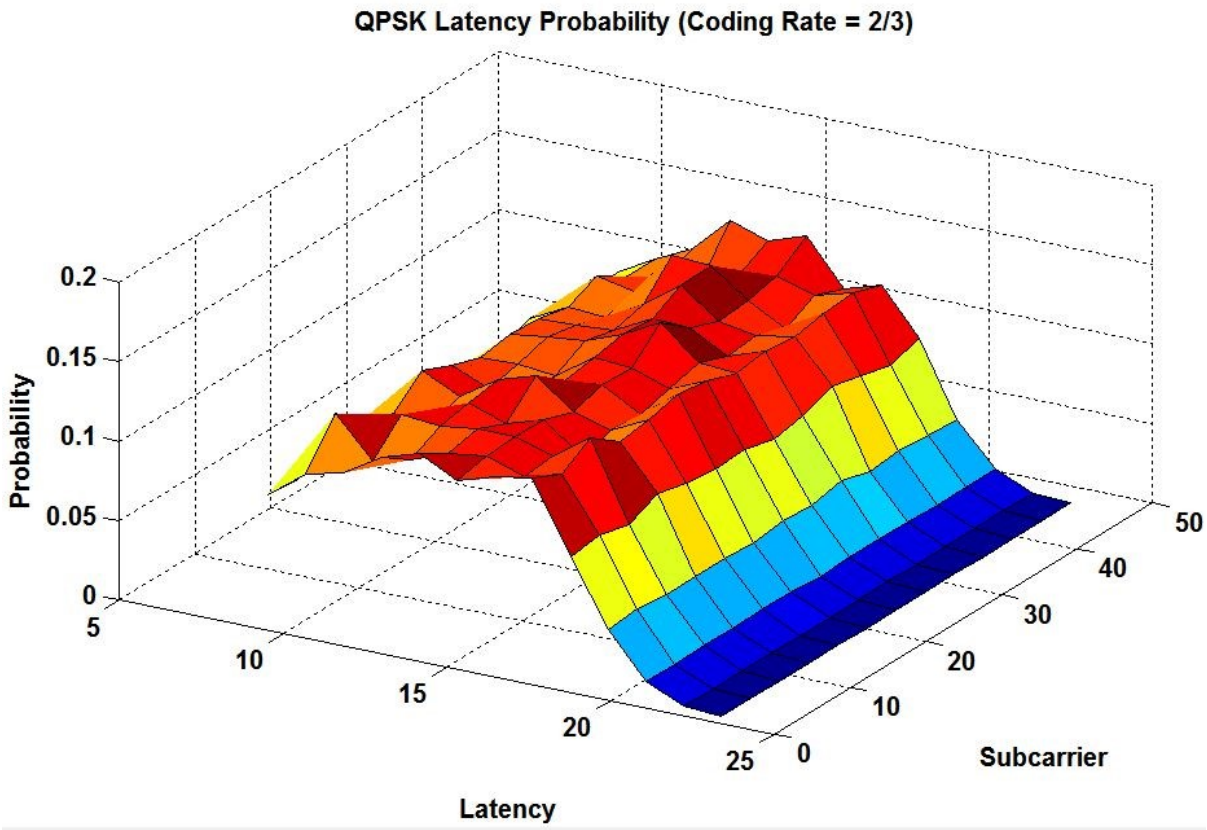

Figure 6-6 - Latency Results Using QPSK Modulation and a Coding Rate of 2/3

The packet success probability threshold is visible in each graph with a steep incline between higher latency and lower latency probabilities. The higher latencies are due to higher bit-error rates occurring at low SNR levels of 0-3dB which require further iterations in the Turbo-Decoder and in worst-case scenarios, retransmission of packet.

6.5 16QAM RESULTS

The 16QAM latency results for coding rates of $1/3$ and $2/3$ are represented by Figure 6-7 and Figure 6-8 respectively. The un-coded 16QAM results were presented and compared against a waterfilling resource allocation scheme in [44].

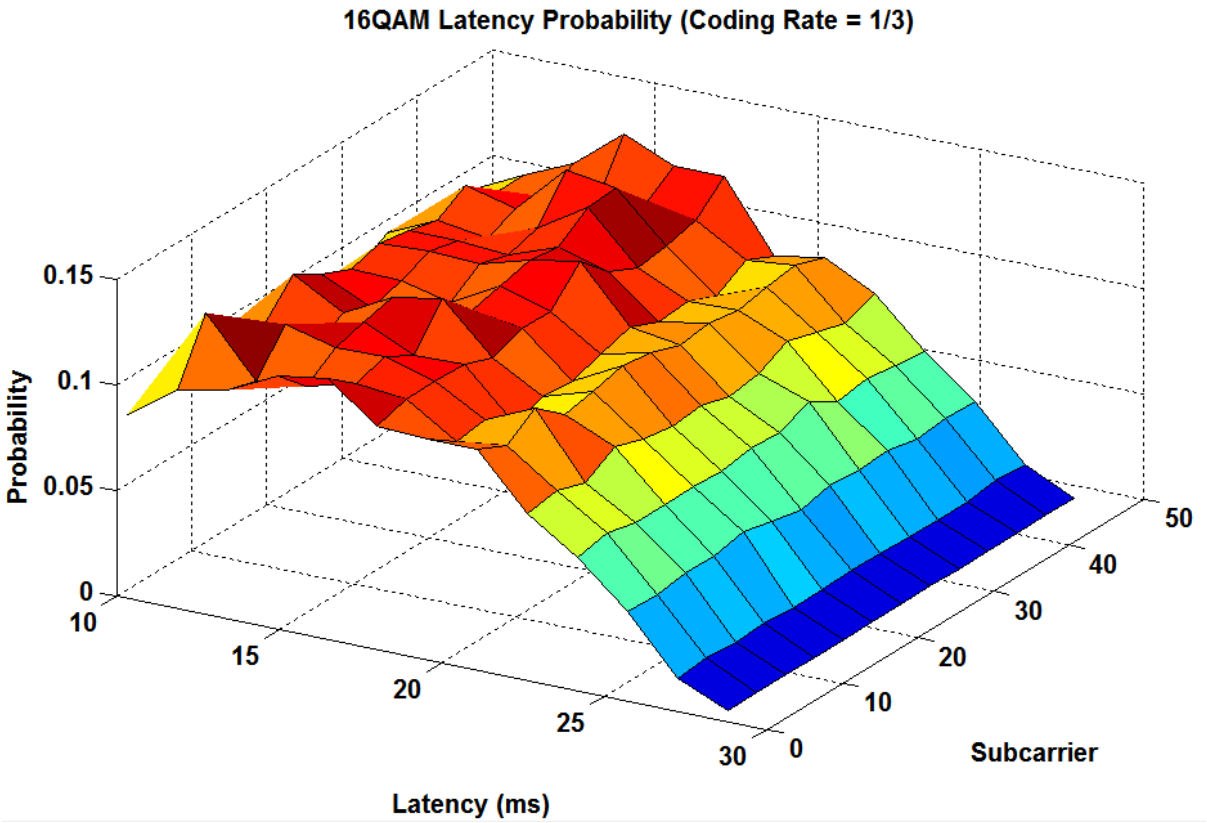

Figure 6-7 - Latency Results Using 16QAM Modulation and a Coding Rate of 1/3

The latency of a 16QAM modulated packet with a Turbo-Coding rate of $1/3$ will face a latency of approximately 10 – 20ms. The variability in the latency probability is reduced in Figure 6-7 by the extra redundant bits used by a $1/3$ Turbo Encoder. This provides higher packet success probabilities thus lowering the required number of packet retransmissions. This in turn increase the probability of lower latency transmissions.

The latency of a 16QAM modulated packet with a Turbo-Coding rate of $2/3$ will face a latency of approximately 7 – 15ms. There is a large degree of variability in the low latency end of Figure 6-8. This is caused by the relationship between the packet success probability and lower error correction capabilities of the $2/3$ Turbo Code. At the peaks visible in Figure 6-8 the UEs have overcome the lower bound of the Bit Error Rate displayed in Figure 5-9. At this point, the Turbo-Decoder is able to correct all errors and give a modest gain in performance yielding a lower latency at a higher probability.

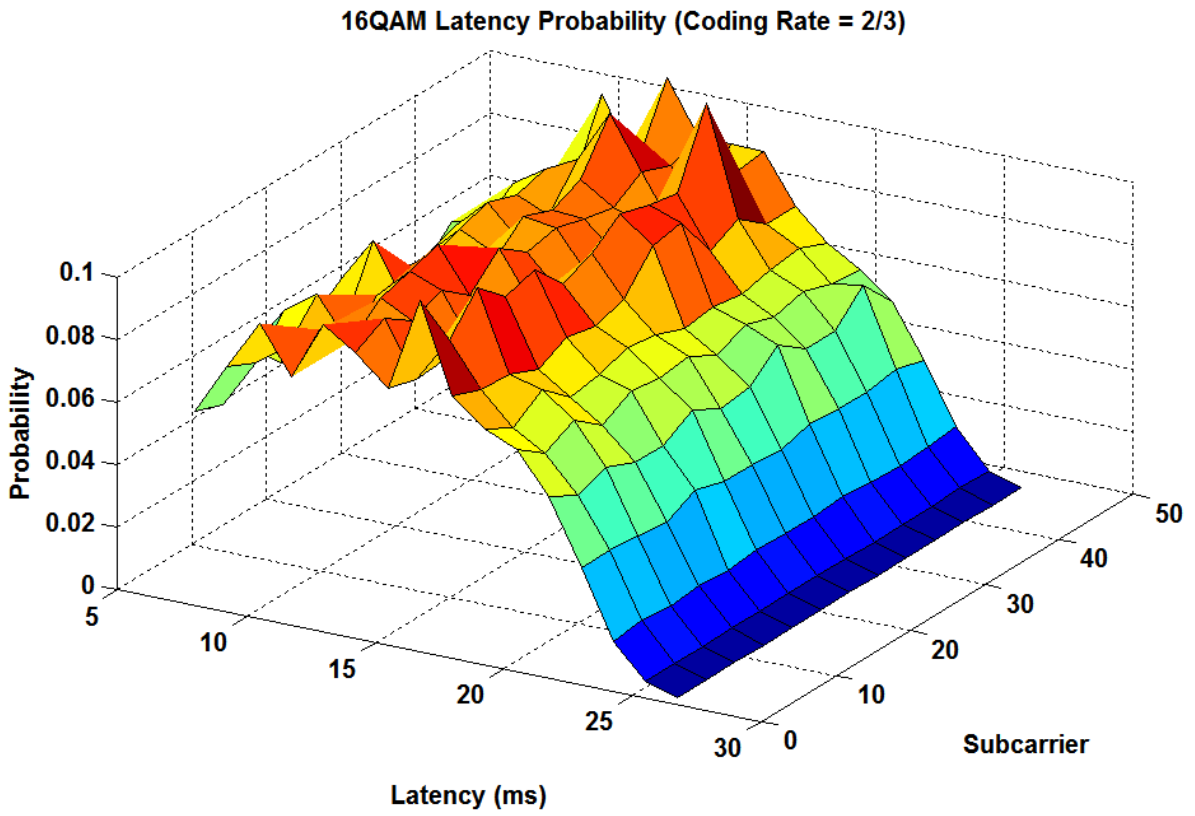

Figure 6-8 - Latency Results Using 16QAM Modulation and a Coding Rate of 2/3

Due to 16QAM's packet success probability being low for low SNR values, the tail of the graph is much longer than displayed in the QPSK results. QPSK results were subject to high packet success probabilities for low SNR values creating a more visible difference between lower latency and higher latency results. The incline in 16QAM results is not as steep due to low SNR UEs requiring packet re-transmission which increases latency. Even with the higher probability of bit errors causing lower packet success probabilities, the results for 16QAM still provide low latency similar to those in Section 6.4 which were subject to greater packet success probabilities over all SNRs. This is achievable due to an increase in the number of bits per symbol afforded by the 16QAM modulation scheme. This effectively increases the bit rate reducing the number of transmitted symbols thereby reducing latency marginally.

6.6 64QAM RESULTS

The 64QAM latency results for coding rates of $1/3$ and $2/3$ are represented by Figure 6-9 and Figure 6-10 respectively.

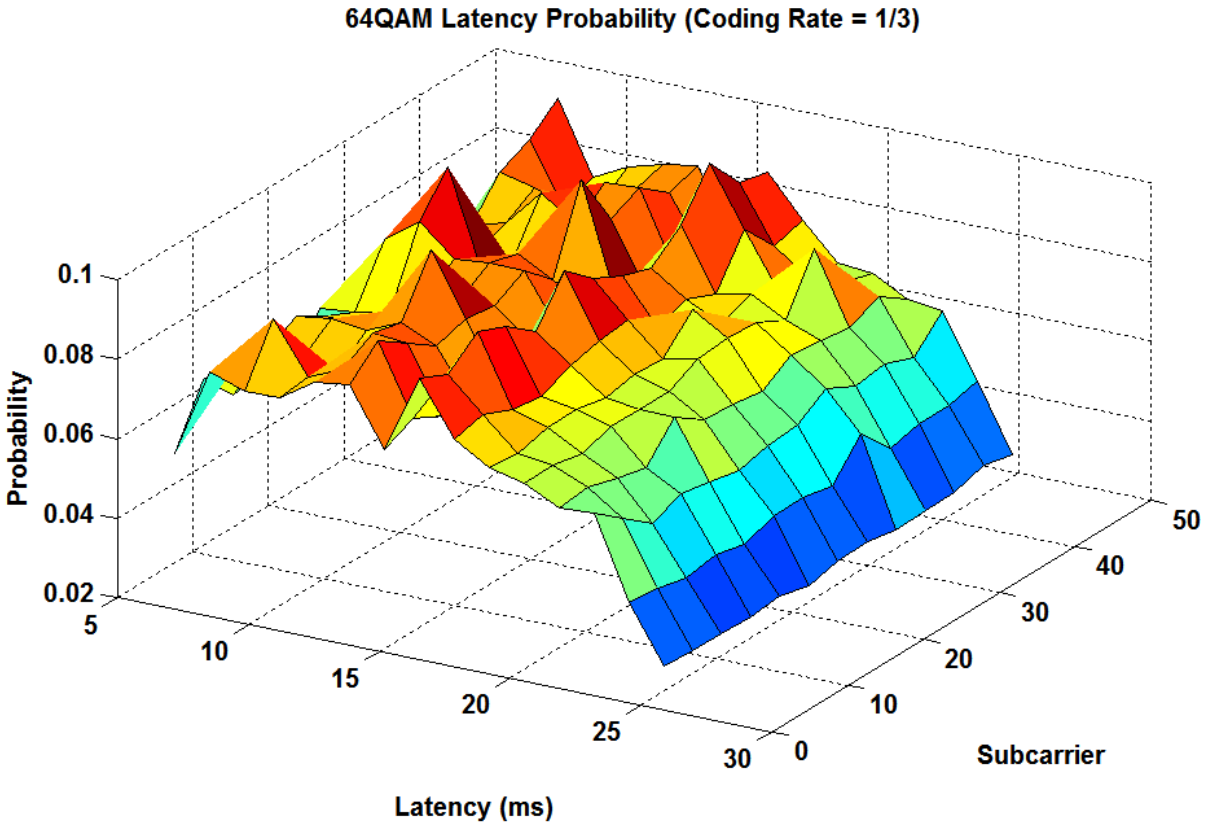

Figure 6-9 - Latency Results Using 64QAM Modulation and a Coding Rate of 1/3

The latency of a 64QAM modulated packet with a Turbo-Coding rate of $1/3$ will face a latency of approximately 5 – 20ms. This is similar to the results when Turbo-Coding at a rate of $2/3$ as displayed in Figure 6-10. The peaks denote areas of higher probability of packet transmission occurring at the latency recorded. These peaks occur at lower latency due to the situation where UE SNR have surpassed the threshold as displayed in Figure 5-9. This creates an area of low bit error rate and thus high packet success rate. So it can be quantitatively stated that the peaks represent areas of low packet retransmission probability. Areas outside the peaks are still subjected to low latency however the probability of attaining these latencies is much lower.

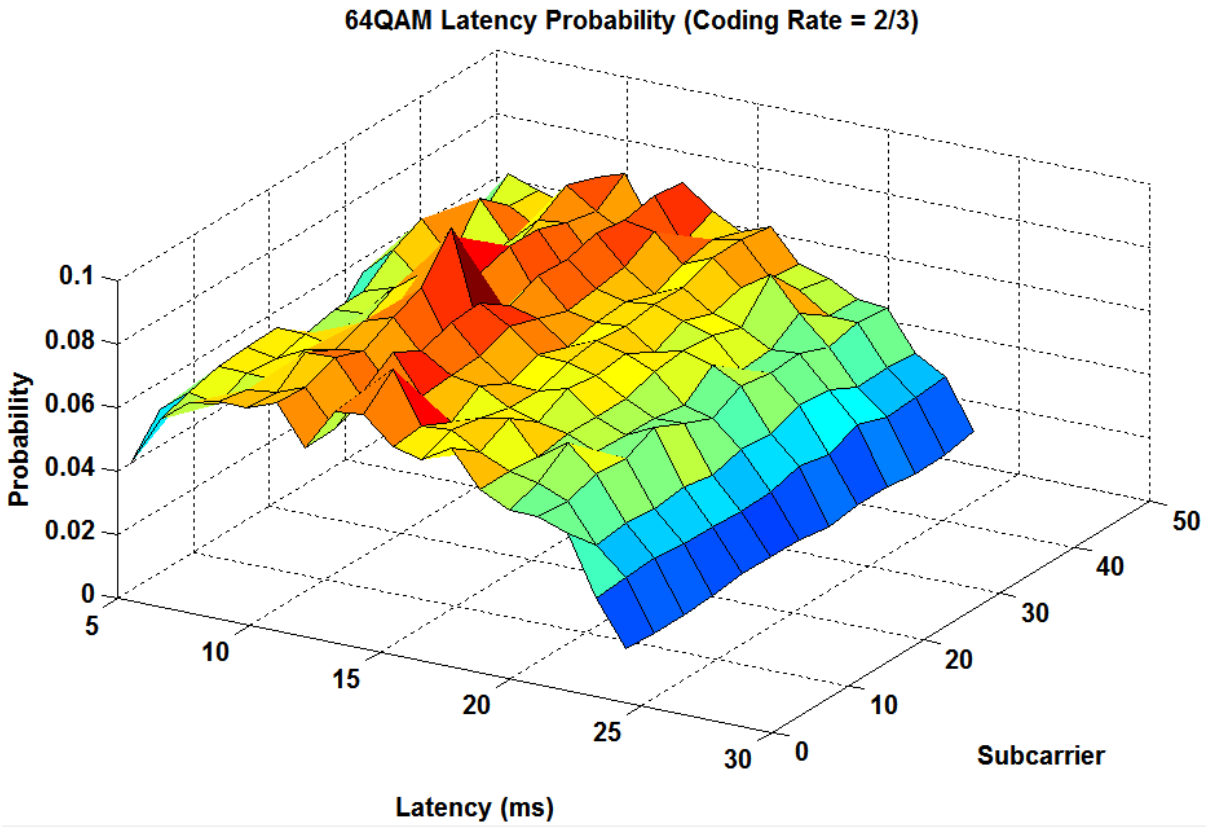

Figure 6-10 - Latency Results Using 64QAM Modulation and a Coding Rate of 2/3

The larger spread in latency values displayed in Figure 6-9 and Figure 6-10 is based on two conditions. The lower latency recorded by 64QAM is due to higher bits per symbol increasing the data rate coupled with UEs operating at higher SNRs. The higher latency results are caused by low SNR UEs requiring re-transmitted packets due to higher bit error rates and lower packet success probabilities.

The modulation latency results have displayed a few key relationships. The latency probability distribution can be defined by two surfaces, a typically constant probability surface with inherent variability and a declining region of low probability. The typically constant surface can contain peaks that represent areas of low packet re-transmission probabilities. The length of the surface is directly related to the trade-off between higher data rates due to increased symbol size and the increasing bit error rates of higher order modulations at lower SNR values.

The tail length and gradient of the declining region is based on the number of UEs operating at below the modulation threshold as displayed in Figure 5-9. As the

modulation order increases, the differentiation between symbols in the constellation decreases causing higher bit and symbol error rates. However, once the SNR threshold for the modulation mode has been surpassed the system provides low bit error rates thus increasing the probability of successful packet transmissions. This decreases the latency by removing the requirement for packet re-transmissions. This means that at higher order modulations, the tail will be longer due to more UEs operating below optimal SNRs.

On average, the latency of the $1/3$ Turbo-Coded results increased the latency marginally. This difference between the latency of the 1/3 and 2/3 coded rates is due to the serial nature of the coding, which requires more bits in the 1/3 to be coded before it can be transmitted. This produces additional coding, decoding and propagation delays in the transmission of the packet thus increasing overall latency.

6.7 QUEUE LATENCY

In this section this research will analyse the effect of queue latency in respect to queue length for both sporadic and periodic traffic. As defined in Section 3.2.1, this research identifies two type of traffic: sporadic and periodic. Sporadic traffic is defined as unscheduled traffic that is created by either user requirement or change in state status updates. Periodic traffic is used to describe regular updates that are scheduled and do not occur randomly. The model was simulated in the Matlab Simulink simulation environment and was initialized with the maximum number of packets for each class already in the queue. Each packet was timed in terms of how long from the start of the simulation until it was allocated a subcarrier for transmission over the network. The actual propagation delay was not included in the results. In this section, the packet lengths for the Smart Grid, Data and Voice classes were changed to 200 bytes to best examine the fairness exhibited by the Lotka-Volterra Resource Allocation and Scheduler.

In both Figure 6-11 & Figure 6-12 the black horizontal line displays the latency cut-off for Smart Grid applications which occurs at 200ms. This line represents the latency constraint for Smart Grid applications as defined by Table 2-2. Figure 6-11 represents

the queue latency during sporadic traffic conditions. The fairness of the Lotka-Volterra resource allocation scheme is visible by how close the classes' results are. Queue Latency only exceeds the 200ms cut-off when the queue lengths for the Smart Grid, Data and Voice Classes exceed 3000 packets each. This proves that for high traffic conditions the Lotka-Volterra Resource Allocation Scheduler is able to provide competitive latency with long queue lengths.

This work has stipulated the requirement for Resource Allocator and Schedulers to meet the differing requirements of differing classes of traffic. By removing the difference between the classes the Lotka-Volterra Resource Allocation and Scheduler has proved that given identical requirements will translate to identical results.

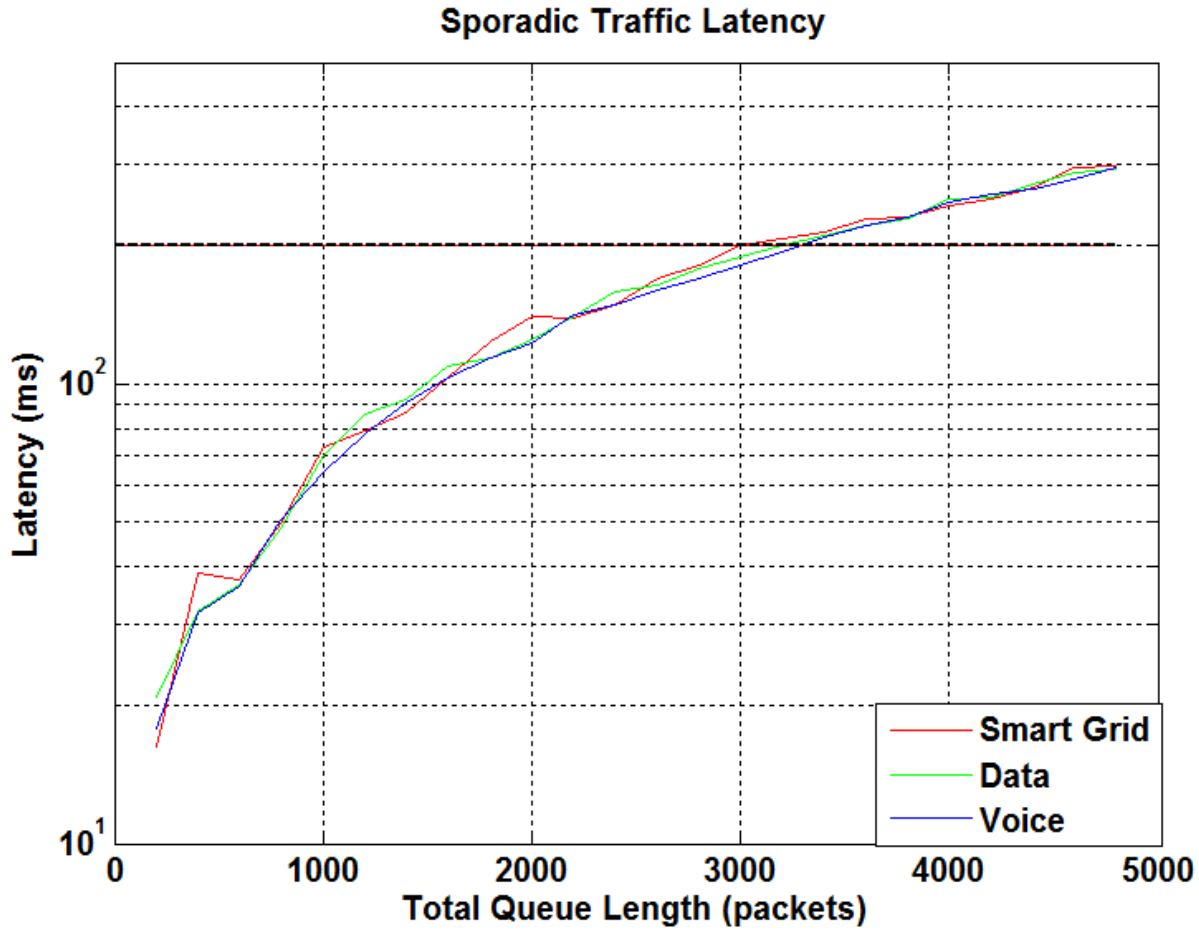

Figure 6-11 - Sporadic Traffic Queue Latency Against Queue Length

The Smart Grid class is contains both SMI and PMU traffic was not modelled to be differentiated between. If differentiated, the system would allocate more resources to

PMU traffic than SMI due its strict latency constraints. This would substantially reduce the latency of PMU traffic whilst exacerbating SMI traffic, which is reasonable.

Figure 6-12 represents the queue latency during periodic Smart Grid traffic conditions. As such the scheduler has allocated Smart Grid packets subcarriers for future transmission. The Scheduler has also allocated more subcarriers to the Smart Grid class due to the growth rate that occurs during periodic traffic conditions. This produces a decrease in the Smart Grid queue latency to the point where it is well under the 200ms threshold for queue lengths exceeding 5000 packets. However, the increased performance in the Smart Grid class is directly related to a marginally decreased performance in the Data class, and a drastic decrease in performance in the Voice class. This is reflected by the normalized growth rates of those classes during times of periodic Smart Grid traffic.

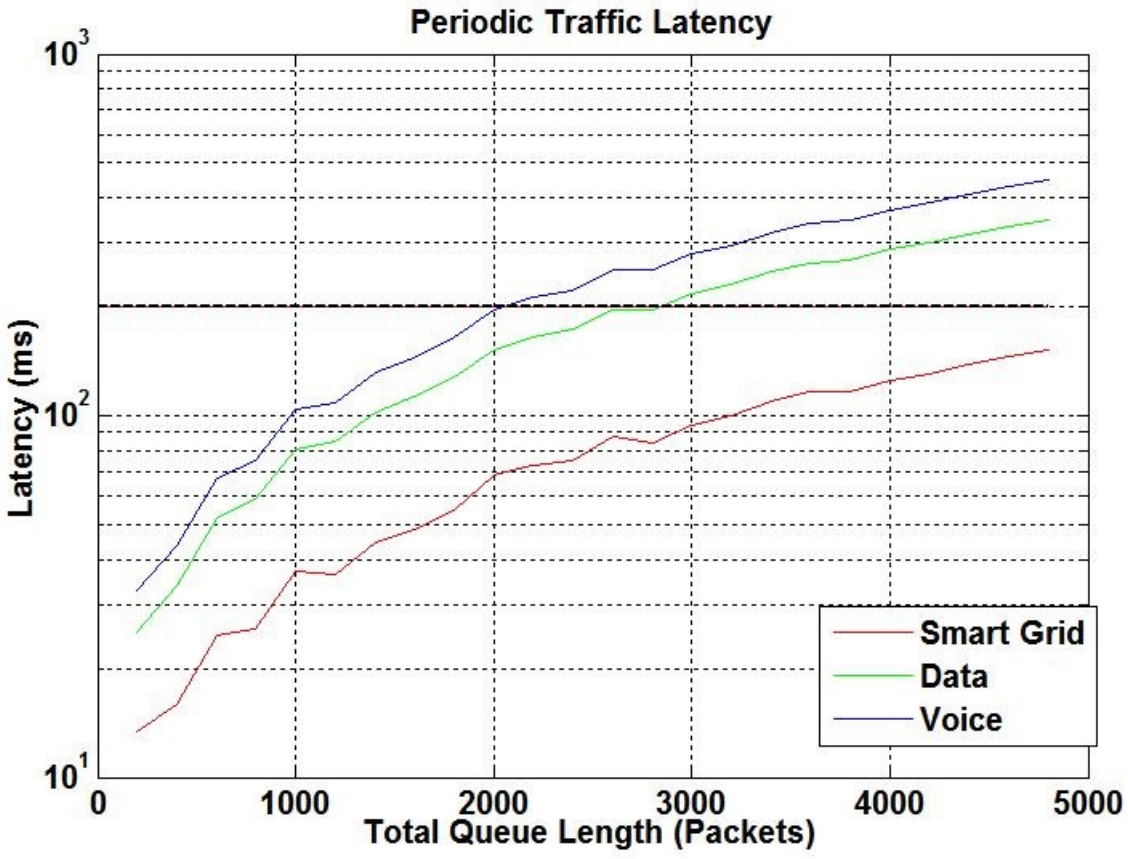

Figure 6-12 - Periodic Traffic Queue Latency Against Queue Length

During periods of sporadic traffic the Scheduler allocates resources fairly between the classes with impartiality. With latencies already approaching the 200ms mark and not

including latencies invoked by processing of packets, it is apparent that the Lotka-Volterra system is required to ensure low latency transmission of high priority Smart Grid packets. When imposed with Smart Grid Periodic Traffic conditions including stringent QoS requirements, the Lotka-Volterra Resource Allocation and Scheduler is able to adapt to these QoS requirements to ensure low latency transmission of packets. This is of vital importance due to the time critical nature of Smart Grid packets and their impact on the stability of the Power Grid.

6.8 LATENCY ANALYSIS SUMMARY

The Lotka-Volterra Resource Allocation Scheme has produced low latency transmission and queue lengths for Smart Grid data packets. The latency results for two sets of Turbo-Coding rates, and three sets of modulation are analysed. Furthermore, the latency results are broken into two separate streams: transmission and queue latencies.

Transmission latencies were contained within 30ms and a minimum latency of 5ms was achieved using the Lotka-Volterra Resource Allocation and Scheduler Scheme. Whilst this latencies are within LTE specifications, the overall high probability for low latency transmission over a Rayleigh fading channel shows optimal use of the channel and high levels of multi-user gain. All of which is the result of Lotka-Volterra Resource Allocation and Scheduling based on current and future communications traffic requirements, growth rates of individual classes, and individual class QoS requirements.

Queue delays were minimized for Smart Grid traffic during times of periodic traffic. This is provided by smart pre-allocation of optimal subcarriers to Smart Grid packets during intervals of periodic traffic. Outside of these times, the QoS requirements, growth rates and queue lengths determine the subcarrier allocation and subsequent latency.

This chapter has provided an in depth analysis of the latency results collected from the traffic, channel, and radio resource management set out in Chapter 3 & Chapter

4. The latency results contained within show the viability of the proposed Lotka-Volterra Resource Allocation and Scheduler scheme for providing support for the Smart Grid over a wireless telecommunications network. Furthermore, the scheme also highlights the marginal impact of Smart Grid inclusion in a pre-existing, high traffic network due to the dynamics of the Lotka-Volterra Equation. Whilst latency is not improved by using this scheme, it supports the co-existence of regular communications traffic and Smart Grid traffic with no extra capital investiture required. This has real-world effects as Governments and Grid Operators will be more willing to apply Smart Grid technologies if there is no requirement to build a dedicated Smart Grid communications network (which may cost more than the technologies and applications it will support). The next chapter analyses the throughput of the Lotka-Volterra Resource Allocation Scheme and how it performs against other schemes.

Chapter 7.
Throughput Analysis & Results

Throughput is a key metric for calculating the quality of a wireless data link. It is the measure of the number of information bits received without error per second. Following popular convention, it will be quantified in bits/second in this research. Certainly, this quantity should ideally be as high as possible. Therefore the optimization of the throughput in a wireless data network is paramount. This thesis explores the current throughput optimization models in literature and then evaluates it against the proposed Lotka-Volterra algorithm designed in the previous section.

This chapter looks at the problem of optimizing throughput for a packet based OFDM wireless data transmission scheme. It does so by allocating the subcarriers in an LTE OFDM downlink environment based on the population dynamics as modelled by the Lotka-Volterra equations. The Lotka-Volterra Resource Allocation Scheme allocates subcarriers to users based on current and future user requirements. Future requirements of certain classes of communication data can be ascertained by previous history of repetitive nature. This differs from other research in that the L-V Resource Allocation Scheme also provides fairness and differentiation between differing classes of communication data. Whilst the number of classes in this research was chosen to be three, it is in fact limitless providing the basis for uses in other fields where resource allocation can provide performance gains.

7.1 ASSUMPTIONS

Because this research is based on allocation of a large scale telecommunications network with many factors that could affect its performance, it was necessary to employ certain assumptions in the simulation and analysis of the results in this thesis. The wireless communication channel is home to many differing factors that can affect the received signal.

In this research, path loss, shadowing and multi-path were considered in the modelling of the communications channel. Each of these sources of degradation in the received signal are stochastic quantities that vary over time. The channel model used in this research was a Rayleigh fading channel inherent with randomness but was chosen not to vary over time. The time varying nature of the Rayleigh fading channel was not included as it provided no extra insight into the validity of the Lotka-Volterra Resource Allocation Scheme and would have added further complexity. The Lotka-Volterra Resource Allocation Scheme re-evaluates the communication environment every 20ms time block (i.e. every LTE time slot) and allocates resources based on class requirement and queue sizes which is unaffected by a changing channel. As Smart Grid devices will be stationary, their channel variance overtime will be close to zero, thereby alsonullifying the need for a changing channel.

The mobility of users was embedded in the Rayleigh Channel design incorporating a certain degree of temporal variation. However, actual mobility was not modelled or considered due to Smart Grid devices being stationary and the extra complexity in the model to introduce mobility. As stated previously, resource allocation by the Lotka-Volterra scheme is not based on parameters affected by mobility of users.

7.2 QUEUE INITIALIZATION

The packet transmissions in a wireless telecommunication system are so numerous that there is seldom enough bandwidth for all devices seeking to communicate, or be communicated with, to be allocated a communications channel concurrently.

Therefore telecommunications systems utilize queues to store data awaiting processing and transmission. When a communication channel is released and is available, the channel is allocated to the next user in the queue. This ensures that packets are communicated instead of being dropped by system during periods of high traffic.

During initialization of the system the queue size is zero and all packets are allocated to available subcarriers. As packet and transmission requests increase overtime, the number of allocated subcarriers reaches its limit. Therefore, a queue is used to store any packets awaiting to be transmitted. The Lotka-Volterra Resource Allocation Scheme Scheduler is able to determine the type of packet by header information and places the packets into either the Data, Voice or Smart Grid queue.

7.3 BANDWIDTH REQUIREMENTS

Unlike other Resource Allocation schemes, the Lotka-Volterra Resource Allocation Scheme uses both prior and upcoming periodic traffic events (e.g. update requests) to ensure optimal bandwidth allocation to classes. The effect and optimal scheduling of periodic traffic will be explored further in Chapter 8 however it does affect the allocation between the classes and will therefore be briefly explored in this chapter. The growth rate, as determined by Lotka-Volterra Resource Scheduler by examining queue lengths and upcoming periodic traffic provides the basis for the bandwidth allocated to each class. Figure 7-1 shows the packet requests for the three classes of information in the network: Voice; Data; and Smart Grid. As defined, the Data class clearly transmits the most packets over the network, followed by Voice and Smart Grid classes respectively. The number of packets transmitted by the system clearly passes the threshold number of subcarriers and therefore must use a queue.

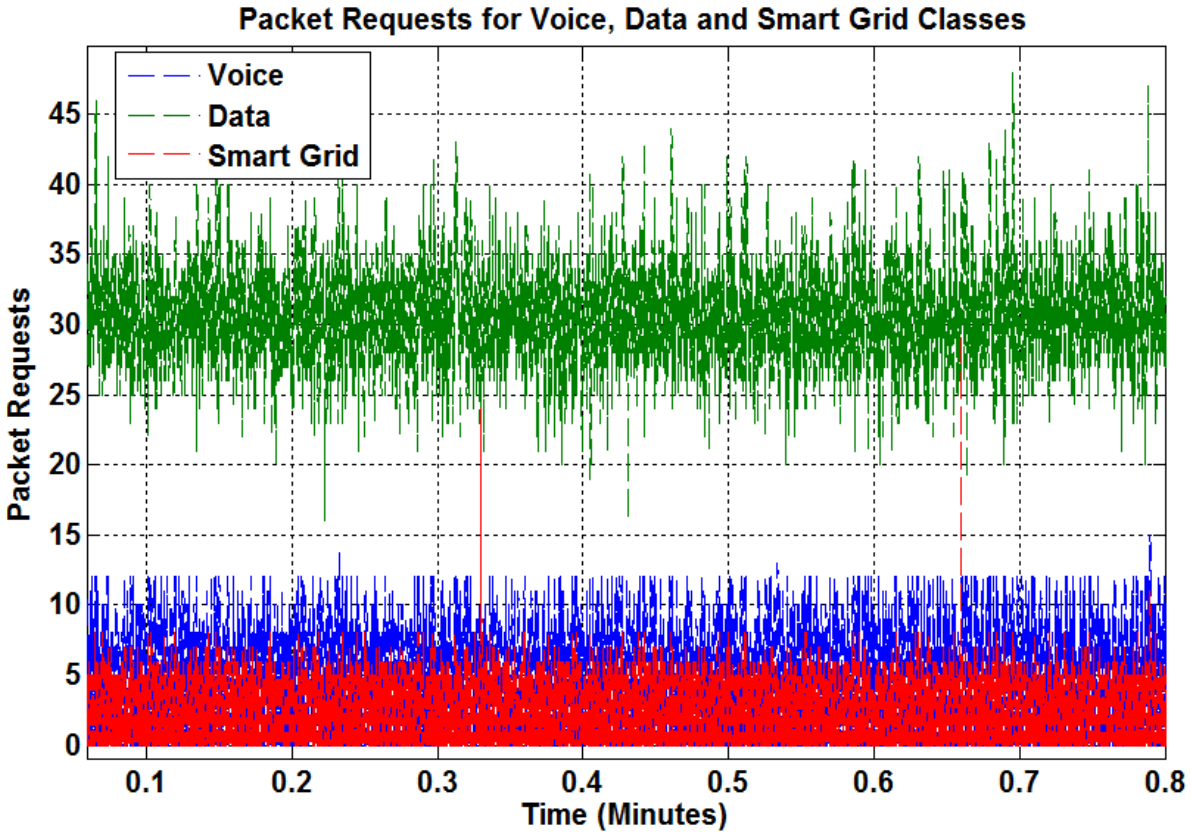

Figure 7-1 - Packet Requests for the Three Classes; Voice; Data; Smart Grid

7.4 POWER ALLOCATION TO SUBCARRIERS

Multi-User Gain is used to describe the improved performance when the QoS requirements of a Multi-User environment is exploited as opposed to using random or sequential resource allocation. OFDMA matches well to the Multi-User Diversity scenario: a subcarrier that is of low quality to one user may be of high quality to another user and can be allocated accordingly [18]. This is the basis of the Resource Allocation scheme in this research. The power allocated to the LTE subcarriers is non-uniform as shown in Figure 7-2. By applying a Gaussian relationship to the power allocated to the subcarriers, the system is able to provide a further level of diversity and such can suit the requirements of a Multi-User environment better. For example, a user with poor channel conditions and suffering from high path loss due to low proximity to the eNB should still be able to access the network. In this example, the user would be allocated a subcarrier with high power to ensure acceptable QoS.

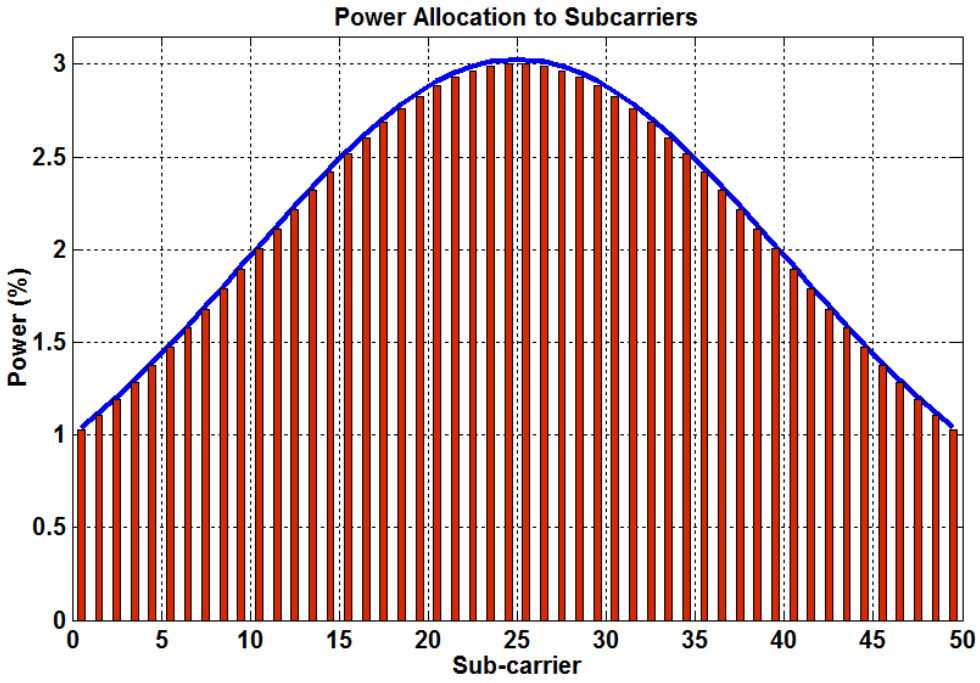

Figure 7-2 - Non-Uniform Power Allocation To Subcarriers

7.4.1 Subcarrier Allocation to Classes

Thus far, the system has determined the growth rates of each class and also calculated the length of each class queue. Both quantities are used by the Lotka-Volterra Resource Allocation Scheme. The growth rate determines the token order in which the classes can select subcarriers. Each iteration, the class with the greatest growth rate, has first choice of remaining subcarriers.

Once the classes have 'bought' all the subcarriers, the allocation of each subcarrier to a user must commence. The allocation, as explained in Chapter 4, is based on attaining the highest average Multi-User Gain. This takes into account the Power Allocated to the Subcarriers, the Channel Gain experienced by the UEs, and the sharing of the resultant gains between the UEs. This ensures that, just because a UE is closer to the eNB, it is not necessarily allocated the subcarrier that would produce the highest Multi-User Gain. This guarantees access to high quality channels to UEs close to the boundary, thereby increasing average Multi-User Gain at the expense of the Maximum Attainable Gain.

A snapshot of the final bandwidth allocated by the Lotka-Volterra algorithm is shown in Figure 7-3. The cyclical nature of the Smart Grid traffic can be seen in the formation of the peaks at 0.1 & 0.3 minute intervals. At these times, the Periodic Traffic is being transmitted and the Smart Grid. In between the large peaks, the Smart Grid is communicating Sporadic Traffic only.

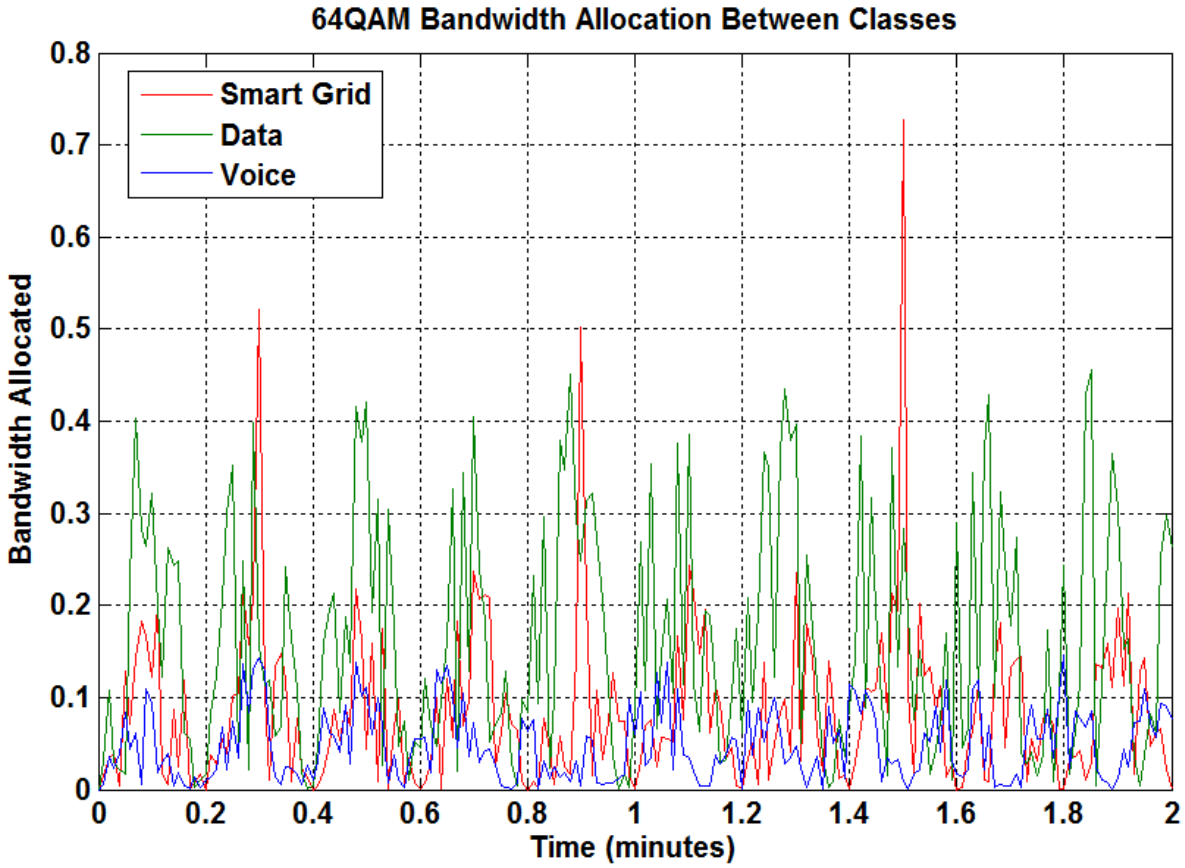

Figure 7-3 - Bandwidth Allocation Between Classes Over Time

During the peaks the Smart Grid class requires a large percentage of the bandwidth. This correlates to times when all the SMI and/or PMU UEs are receiving a status/update packet at the same time. The update times of both PMU and SMI networks were chosen to update at coinciding intervals to showcase a worst case scenario. At this time, the system is seen to allow more bandwidth for the Smart Grid class to ensure low latency and high throughput. The Periodic Traffic have thin spikes and quick recovery due to the L-V scheduler being aware of upcoming mass packet transfer by the SG class and pre-allocating resources. This ensures that the system can quickly dispatch the Smart Grid packets with the effect on UEs in the Data and Voice classes minimized. As mentioned above, voice calls transmit no data for

approximately fifty per-cent of the time. This is represented in Figure 7-3 by the on/off nature of the voice traffic.

7.5 THROUGHPUT ANALYSIS

The throughput results were calculated using the following equation:

$$T = \left(\frac{L-B}{L}\right)\left(\frac{\frac{P}{N_0}}{SNR}\right)P_s \tag{7-1}$$

Where P_s is the recorded Packet Success Rate in Figure 4.12 and SNR is displayed in Figure 4.13. L is the length of the information in bits. B is the error correcting bits required as defined by the coding rates described in Section 4.3.2.3. This essentially bases the throughput calculations on the SNR of the UE. The Power of the allocated subcarrier is based on Figure 7-2 and the packet lengths are defined in Table 4-1. The individual allocation of subcarriers to each UE is defined by the following relation:

$$\sum_{u=0}^{U} max \sum_{n=0}^{N} \frac{T_{u,n}}{T_{avg_{u,n}}} \tag{7-2}$$

which maximizes average user throughput. This is the basis of the subcarrier selection defined in Algorithm 7-1 below.

1: Algorithm for Subcarrier Allocation
2: %INITIALISE%
3: Let N be the set of available subcarriers at time interval t
4: Let U be the set of schedulable individual class UEs
5: %MAPPING subcarriers to UEs%
6: ***For*** $i = 0$ *to* n ***do***
7: calculate T_n based on buffer status reports and channel conditions
8: map data packets of *i*th UE to require subcarriers
9: **End For**
10: Sort U in ascending order in terms of SNR
11: **While** $\{U\} \neq 0$ **do**

12: find $n \in \{N\}$ with $max(T_n)$
13: **if** n is not allocated for future periodic traffic **then**
14: assign $[Index : Index + n]$ subcarriers to u
15: $\{N\} \setminus \{index + n\}$
16: $\{U\} \setminus \{u\}$
17: **End if**
18: $Index = Index + n$
19: **End While**

Algorithm 7-1 - Subcarrier Allocation to Individual UEs

This maps subcarriers to UEs by maximizing the average throughput rate. The results of such an allocation relationship are displayed in the following sections.

7.6 LOTKA-VOLTERRA RESOURCE ALLOCATION RESULTS

The results of the Lotka-Volterra Resource Allocation Scheme are displayed in the figures below. The model was tested using three modulation methods, namely QPKS (4QAM), 16QAM & 64QAM. When optimizing individual class throughput, the class is divided into three categories defined by their SNR. These categories are SNR of {0-10} for UEs close to boundary; {10-20}; and {20+} for UES near the eNB (see Equation 7-3). This is clearly shown in Figure 7-4 to Figure 7-12, with a discontinuation of SNR to throughput relationship occurring at 10 and 20 dB. These results were presented as throughput analysis in [45] for the proposed Lotka-Volterra Resource Allocation and Scheduler Scheme.

$$SNR = \begin{cases} 0-10 & \rightarrow Category\ A \\ 10-20 & \rightarrow Category\ B \\ 20+ & \rightarrow Category\ C \end{cases} \quad (7\text{-}3)$$

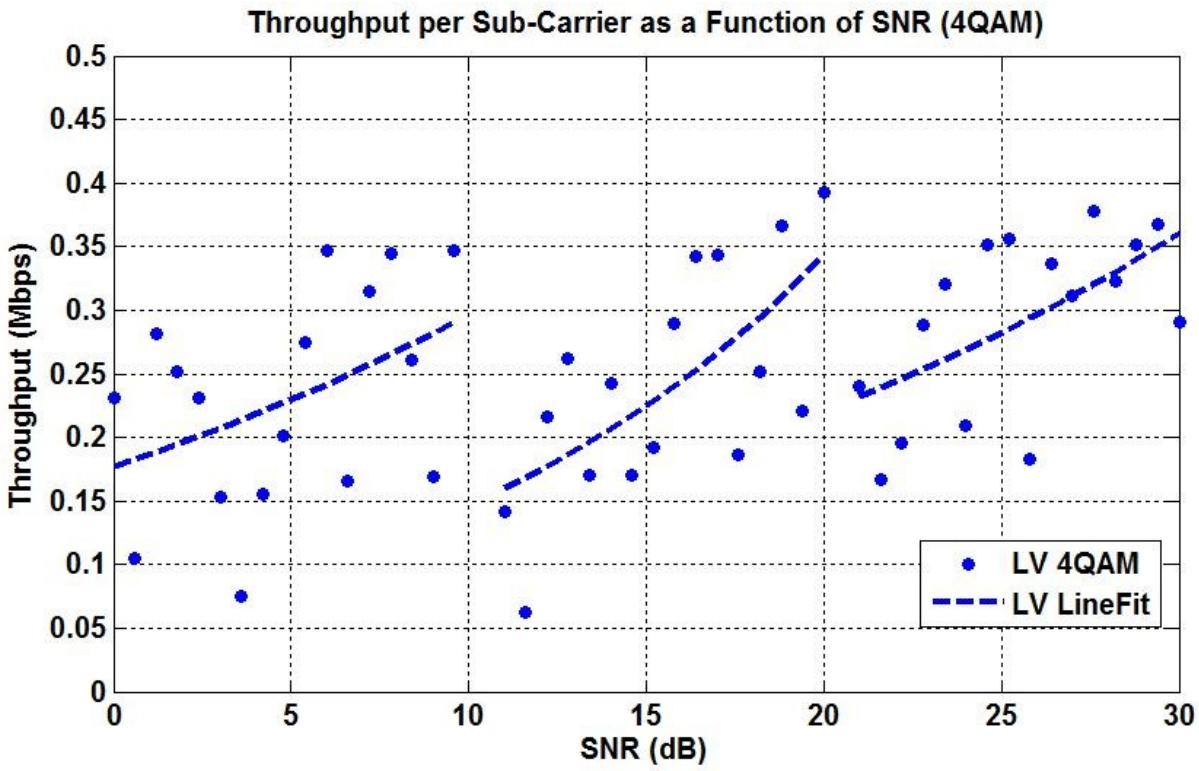

Figure 7-4 - Lotka-Volterra Resource Allocation Scheme Throughput per Sub-Carrier as a function of SNR on 4QAM Modulation

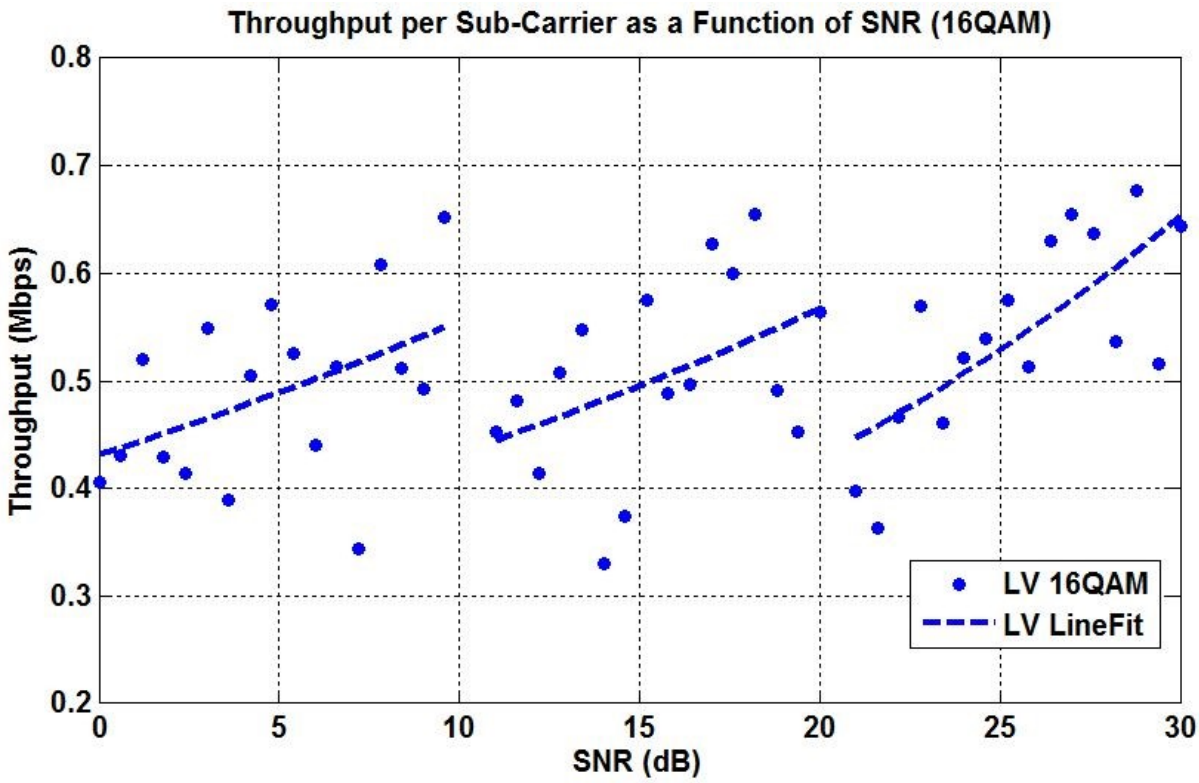

Figure 7-5 - Lotka-Volterra Resource Allocation Scheme Throughput per Sub-Carrier as a function of SNR on 16QAM Modulation

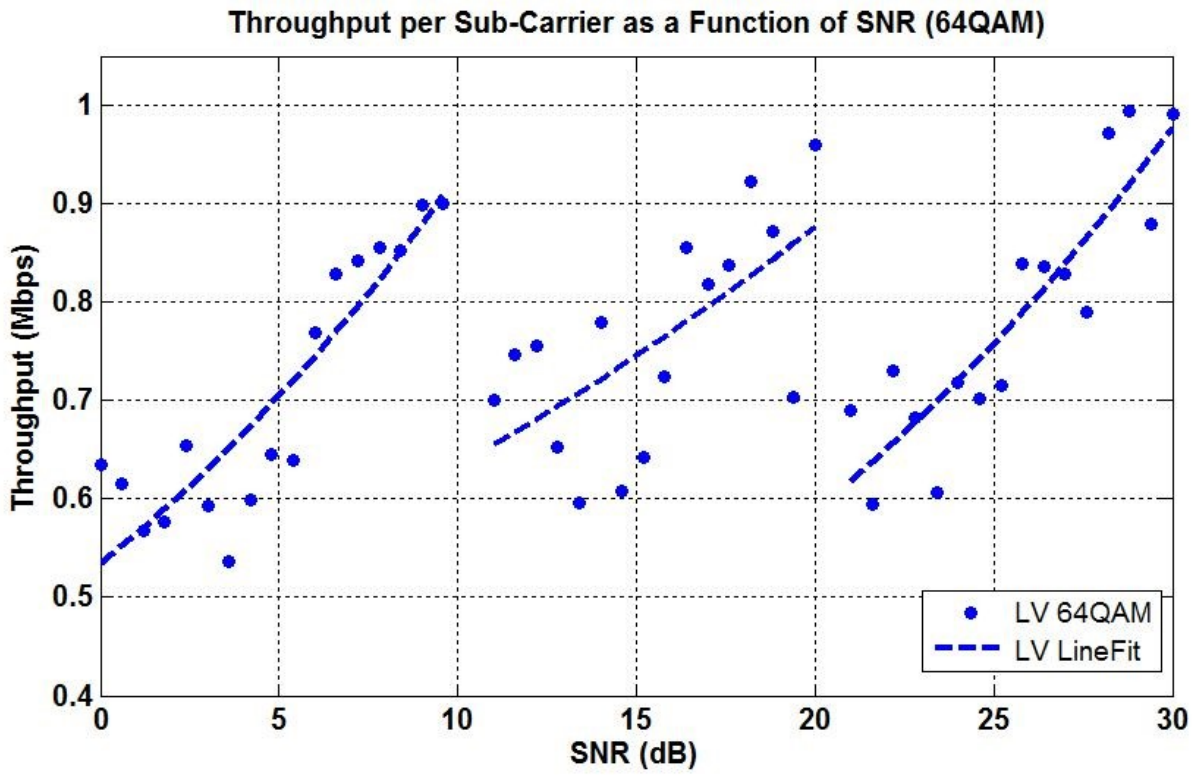

Figure 7-6 - Lotka-Volterra Resource Allocation Scheme Throughput per Sub-Carrier as a function of SNR on 64QAM Modulation

The throughput of the differing modulation modes in Figure 7-4 to Figure 7-6 follow an exponential distribution as their SNR increases. The figure shows that the lower bound of the LV algorithm is higher than if the class was not fragmented into three categories. This slightly affected the maximum rate by decreasing it marginally. However, it provided higher average rates to users with an SNR below 20dB.

Figure 7-4 shows the performance of the Lotka-Volterra Resource Allocation Scheme using QPSK Modulation. The throughput reaches a maximum of just under 0.4Mbps and a minimum around 0.075Mbps. The throughput at low SNRs were affected by signal degradation produced by high attenuations. The average throughput remained high for all three categories, rising exponentially with SNR.

The 16QAM modulation results of the Lotka-Volterra Resource Allocation Scheme are shown in Figure 7-5. The best performance is found in Category C and is due to high SNR values

The spread of results are very high in the 16QAM & QPSK modulation schemes, most noticeably in Category A ({0-10} SNR). This is due to higher SNR requirements for

Error Correction Coding at low modulations which in turn produced higher errors, and thus more re-transmissions.

As expected, the throughput is highest in 64QAM mode as shown in Figure 7-6. However, the largest range of values was also found in the 64QAM modulation mode which could be due to the higher BER in 64QAM. As the SNR decreases, the number of errors or possible re-transmissions will increase. This is a factor in the diminished performance of the 64QAM mode in Category A.

In each of the three Modulation Modes, the fairness is apparent in the Lotka-Volterra Resource Allocation Scheme. This can be measured by the number of low performing (below average) UEs in each Category remaining constant. Whilst the system could have allocated all UEs in Category C high-gain subcarriers, the high gradient of the average (particularly in 16QAM & 64QAM) signifies that it in fact allocated low-gain subcarriers to the advantage of UEs with low SNR.

7.6.1 Class Differentiation in Lotka-Volterra Resource Allocation Scheme

Thus far, the results have only highlighted the throughput of UEs and have not yet differentiated between the classes the UE belonged to. Section 7.6.1 will explore the throughput of the three classes: Smart Grid; Voice; & Data. As with the previous section (Section 7.6), the Lotka-Volterra Resource Allocation Scheme is examined in QPSK, 16QAM and 64QAM modulations. It should be noted that the subcarrier numbers are not the same as those Figure 7-2 as they have been arranged in an ascending order.

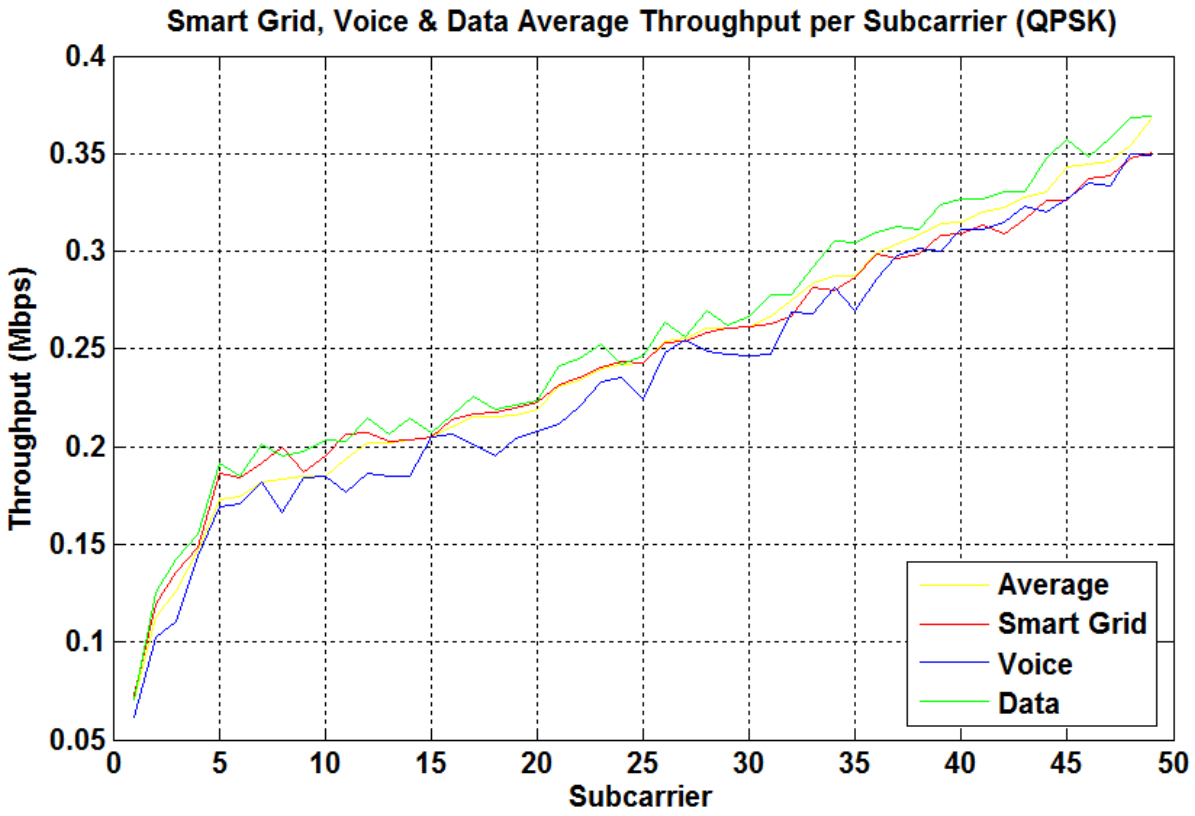

Figure 7-7 - Average Throughputs for Smart Grid, Voice and Data Classes Using QPSK Modulation

Figure 7-7 shows the throughputs of the Smart Grid, Voice & Data classes using QPSK modulation. The throughput roughly follows a linear relationship apart from subcarriers 1 ↔ 5. This could be due to high channel interference or low received signal power due to fading, or a combination of both. The linear region of Figure 7-7 accounts for a linear Multi-User Gain, which correlates to high fairness. This is confirmed by the absence of an exponential growth relationship for one of the classes, which is indicative of random resource allocation.

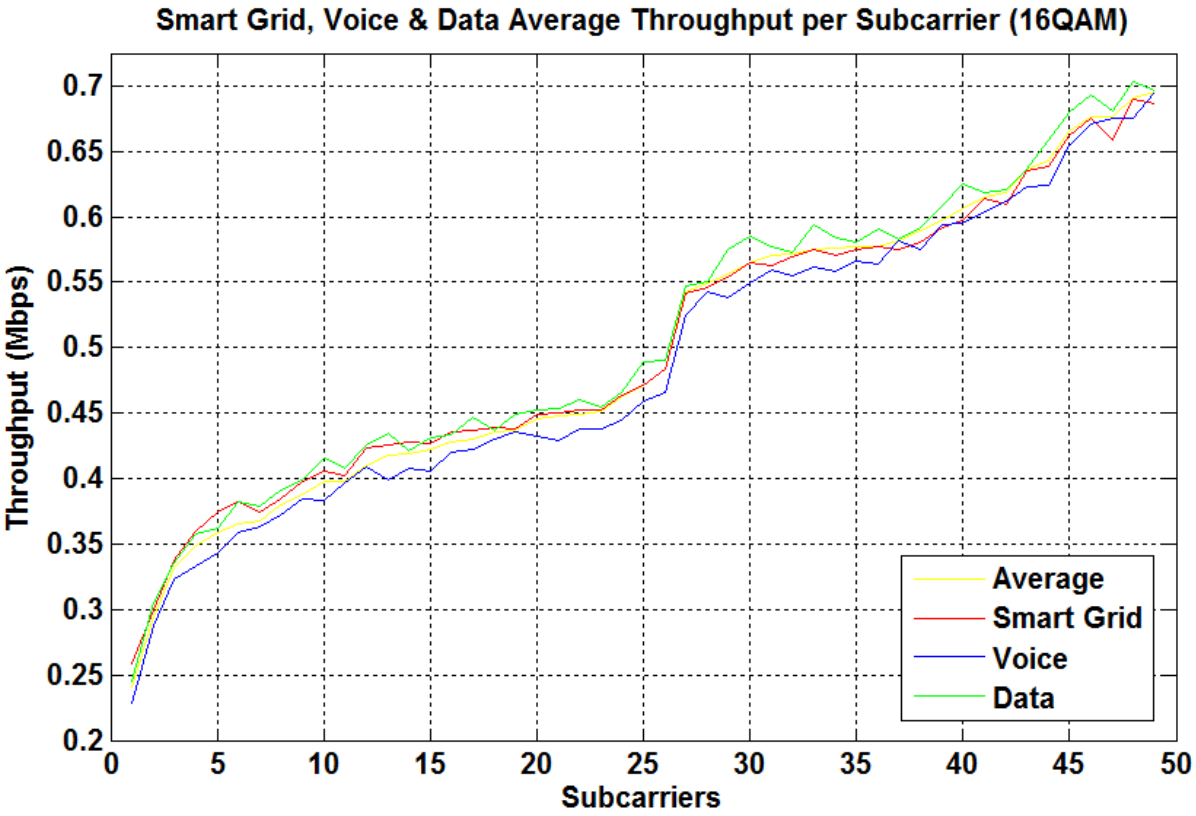

Figure 7-8 - Average Throughputs for Smart Grid, Voice and Data Classes Using 16QAM Modulation

The throughput results for the differing classes using 16QAM Modulation are shown in Figure 7-8. The throughput relationship between the subcarriers is roughly linear with some regions of higher growth. Subcarriers 1 ↔ 3 provide the lowest performance most probably due to UE remoteness from the eNB or poor channel conditions. Conversely, subcarriers 45 ↔ 50 provide high throughput to their allocated UEs due to close proximity to the eNB and/or good channel conditions. There is also a region of rapid growth in throughput in the region of the twenty-seventh subcarrier. This growth is due to the higher bit rate afforded by higher order 16QAM modulation mode. At higher SNR ratios, the system has lower bit error rates due to more precise mapping of symbols at the receiver demodulator. It is due to this higher bit rate that the throughput for 16QAM is higher than that in QPSK (4QAM) modulation mode.

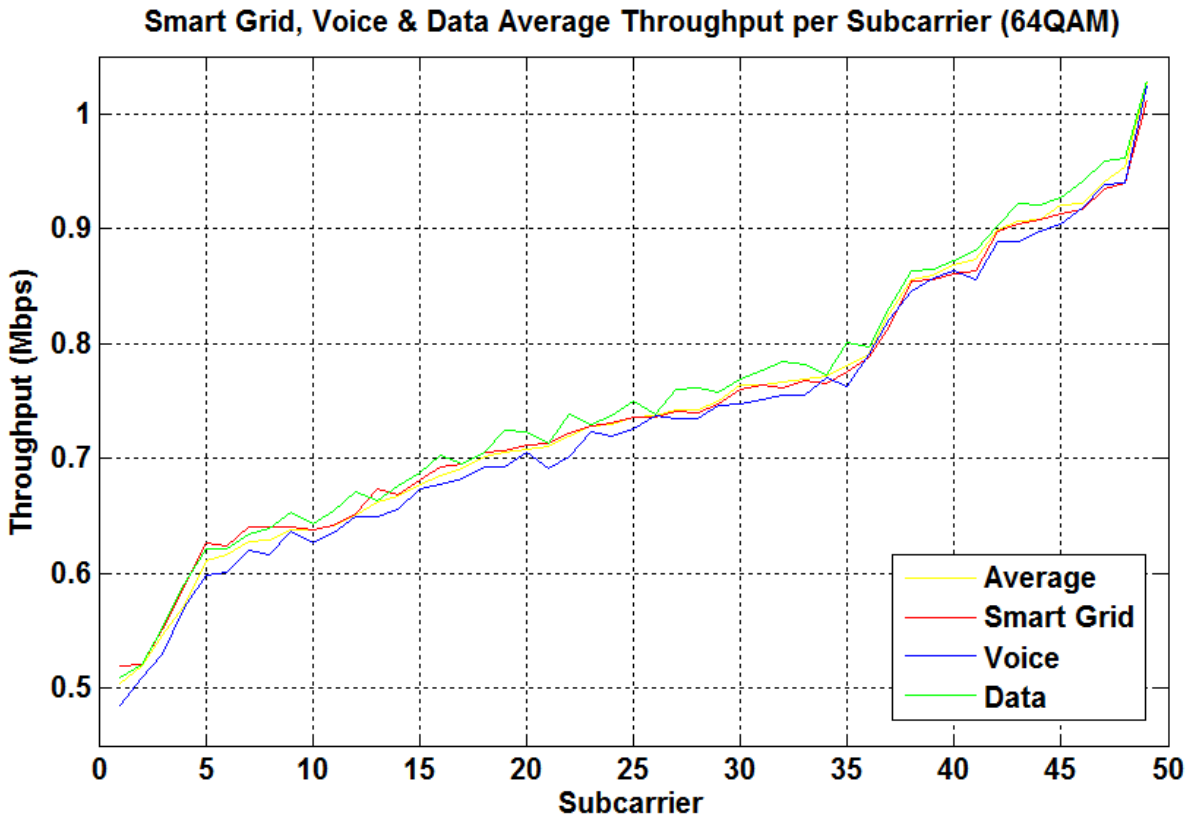

Figure 7-9 - Average Throughputs for Smart Grid, Voice and Data Classes Using 64QAM Modulation

Figure 7-9 shows the throughput of Smart Grid, Voice and Data classes using 64QAM modulation. As with the previous modulation modes, the first few subcarriers afford a low throughput due to poor channel conditions and/or high path loss. The region of high throughput gain past subcarrier 35 is due to the higher order modulation of 64QAM. The lower resolution of the 64QAM bit-map constellation requires a higher SNR than 16QAM to ensure lower bit error rates by providing precise symbol mapping by the receiver demodulator. It is only at higher SNR that bit error rates reduce (see Figure 5-7 & Figure 5-8), which differs to 16QAM. In 16QAM, the symbol distance in the constellation is larger allowing for higher levels of interference. This means that whilst the data rate for lower order modulation signals may be lower than higher order, the bit error rate may be lower producing higher throughputs, depending on the SNR of the UE.

In all three graphs (Figure 7-7, Figure 7-8 & Figure 7-9), there are slight differences in the throughput on subcarriers gained by the classes. For most subcarriers, the data class was able to achieve the highest throughput. Due to the number of data packets

in the network, the data class is always allocated a large amount of bandwidth. Therefore, when the Lotka-Volterra Resource Allocation Scheme enables the bidding between classes, the data classes gains a minor advantage by having a larger budget of power allocated to it. However, the other classes still closely follow the data class throughput relationship. This is due to the subcarrier allocation based on growth rates. Hence, whilst the data class may have the largest power budget, it does not necessarily mean it will win the best subcarriers. In fact, the power budget size only correlates to the number of allocated subcarriers, not their quality. This allows classes to allocate higher power subcarriers, or subcarriers, that provided the highest gain to UEs that have poor channel conditions or large path fading. This results in an overall higher average throughput for all classes at the expense of the maximum throughput of the network.

7.6.2 Comparison Between Lotka-Volterra & Other Resource Allocation Schemes

A comparison between the two Radio Resource Allocation schemes outlined in Chapter 2 is now examined. The Maximum Sum Rate seeks to maximize the amount of data communicated through the network. This is achieved by maximizing the sum rate of all users given a total transmit power constraint. This often leads to the allocation of most of the resources to the UEs closest to the eNB.

The other RRM scheme compared is the Proportional Rates Constraints scheme. PRC is similar to the MSR in which its objective is to maximize the sum rate of all users, albeit with an added constraint that each user's data rate is proportional to a set of pre-determined system parameters.

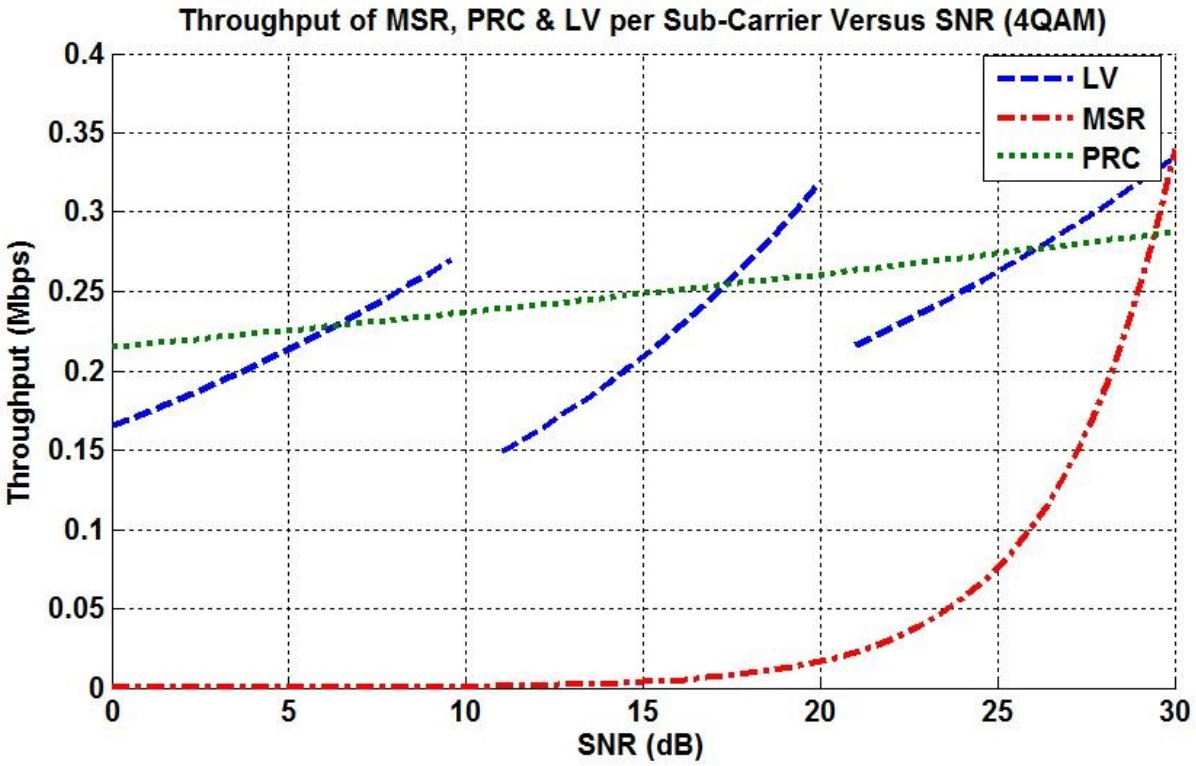

Figure 7-10 - Throughput Comparison Between Maximum Sum Rate (MSR), Proportional Rate Constraints (PRC) & Lotka Volterra Resource Allocation Scheme in 4QAM Modulation

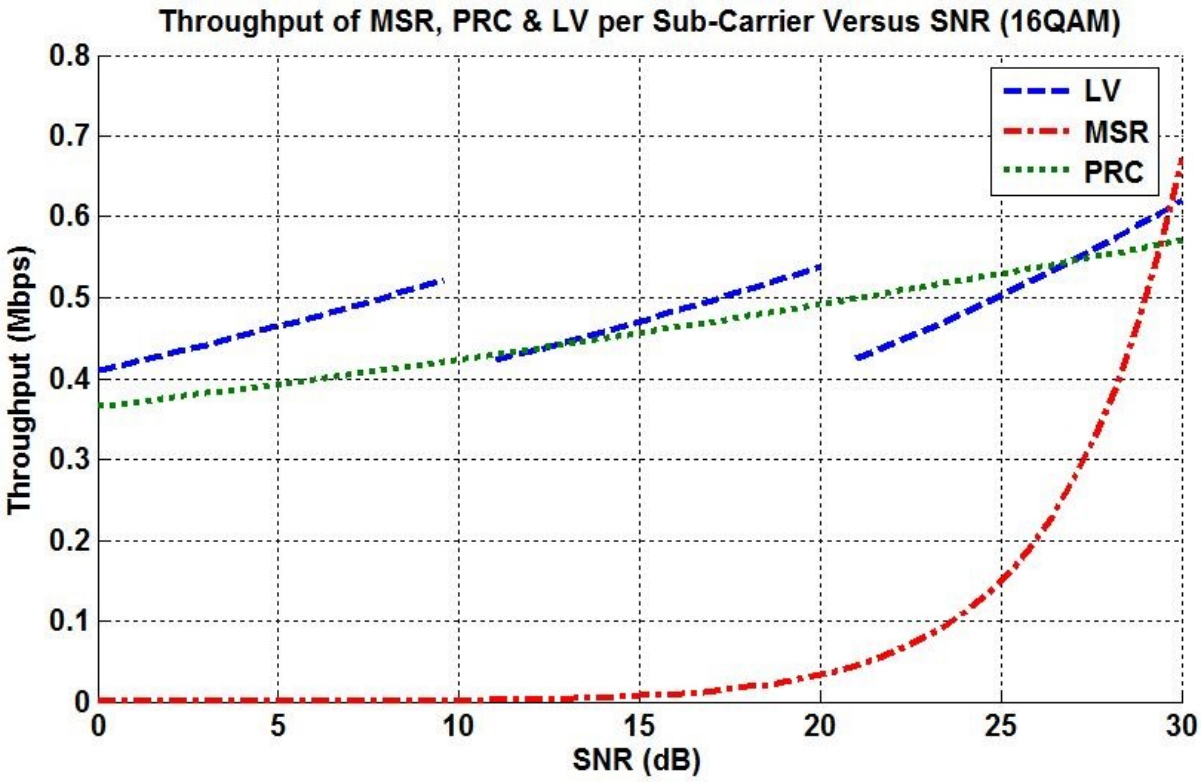

Figure 7-11 - Throughput Comparison Between Maximum Sum Rate (MSR), Proportional Rate Constraints (PRC) & Lotka Volterra Resource Allocation Scheme in 16QAM Modulation

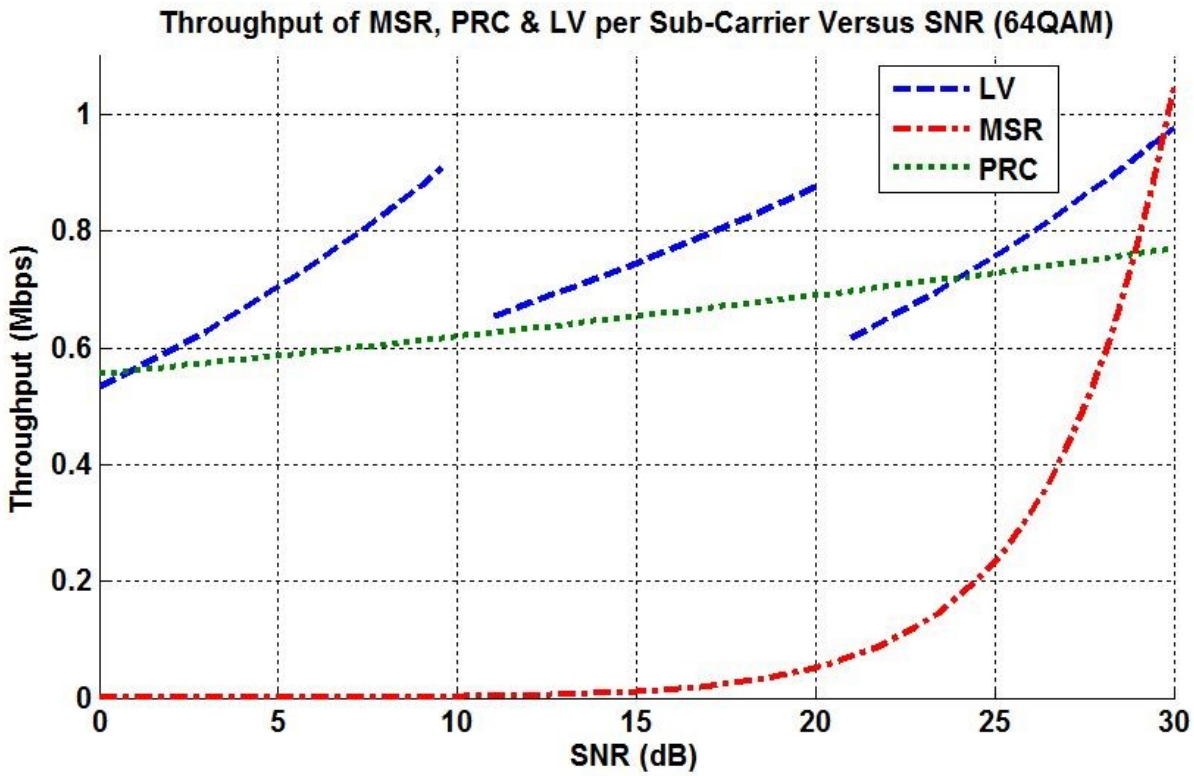

Figure 7-12 - Throughput Comparison Between Maximum Sum Rate (MSR), Proportional Rate Constraints (PRC) & Lotka Volterra Resource Allocation Scheme in 64QAM Modulation

Figure 7-10, Figure 7-11 and Figure 7-12 compares the three schemes, Maximum Sum Rate; Proportional Rates Constraints and Lotka-Volterra Scheme collectively using three differing modulation schemes. The Maximum Sum Rate algorithm performs best at high SNR. However it performs poorly at low SNR, allocating close to no resources to UEs operating further away from the eNodeB. Conversely, the Proportional Rates Constraint algorithm was able to allocate resources proportionately to all users in a linear relationship to the increasing SNR. This produced a lower peak data rate and does not fully optimize QoS by exploiting the diversity of a multi-user environment. The Lotka-Volterra algorithm was found to share resources well between users, favoring those that had higher SNR to quickly release the sub-carrier thus reducing latency. However, the subcarriers with large amounts of power (and consequently most sought after) are shared equally between the categories of SNR, allowing an overall higher average throughput.

In Figure 7-10, the three schemes are compared using QPSK modulation. The Lotka-Volterra Resource Allocation Scheme provides throughput in the range of 0.15 to

0.325Mbps almost eclipsing the MSR maximum throughput value of 0.34Mbps. The MSR can achieve much higher throughput. However, in a high traffic environment the subcarriers are still to a certain degree shared, even if it is only for UEs operating at higher SNR values. On average, using QPSK modulation, the PRC scheme performs better than the Lotka-Volterra Resource Allocation Scheme. This provides a higher minimum throughput at the expense of achieving much higher maximum throughputs.

In both the 16QAM and 64QAM results as shown in Figure 7-11 and Figure 7-12 respectively, the Lotka-Volterra Resource Allocation Scheme performs much better than the PRC scheme. The PRC has slightly higher throughputs at the low end of the high SNR category {20-30} SNR. This can be accounted to the inherent fairness in the Lotka-Volterra Resource Allocation Scheme. The average throughput is increased by allocating a high-power or high-gain subcarrier to a low SNR UE instead of a high SNR UE. It should be noted that at the low ends of the two higher ranges of SNR (i.e. {10 – 20} & {20 – 30}), the throughputs are comparable to that of the low end of the {0 – 10} SNR range. Not only does this prove that the Lotka-Volterra Scheme fairly distributes subcarriers, but also that doing so achieved higher average throughputs than the PRC, which has an inbuilt fairness constraint.

7.7 THROUGHPUT ANALYSIS SUMMARY

The Lotka-Volterra Resource Allocation Scheme produced high average throughput and fairness between the different classes of traffic. It also provided much higher throughput for UEs operating on the 64QAM modulation scheme than those on the 16QAM or 4QAM (QPSK) mode, as to be expected. The spread of data in the 64QAM modulation mode shows that the system is best suited to that modulation. However, it still provides high throughput thereby satisfying QoS requirements in all three modulation modes.

Signals modulated using 16QAM provided the most linear relationship of throughput produced by the fair allocation of subcarriers. This is due to the balance between the extra bits per symbol used in 16QAM, and the moderate spacing between modulated

symbols in the constellation. This provided a higher data rate than QPSK to UEs without compromising the bit error rate which occurs in 64QAM.

The throughput for Periodic Traffic packets from UEs with poor channel conditions and/or high path fading still receive good levels of throughput. This is to be expected as the scheduler will try allocate optimal subcarriers to UEs during periodic communication. In doing so, the subcarrier can be re-allocated for users with lower SNR thereby ensuring higher average throughput with diminished latency.

This chapter provided an in depth analysis of the throughput results collected from the traffic, channel and Lotka-Volterra Resource Allocation and Scheduler set out in Chapter 3 & 4. The results proved that the Lotka-Volterra Resource Allocation Scheme is capable of sharing bandwidth between multiple classes thus improving on Multi-User Gain over other Resource Allocation Schemes. The average throughput for modulation methods QPSK, 16QAM & 64QAM show increased average throughput over the PRC and MSR Resource Allocation Schemes. It is also the case that the Lotka-Volterra Resource Allocation scheme produced higher throughputs when the received signal quality is poor. Chapter 8 builds on this by analysing the fairness of the Lotka-Volterra Resource Allocation Scheme and how it performs against other schemes.

Chapter 8.
Fairness & Smart Grid Optimization Results

This chapter delves into the fairness and optimization of the proposed Lotka-Volterra Resource Allocation and Scheduler Scheme. The fairness of the proposed model was compared against the familiar and popular Proportional Rate Constraints and Maximum Sum Rate opportunistic schedulers.

Fairness is a seldom used metric to measure the performance of a resource allocation and scheduler scheme. Due to varying channel conditions in a wireless network fairness is a desirable property as it provides protection between users. It does this by ensuring that no UE is over served at the detriment of underserved UEs. In opportunistic schedulers, such as the Maximum Sum Rate, UEs with favourable channel conditions are allocated a large proportion of the communications bandwidth. Whilst this produces high network throughput, the UEs with poor channel conditions are consistently denied access. For Smart Grid applications, there is a real necessity to ensure access to the communications channel regardless of the respective UE channel conditions. This requires a fairness criteria to be enacted on the scheduling and resource allocation of all UEs operating in wireless network.

8.1 CRITERIA FOR FAIRNESS

As there is no quantitative value that measures the fairness of the system, it became incumbent to define a scenario to measure the embedded fairness in the Resource Allocation and Schedulers examined. The scenario chosen was to measure the performance of each Opportunistic Scheduler (Proportional Rates Constraints, Maximum Sum Rate & the proposed Lotka-Volterra Resource Allocation and Scheduler) in terms of throughput of the UE with the lowest average Signal to Noise Ratio. The schemes were evaluated on their ability to provide high performance throughput over all subcarriers. The schemes were also evaluated on their ability to allocate resources to the minimum user with an increasing number of UEs operating in the wireless environment.

8.2 FAIRNESS RESULTS

The fairness results for both the Proportional Rates Constraints, Maximum Sum Rate and Lotka-Volterra Resource Allocation and Scheduler schemes will be examined and analysed in this section. As Figure 8-3 will demonstrate, there is no requirement for a figure displaying the throughput analysis for the minimum user using the Maximum Sum Rate algorithm.

During each iteration of the simulation, the minimum user is the UE with the lowest channel gain for the individual subcarrier. The number of UEs accessing the wireless channel is then increased to 200 to examine the fairness exhibited by each scheme during high traffic conditions.

8.2.1 Proportional Rates Constraints Results & Analysis

The results for the analysis of the Proportional Rates Constraints Opportunistic Scheduler are displayed in Figure 8-1. As expected, when the network is flooded with extra UEs the minimum user is affected by lower throughput. This is apparent in Figure

8-1 by the decreasing throughput profile. At this time, the throughput of the minimum user decreases from approximately 0.4 Mbps to 0.3 Mbps.

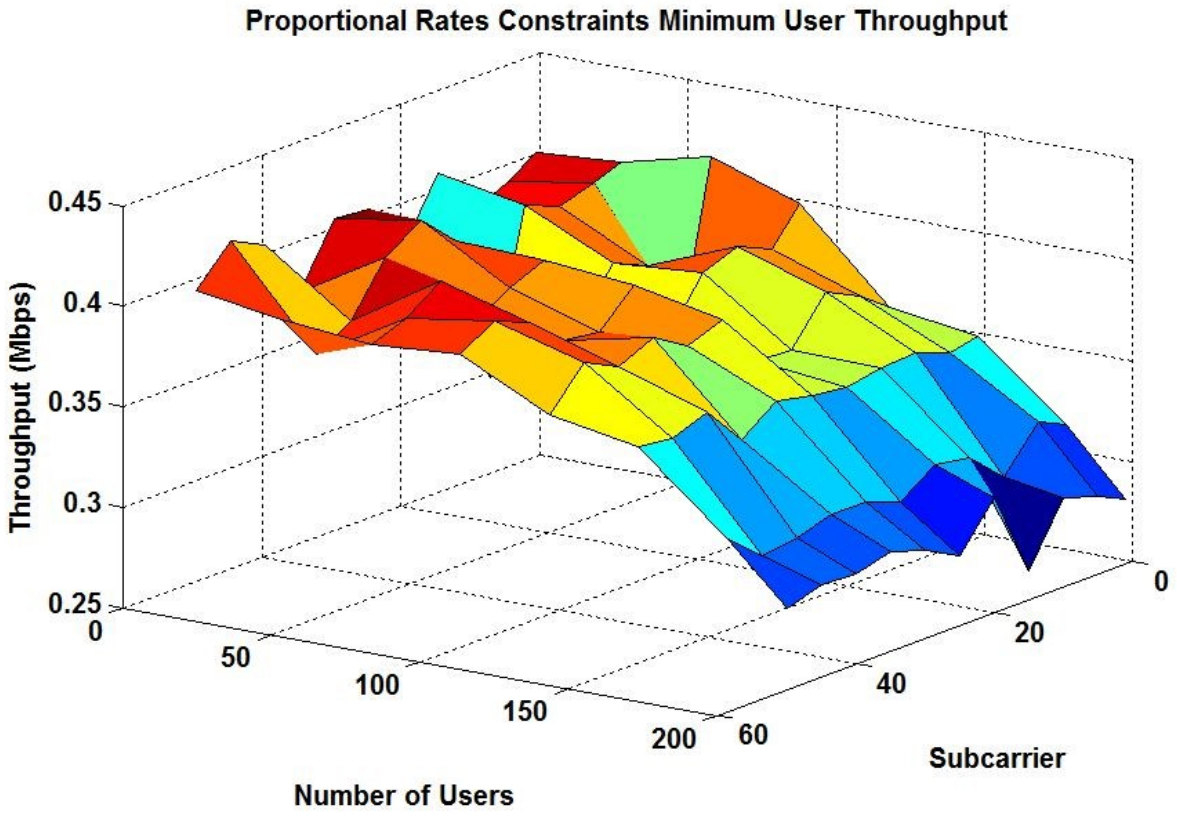

Figure 8-1 - Minimum User Proportional Rate Constraints Allocated Throughput

In some cases, variability in a systems' results or performance can show its ability to adapt dynamically to changing parameters. However, with regards to a wireless communications network, variability is synonymous with unpredictability. The variability in the performance of the PRC opportunistic scheduler results showcase the possibility of a large difference in performance with a slight change in system parameters, such as number of users or allocated subcarrier. This is a basic definition of non-linear systems that exhibit chaos. There is a possibility, then, of a change of state occurring that could produce substantial differences in performance. Therefore, the use of the PRC for scheduling Smart Grid traffic in high traffic wireless channels cannot be ensured with a high probability of confidence.

8.2.2 Lotka-Volterra Resource Allocation and Scheduler Results & Analysis

The results for the analysis of the Proportional Rates Constraints Opportunistic Scheduler are displayed in Figure 8-2. Just as with the PRC Opportunistic Scheduler the Lotka-Volterra Resource Allocation and Scheduler suffers from impaired performance when the number of UEs increase and floods the network with traffic.

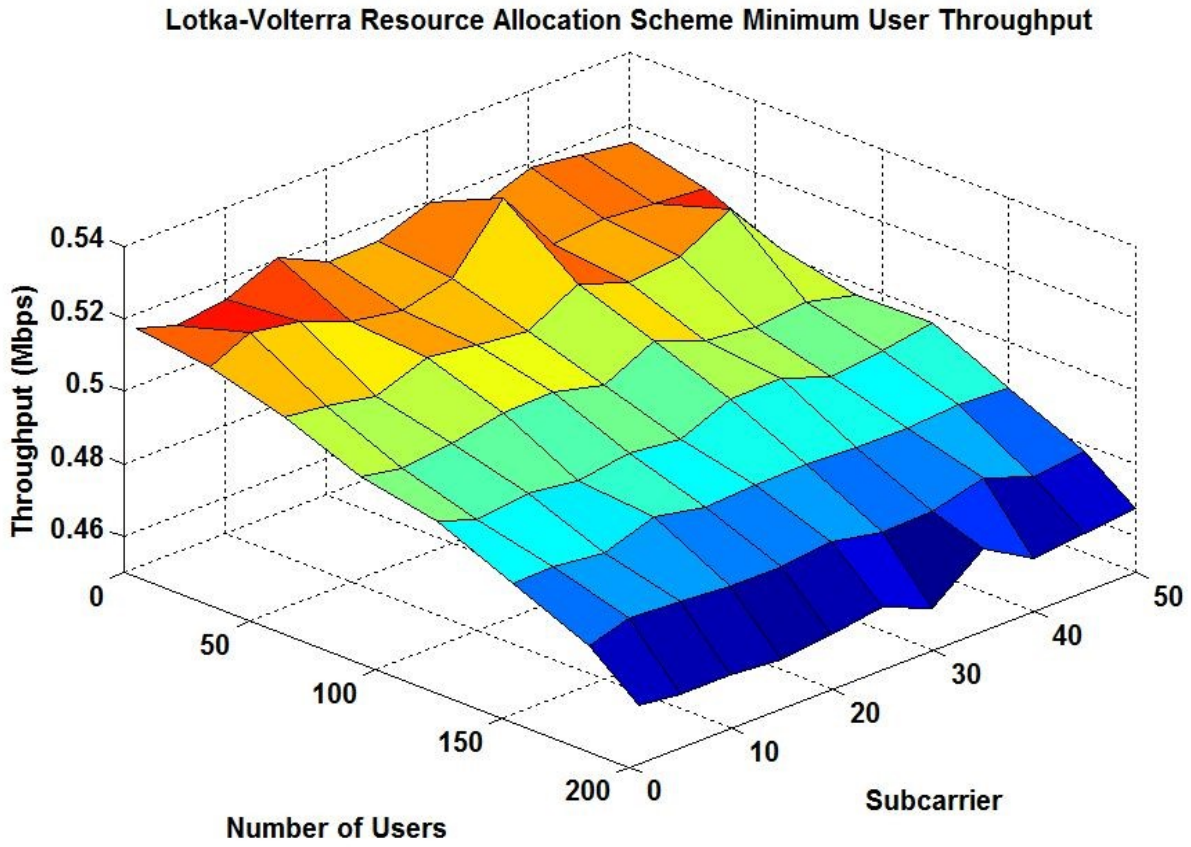

Figure 8-2 - Minimum User Lotka-Volterra Allocated Throughput

The performance of the Lotka-Volterra Resource Allocation and Scheduler shows almost flat plane performance. The variability exhibited in the PRC results in Figure 8-1 are non-existent in the LV results. This is due to small perturbations in the system are mapped onto concentric limit cycles as defined by the LV Hamiltonian Function defined in Chapter 4. This ensures that any small perturbations in conditions doesn't result in large fluctuations in the performance of the system.

Higher performance is also evident in the Lotka-Volterra Resource Allocation and Scheduler Scheme. The LV scheme allocates resources based on the following condition:

$$\sum_{n=0}^{N} max \sum_{s=0}^{S} \frac{T_{n,s}}{T_{avg_{n,s}}} \tag{8-1}$$

which is used to maximize average user throughput. Where $T_{n,s}$ is the throughput of UE n allocated to subcarrier s. The users are selected from the lowest SNR to the maximum SNR. This allows the UEs that would be under-served in most other Opportunistic Schedulers to attain a high performance subcarrier based on their channel conditions. By improving average UE throughput and successfully mapping total transmit power to classes based on the dynamics of the telecommunications environment the minimum user is better served. This showcases not only high levels of fairness, but through embedded flexibility, a level of average throughput performance.

Figure 8-3 compares the minimum user (subcarrier averaged) throughput between the three Opportunistic Schedulers. The subcarriers are averaged to provide easy system comparison between the Opportunistic Schedulers. On average, the Maximum Sum Rate Opportunistic Scheduler performs the poorest. The performance for a singular UE (the minimum UE) provides throughput higher than either the PRC or LV schemes. However, this performance gain is lost once the number of UEs operating in the wireless environment increases. With an increase of UEs operating the performance gain of the minimum user utilizing either the LV or PRC over the MSR scheme is clearly visible.

The throughput performance of the Lotka-Volterra Resource Allocation and Scheduler remains higher than the Proportional Rates Constraints Scheme for all number of UEs. This is achieved by allowing the minimum user first choice of subcarrier by the LV scheme. This helps maximize the channel gain afforded to the minimum user.

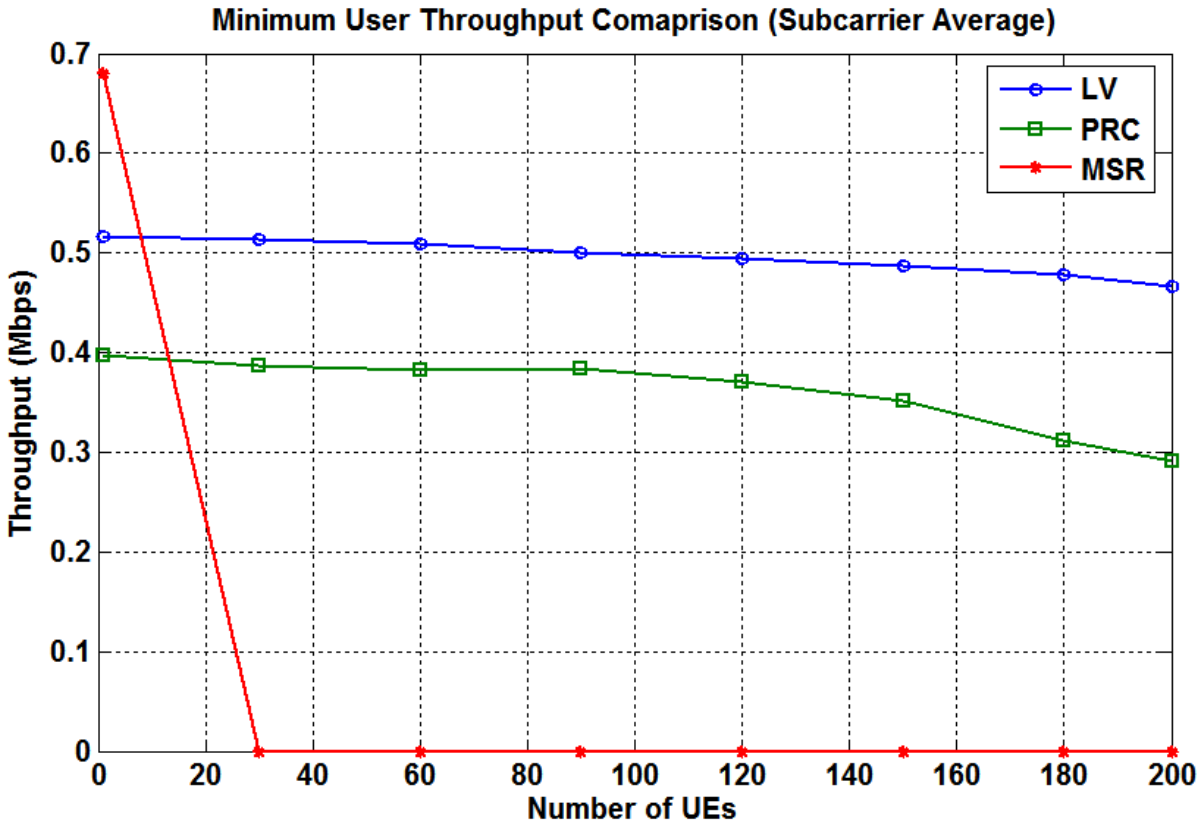

Figure 8-3 - Minimum User Throughput Comparison

Not only is the throughput higher in the Lotka-Volterra Resource Allocation scheme, it also more closely resembles a linear relationship with regards to increasing users. In wireless subcarrier allocation, a linear relationship is beneficial. It can provide incomplete channel state information to the eNB to allow for optimal allocation of subcarriers.

8.3 SMART GRID RESOURCE ALLOCATION OPTIMIZATION

The optimization of subcarrier allocation is pivotal in ensuring the network operates at the highest attainable limits. To optimize Smart Grid traffic, the scheduler pre-allocates subcarriers to Smart Grid packets that occur at periodic intervals. The algorithm used to allocate the subcarriers to SG UEs undergoing periodic traffic can be found in Algorithm 8-1:

1: Algorithm for Smart Grid UE Optimization
2: %INITIALISE%
3: Let N be the set of available subcarriers at time interval t
4: Let U be the set of schedulable SG UEs
5: Sort U by SNR, with $U_1 = lowest\ SNR\ SG_{UE}$
6: **For** n = 1 to size(U)
7: **For** j = 1 to size(N)
8: determine acceptable subcarriers for U_n based on achievable throughput:

$$T_{n,j} = \left(L - \frac{B}{L}\right)\left(\frac{\frac{P}{N_0}}{SNR}\right)P_s$$

9: Sort T_n in descending order
10: **For** i = 1 to size(T_n)
11: **if** (subcarrier i is not allocated)
12: allocate subcarrier i to user n
13: $\{N\} = \{N\} \setminus \{N_i\}$
14: **else**
15: allocate any available subcarrier to user n
16: **End if**
17: **end**
18: **end**
19: **end**

Algorithm 8-1 - Smart Grid Subcarrier Allocation Algorithm During Periodic Traffic

The algorithm determines acceptable subcarriers that can be allocated to a UE based on their throughput requirements. Any single subcarrier that meets the minimum throughput requirement is said to be an optimal subcarrier. UEs are ordered based on increasing SNR and are allocated their first choice of subcarrier (on the condition it hasn't already been scheduled). If no optimal subcarriers are available to be allocated the UE is allocated a non-optimal subcarrier on the basis that in the next iteration an optimal subcarrier may become available. This process ensures swift allocation of subcarriers to Smart Grid traffic with minimal queue latencies. The fixed nature of Smart Grid UEs also enables prior channel state information to be used further speeding up the process of mapping subcarriers to the Smart Grid traffic. The pre-allocation of Smart Grid traffic also provides rapid recovery of the system to sporadic traffic conditions.

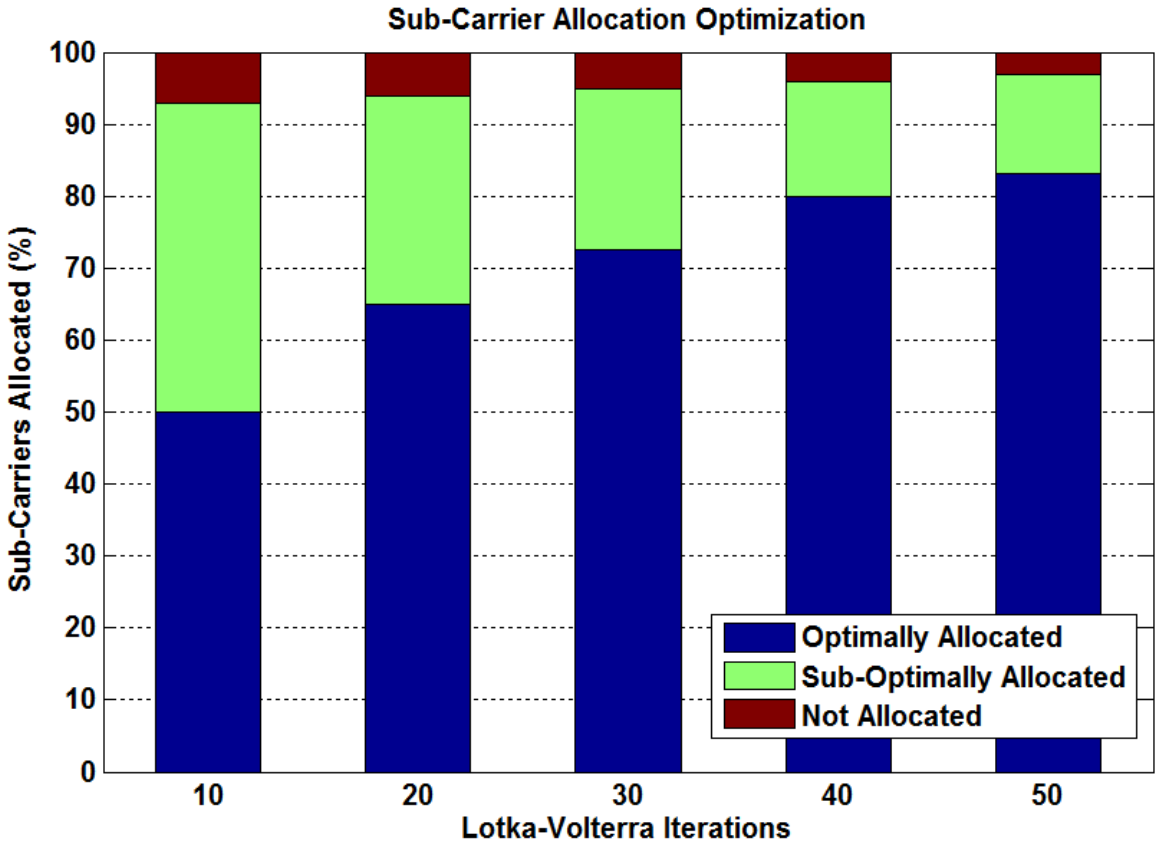

Figure 8-4 - Optimization of Sub-Carrier Allocation Over Lotka-Volterra Algorithm Iterations

The optimization shown in Figure 8-4 shows the proportion of Smart Grid UEs are provided with an optimal subcarrier to communicate over. The system reaches an optimization limit of ~83% regardless of number of iterations involved. This is due to subcarriers not pre-allocated and already allocated before the network is flooded with periodic traffic. Sub-optimal allocation occurs when two or more UEs have the same optimal subcarrier. In this case, the subcarrier is allocated in a first come first served basis. However, due to the cyclical nature of the LV solution, it will still result in the UEs sharing the subcarrier at some point. This optimization can be utilized for any fixed wireless communication device and need not be confined to Smart Grid optimization problems.

8.4 FAIRNESS & OPTIMIZATION SUMMARY

The Lotka-Volterra Resource Allocation Scheme produces high levels of fairness as measured by throughput performance for low SNR UEs. The throughput recorded by the Lotka-Volterra scheme outperformed the Proportional Rates Constraints and Maximum Sum Rate Opportunistic Schedulers.

The throughput of the Lotka-Volterra Resource Allocation and Scheduler provides almost linear performance measured against increasing number of users. This can provide invaluable data to eNBs facing subcarrier allocation decisions with incomplete or missing channel state information. The linear relationship is based on the mapping of wireless network variability to Lotka-Volterra Hamiltonian Limit Cycles. This provides higher performance than the PRC Opportunistic Scheduler that exhibits volatility when the system is slightly perturbed.

Smart Grid traffic is also better optimized by utilizing the Lotka-Volterra Resource Allocation Scheme. The optimization is provided by pre-allocating subcarriers to periodic Smart Grid traffic. Over multiple iterations of the Lotka-Volterra Resource Allocation and Scheduler Scheme faces an optimization limit of approximately 80%. This still provides high level of optimal subcarrier allocation to Smart Grid traffic which carries information of critical importance regarding the stability and security of each nations' largest single piece of infrastructure.

The next chapter provides the concluding remarks of this thesis. It also includes an insight into further research that can build upon the results garnered from this thesis.

Chapter 9.
Conclusion, Limitations & Future Directions

The results contained within this thesis have concluded that the Latency & Throughput requirements for Smart Grid applications have been satisfied, with minimized effect on pre-existing communications traffic. By satisfying the QoS requirements of Smart Grid applications tabulated in Chapter 2, it is this theses view that support for higher Renewable Energy Resources distributed within the Distribution Grid is possible by use of a WAMPAC scheme operating on a wireless OFDM network.

This research has presented a model for harnessing the dynamic nature of telecommunications environments by utilizing the population dynamic Lotka-Volterra equations. Subcarrier allocation to each class is based on growth rates determined by the closed limit cycle solutions of the Lotka-Volterra equations. Subcarrier allocation is applied to future traffic to ensure minimal queue latency in the modelled high traffic environment. By mapping subcarriers based on a population dynamics model it was possible to optimally allocate users to reduce overall latency and increase total system throughput.

With queue wait time included, the latency constraints of 20-200ms for Wide Area Situation Awareness is achievable using the Lotka-Volterra Resource Allocation Scheme. The bandwidth requirements of 600kbps to 1500kpbs are also achievable, with ~forty percent of users able to transmit with throughput higher than 1500kbps and ~seventy percent able to transmit with throughput higher than 600kbps.

The throughput results displayed in Chapter 7 show higher average throughput for the Lotka-Volterra Resource Allocation Scheme than the other Opportunistic Schedulers examined. The proposed Opportunistic Scheduler provided best results for the 64QAM mode of modulation, however, increases in average throughput over other schemes was still evident in 16QAM and QPSK modulation modes.

Chapter 8 examined the fairness exhibited by the Opportunistic Schedulers. The Lotka-Volterra Resource Allocation and Scheduler overwhelmingly provided higher levels of fairness than the other Opportunistic Schedulers. Low variability was recorded by the fairness analysis of the Lotka-Volterra Resource Allocation and Scheduler Scheme. This produces low levels of unpredictability which better suits the wireless communications network which exhibits a high degree of volatility.

Principally, the largely significant results of this thesis prove that an OFDMA based wireless network, such as LTE & LTE-A, can provide support for Smart Grid communications with minimal effect on pre-existing wireless traffic in the network. This has real-world applications due to major disparity in the research community regarding the facilitation of a Smart Grid communications network.

The Lotka-Volterra Resource Allocation Scheme was shown to model a communications environment effectively. The Lotka-Volterra equations provided the ability to quickly adapt to the changing requirements of UEs operating and allocate resources to ensure high QoS. This research has shown that current day telecommunications infrastructure can incorporate Smart Grid traffic without adversely affecting pre-existing data and voice communications in a large way. This paves the way for substantial increases in renewable energy generators operating on the power grid. This is based on the results contain herein that allows for Smart Grid applications to be able to operate successfully in high traffic wireless networks. By doing so, the level of available monitoring and control techniques the Smart Grid can utilize is

increased which can ensure the effective integration of such Renewable Energy Resources.

This research has proven that, utilizing the proposed Lotka-Volterra Resource Allocation and Scheduler scheme, LTE is a viable network for incorporating Smart Grid applications, even in high traffic networks.

This research can also be used as a basis of increasing throughput to fixed position UEs.

9.1 RESEARCH CONTRIBUTIONS

- Successful integration of Smart Grid communications traffic in a high traffic OFDM network. This has real world applications whereby Governments or TSO's could reduce capital expenditure in installing Smart Grid applications by utilizing pre-existing LTE networks.
- Development of a novel Lotka-Volterra based resource allocation and scheduler scheme. The Lotka-Volterra model was able to successfully adapt to a dynamic telecommunications environment and allocate resources accordingly.
- A two tiered approach to resource allocation. Firstly a subset of total transmit power was allocated to each class dependent on their queue growth rate. This growth rate was average sporadic traffic and also incorporated future periodic traffic. Using the allocated power like bidding chips, the classes were able to accumulate selected subcarriers. These subcarriers were then allocated to individual UEs based on their achievable multi-user gain. To ensure fairness, low SNR UEs were given first choice.
- The effects of modulation and coding on reliability, throughput and latency performance was analyzed. The results showed that UEs with low SNR could choose a lower order modulation with higher coding rate to ensure successful delivery of a frame. In the long run, this reduces latency and increases throughput due to negligible frame retransmissions.

- Smart Grid Quality of Service requirements for strict latency, reliability and throughput were satisfied utilizing the proposed Lotka-Volterra Resource Allocation and Scheduler scheme.
- Lotka-Volterra Resource Allocation and Scheduler was able to find an optimal operating point where the integration of Smart Grid traffic had a minimized effect on pre-existing traffic whilst still satisfying Smart Grid application QoS requirements.
- Fairness exhibited by the model exceeded that of common opportunistic schedulers examined. The flat performance for the Lotka-Volterra Resource Allocation and Scheduler can allow eNBs to allocate subcarriers optimally with little channel state information required.
- Optimization of Periodic Smart Grid traffic produced decreased queue latencies at the cost of Voice and Data queue latencies. However, overall queue latency was improved for all classes by Scheduler awareness and allocation of future periodic traffic.
- By satisfying the QoS requirements for WAMPAC, the successful integration of higher total capacity of Renewable Energy Resources is now possible. This can reduce the requirement for carbon-intensive power generation, thus providing direct action against global warming.
- Results need not be constrained to Smart Grid applications. The stationary nature of Smart Grid UEs were utilized to provide optimization of subcarrier allocation. This can be applied to any stationary UE operating in a wireless telecommunications domain.

9.2 LIMITATIONS

In future research, an examination into changing channel conditions and also mobility of users within the cell will be provided. This can be provided by a random walk process and will provide mobility variability in the model. There is no model that can satisfactorily model a wireless channel over time, however, models used in other research are much more extensive. It was chosen to limit the randomness apparent

in the system as it didn't greatly affect the results this thesis provided and should not diminish their merit.

9.3 FUTURE DIRECTIONS

In the future, the uplink communications can be investigated to ensure that LTE SC-FDMA has the capability to uphold Smart Grid QoS requirements whilst also guaranteeing available bandwidth for differing classes of users (for example: smart phone, tablet, fixed & mobile broadband, laptops etc) in the wireless cell.

In this research, the power allocated to subcarriers followed a normal distribution. Whilst this provides greater flexibility for allocating subcarriers in a multi-user diverse environment it contradicts the dynamical nature of the Lotka-Volterra Resource Allocation Scheme. In future research, it would be worthwhile to apply a dynamic power allocation scheme to ensure complete exploitation of the multi-user diversity and the communications gain that can be achieved. This involves subcarrier power allocation to suit individual user requirements, satisfying the constraint that:

$$\sum_{i=1}^{n} P_i < P_{total}, \tag{9-1}$$

where P_i is the power allocated to the i-th subcarrier.

Furthermore, we would like to look at reducing overall power consumption at the eNodeB and also at UEs operating on battery. In this research, the EnodeB supplied a higher bitrate than required if it was possible to do so. By constraining the system to provide QoS requirements without exceeding them we can reduce the overall power consumption and find an efficient operating point.

Bibliography

[1] M. Biabani, M.A. Golkar, A. H. Z. Kasiry, M. Akbari, "Smart grid in Iran: Driving factors, evolution, challenges and possible solutions, "*2011 10th International Conference on Environment and Electrical Engineering (EEEIC),* , vol., no., pp.1-4, 8-11 May 2011.

[2] T. Chong, Y. Kai, C. Shi, S. Han, W. Haifeng, B. Zhiyong, "Distributed channel allocation scheme based on LTE system in smart grid,"Control Conference (CCC), 2012 31st Chinese , vol., no., pp.5582,5585, 25-27 July 2012

[3] P. Hines, K. Balasubramaniam, E. C. Sanchez, "Cascading failures in power grids, "IEEE Potentials", , vol.28, no.5, pp.24-30, September-October 2009.

[4] C. G. Elsworth, The Smart Grid and Electric Power Transmission (1st Edition), Nova Science (New York, 2010)

[5] B. Ummels Wind Integration: Power System Operation with Large-Scale Wind Power in Liberalised Environment, ,Denmark, 2009, Technische Universiteit Delft

[6] C. Li, Y. Sun, X. Chen, "Analysis of the blackout in Europe on November 4, 2006," Power Engineering Conference, 2007. IPEC 2007. International , vol., no., pp.939,944, 3-6 Dec. 2007

[7] X. Chen, C. Deng, Y. Chen, C. Li, "Blackout prevention: Anatomy of the blackout in Europe," Power Engineering Conference, 2007. IPEC 2007. International , vol., no., pp.928,932, 3-6 Dec. 2007

[8] European Photovoltaic Industry Association (EPIA), Connecting the Sun: Solar photovoltaics on the road to large-scale grid integration (September, 2012) <http://www.epia.org/fileadmin/user_upload/Publications/Connecting_the_Sun_Full_Report_converted.pdf> (Accessed: December, 2013)

[9] A. Ghosh, J. Zhang, J.G. Andrews, R. Muhamed, Fundamentals of LTE (1st Edition), Pearson Education (Boston, 2010)

[10] G. Ozcan, M. C. Gursoy, "Cognitive Radio Transmissions Exploiting Multi-User Diversity under Channel and Sensing Uncertainty,"*Communications Letters, IEEE*, vol.17, no.9, pp.1714,1717, September 2013

[11] M. Obaidat, "Keynote 1," *Next Generation Mobile Applications, Services and Technologies (NGMAST), 2011 5th International Conference on* , vol., no., pp.xii,xiii, 14-16 Sept. 2011

[12] S. Lashgari, A. S. Avestimehr, "Timely Throughput of Heterogeneous Wireless Networks: Fundamental Limits and Algorithms," *Information Theory, IEEE Transactions on* , vol.59, no.12, pp.8414,8433, Dec. 2013

[13] W Rhee, J. M. Cioffi, "Increase in capacity of multiuser OFDM system using dynamic subchannel allocation," *Vehicular Technology Conference Proceedings, 2000. VTC 2000-Spring Tokyo. 2000 IEEE 51st* , vol.2, no., pp.1085,1089 vol.2, 2000

[14] Z. Shen, J. G. Andrews, B. L. Evans, "Optimal power allocation in multiuser OFDM systems," Global Telecommunications Conference, 2003. GLOBECOM '03. IEEE , vol.1, no., pp.337,341 Vol.1, 1-5 Dec. 2003

[15] W. Xu, C. Zhao, P. Zhou, Y. Yang, "Efficient Adaptive Resource Allocation for Multiuser OFDM Systems with Minimum Rate Constraints," Communications, 2007. ICC '07. IEEE International Conference on , vol., no., pp.5126,5131, 24-28 June 2007

[16] I. C. Wong, Z. Shen, B. L. Evans, J. G. Andrews, "A low complexity algorithm for proportional resource allocation in OFDMA systems," Signal Processing Systems, 2004. SIPS 2004. IEEE Workshop on , vol., no., pp.1,6, 13-15 Oct. 2004

[17] P. Svedman, S. K. Wilson, L. J. Cimini, B. Ottersten, "Opportunistic Beamforming and Scheduling for OFDMA Systems," Communications, IEEE Transactions on , vol.55, no.5, pp.941,952, May 2007

[18] S. Pietrzyk, OFDMA For Broadband Wireless Access (1st Edition), Artech House Mobile Communications (Norwood, 2006)

[19] P. McDaniel, S. McLaughlin, "Security and Privacy Challenges in the Smart Grid, "*IEEE Security & Privacy,* , vol.7, no.3, pp.75-77, May-June 2009.

[20] V. K. Sood, D. Fischer, J. M. Eklund, T. Brown, "Developing a communication infrastructure for the Smart Grid," *IEEE Electrical Power & Energy Conference (EPEC), 2009*, vol., no., pp.1-7, 22-23 Oct. 2009.

[21] T. M. Overman, R. W. Sackman, "High Assurance Smart Grid: Smart Grid Control Systems Communications Architecture," *First IEEE International Conference on Smart Grid Communications (SmartGridComm), 2010*, vol., no., pp.19-24, 4-6 Oct. 2010.

[22] K. Moslehi, R. Kumar, "A Reliability Perspective of the Smart Grid, "*IEEE Transactions on Smart Grid,* vol.1, no.1, pp.57-64, June 2010.

[23] D. G. Hart, "Using AMI to realize the Smart Grid,"*IEEE Power and Energy Society General Meeting - Conversion and Delivery of Electrical Energy in the 21st Century, 2008*, vol., no., pp.1-2, 20-24 July 2008.

[24] E. Miller, Renewable Energy Focus, *Renewables on the Smart Grid,* (11th May, 2009) http://www.renewableenergyfocus.com/view/1751/renewables-and-the-smart-grid-/ (Accessed: October, 2011).

[25] M. M. He, E. M. Reutzel, J. Xiaofan, R.H. Katz, S. R. Sanders, D. E. Culler, K. Lutz, ,"An Architecture for Local Energy Generation, Distribution, and Sharing," IEEE Energy 2030 Conference, 2008. ENERGY 2008., vol., no., pp.1-6, 17-18 Nov. 2008.

[26] Australian Government: Department of Resources, Energy and Tourism, Smart Grid, Smart City: Factsheet, <http://www.ret.gov.au/energy/Documents/smart-grid/smart-grid-factsheet1.pdf> (Accessed August, 2011)

[27] American Physical Society (APS), Integrating Renewable Electricity on the Grid: A Report by the APS Panel on Public Affairs, <

http://www.aps.org/policy/reports/popa-reports/upload/integratingelec.pdf>, (Accessed: October, 2011)

[28] International Energy Agency, Renewables Information: Beyond 2020 Documentation (2012 edition), < http://wds.iea.org/wds/pdf/Documentation%20for%20Renewables%20Information%202012.pdf> (Accessed: November, 2013)

[29] Australian PV Institute, Mapping Australian Photovoltaic Installations, <http://pv-map.apvi.org.au/historical> (Accessed: December, 2013)

[30] Australian Government, Bureau of Resources and Energy Economics (BREE), 2013 Australian Energy Statistics Update, <http://www.bree.gov.au/publications/australian-energy-statistics> (Accessed: November, 2013)

[31] World Wind Energy Association (WWEA), Key Statistics of World Wind Energy Report 2013, < http://www.wwindea.org/webimages/WWEA_WorldWindReportKeyFigures_2013.pdf> (Accessed: November, 2013)

[32] International Energy Agency (IEA), World Energy Outlook 2013, < http://www.iea.org/publications/freepublications/publication/WEO2013_Executive_Summary_English.pdf >, (Accessed: November, 2013)

[33] American Wind Energy Association (AWEA), 2012 U.S. Wind Industry Market Update, < http://awea.files.cms-plus.com/FileDownloads/pdfs/AWEA%20U.S.%20Wind%20Industry%20Annual%20Market%20Update%202012_1383058080720_3.pdf >, (Accessed: November, 2013)

[34] Clean Energy Council, There's power in wind: national snapshot (April, 2012), < https://www.cleanenergycouncil.org.au/dam/cec/technologies/wind/fact-sheets/Wind-Energy-Fact-Sheet-Theres-Power-in-Wind-National-Snapshot.pdf>, (Accessed: October, 2013)

[35] Union For The Co-Ordination Of Transmission Of Electricity (UCTE), Final Report – System Disturbance on 4 November 2006, <

https://www.entsoe.eu/fileadmin/user_upload/_library/publications/ce/otherreports/Final-Report-20070130.pdf>, (Accessed: October, 2013)

[36] V. Terzija, G. Valverde, C. Deyu, P. Regulski, V. Madani, J. Fitch, S. Skok, M. M. Begovic, A. Phadke, A, "Wide-Area Monitoring, Protection, and Control of Future Electric Power Networks," Proceedings of the IEEE , vol.99, no.1, pp.80,93, Jan. 2011

[37] R. L. King, "Information services for smart grids," Power and Energy Society General Meeting - Conversion and Delivery of Electrical Energy in the 21st Century, 2008 IEEE , vol., no., pp.1,5, 20-24 July 2008

[38] J. Du, M. Qian, "Research and application on LTE technology in smart grids," Communications and Networking in China (CHINACOM), 2012 7th International ICST Conference on , vol., no., pp.76,80, 8-10 Aug. 2012

[39] J. Brown, J. Y. Khan, "Performance analysis of an LTE TDD based smart grid communications network for uplink biased traffic," Globecom Workshops (GC Wkshps), 2012 IEEE , vol., no., pp.1502,1507, 3-7 Dec. 2012

[40] Cisco Visual Networking Index: Global Mobile Data Traffic Forecast Update, 2013-2018. http://www.cisco.com/c/en/us/solutions/collateral/service-provider/visual-networking-index-vni/white_paper_c11-520862.html (Accessed February, 2014)

[41] 3rd Generation Partnership Project (3GPP), LTE, < http://www.3gpp.org/technologies/keywords-acronyms/98-lte>, (Accessed: October, 2013)

[42] Y. Yang, M. Moretti, W. X. Dong, W. Wang, "Resource allocation for load minimization jointly with admission control in OFDMA wireless networks," Personal Indoor and Mobile Radio Communications (PIMRC), 2013 IEEE 24th International Symposium on , vol., no., pp.1533,1537, 8-11 Sept. 2013

[43] R. Webster, K. Munasinghe, A. Jamalipour, “A Scalable Distributed Microgrid Control Structure,” *IEEE TENCON Spring 2013*, Sydney, Australia, April 2013

[44] R. Webster, K. Munasinghe, A. Jamalipour, “A population theory inspired solution to the optimal bandwidth allocation for smart grid applications,” *IEEE WCNC 2014*, Istanbul, Turkey, April 2014

[45] R. Webster, K. Munasinghe, A. Jamalipour, “Optimal resource allocation for smart grid applications in high traffic wireless networks”, *IEEE SmartGridComm 2014*, Venice, Italy, November 2014

[46] S. Bu; F. R. Yu, P. X. Liu, P. Zhang, "Distributed Scheduling in Smart Grid Communications with Dynamic Power Demands and Intermittent Renewable Energy Resources," *Communications Workshops (ICC), 2011 IEEE International Conference on* , vol., no., pp.1,5, 5-9 June 2011

[47] A. Bose, "Smart Transmission Grid Applications and Their Supporting Infrastructure," *Smart Grid, IEEE Transactions on* , vol.1, no.1, pp.11,19, June 2010

[48] A. Vallejo, A. Zaballos, J. M. Selga, J. Dalmau, "Next-generation QoS control architectures for distribution smart grid communication networks,"*Communications Magazine, IEEE* , vol.50, no.5, pp.128,134, May 2012

[49] A. Zaballos, A. Vallejo, J. M. Selga, "Heterogeneous communication architecture for the smart grid," *Network, IEEE* , vol.25, no.5, pp.30,37, September-October 2011

[50] J. C. Hoag, "Wide-area Smart Grid situational awareness communications and concerns," *Energytech, 2012 IEEE* , vol., no., pp.1,7, 29-31 May 2012

[51] IEEE Standard for Synchrophasor Data Transfer for Power Systems," *IEEE Std C37.118.2-2011 (Revision of IEEE Std C37.118-2005)* , vol., no., pp.1,53, Dec. 28 2011

[52] P. Rengaraju, C. H. Lung, A. Srinivasan, "Communication requirements and analysis of distribution networks using WiMAX technology for smart grids,"*Wireless Communications and Mobile Computing Conference (IWCMC), 2012 8th International*, vol., no., pp.666,670, 27-31 Aug. 2012

[53] M. Levorato, U. Mitra, "Optimal allocation of heterogeneous smart grid traffic to heterogeneous networks,"*Smart Grid Communications (SmartGridComm), 2011 IEEE International Conference on*, vol., no., pp.132,137, 17-20 Oct. 2011

[54] IEEE Standard for Synchrophasor Measurements for Power Systems," *IEEE Std C37.118.1-2011 (Revision of IEEE Std C37.118-2005)* , vol., no., pp.1,61, Dec. 28 2011

[55] North American SynchroPhasor Initiative (NAPSI), Actual and Potential Phasor Data Applications,Jul. 2009, <http://www.naspi.org/phasorappstable.pdf>, (Accessed: December, 2013)

[56] A. Abdrabou, "A Wireless Communication Architecture for Smart Grid Distribution Networks," Systems Journal, IEEE , vol.PP, no.99, pp.1,11, 2014

[57] N. Cherukuri, K. Nahrstedt, "Cooperative congestion control in power grid communication networks,"*Smart Grid Communications (SmartGridComm), 2011 IEEE International Conference on*, vol., no., pp.587,592, 17-20 Oct. 2011

[58] P. Cheng, L. Wang, B. Zhen, S. Wang, "Feasibility study of applying LTE to Smart Grid,"*Smart Grid Modeling and Simulation (SGMS), 2011 IEEE First International Workshop on*, vol., no., pp.108,113, 17-17 Oct. 2011

[59] United States of America Department of Energy (DOE), Communications Requirements of Smart Grid Technologies, *Dep. Of Energy,* <http://www.doe.gov/>, (Accessed: December 2013)

[60] C. P. Nguyen, A. J. Flueck, "Modeling of communication latency in smart grid,"*Power and Energy Society General Meeting, 2011 IEEE*, vol., no., pp.1,7, 24-29 July 2011

[61] M. M. Eissa, A. M. Allam, M. M. A. Mahfouz, H. Gabbar, "Wireless communication requirements selection according to PMUs data transmission standard for smart grid," *Smart Grid Engineering (SGE), 2012 IEEE International Conference on* , vol., no., pp.1,8, 27-29 Aug. 2012

[62] I. Al-Anbagi, M. Erol-Kantarci, H. T. Mouftah, "A low latency data transmission scheme for smart grid condition monitoring applications,"*Electrical Power and Energy Conference (EPEC), 2012 IEEE*, vol., no., pp.20,25, 10-12 Oct. 2012

[63] T. Zhang, Z. Zeng, Y. Qiu, "A Subcarrier Allocation Algorithm for Utility Proportional Fairness in OFDM Systems," *Vehicular Technology Conference, 2008. VTC Spring 2008. IEEE*, vol., no., pp.1901,1905, 11-14 May 2008

[64] I. Al-Anbagi, M. Erol-Kantarci, H. T. Mouftah, "Low-latency smart grid asset monitoring for load control of energy-efficient buildings,"*Smart Grid Engineering (SGE), 2012 IEEE International Conference on*, vol., no., pp.1,4, 27-29 Aug. 2012

[65] Y. Ting, Z. Zhidong, L. Ang, W. Jiaowen, W. Ming, "New IP QoS Algorithm Applying for Communication Sub-Networks in Smart Grid,"*Power and Energy Engineering Conference (APPEEC), 2010 Asia-Pacific* , vol., no., pp.1,4, 28-31 March 2010

[66] T. Zhang, L. Xiao, Z. Zeng, L. Cuthbert, "Performance analysis on subcarrier allocation algorithm for utility fairness in OFDMA systems,"*Statistical Signal Processing, 2009. SSP '09. IEEE/SP 15th Workshop on* , vol., no., pp.297,300, Aug. 31 2009-Sept. 3 2009

[67] H. Li, W. Zhang, "QoS Routing in Smart Grid," *Global Telecommunications Conference (GLOBECOM 2010), 2010 IEEE* , vol., no., pp.1,6, 6-10 Dec. 2010

[68] W. Sun, X. Yuan, J. Wang, D. Han, C. Zhang, "Quality of Service Networking for Smart Grid Distribution Monitoring," *Smart Grid Communications (SmartGridComm), 2010 First IEEE International Conference on* , vol., no., pp.373,378, 4-6 Oct. 2010

[69] L. B. Le, T. Le-Ngoc, "QoS provisioning for OFDMA-based wireless network infrastructure in smart grids," *Electrical and Computer Engineering (CCECE), 2011 24th Canadian Conference on* , vol., no., pp.000813,000816, 8-11 May 2011

[70] C. Muller, M. Putzke, C. Wietfeld, "Traffic engineering analysis of Smart Grid services in cellular networks," *Smart Grid Communications (SmartGridComm),*

2012 IEEE Third International Conference on , vol., no., pp.252,257, 5-8 Nov. 2012

[71] P. Kansal, A. Bose, "Bandwidth and Latency Requirements for Smart Transmission Grid Applications," *Smart Grid, IEEE Transactions on* , vol.3, no.3, pp.1344,1352, Sept. 2012

[72] A. Aziz, H. El-Rewini, "Grid resource allocation and task scheduling for resource intensive applications," *Parallel Processing Workshops, 2006. ICPP 2006 Workshops. 2006 International Conference on* , vol., no., pp.8 pp.,65

[73] M. Pruckner, A. Awad, R. German, "A study on the impact of packet loss and latency on real-time demand response in smart grid," *Globecom Workshops (GC Wkshps), 2012 IEEE* , vol., no., pp.1486,1490, 3-7 Dec. 2012

[74] V. Joseph, G. de Veciana, A. Arapostathis, "Resource allocation: Realizing mean-variability-fairness tradeoffs," *Communication, Control, and Computing (Allerton), 2012 50th Annual Allerton Conference on* , vol., no., pp.831,838, 1-5 Oct. 2012

[75] G. Tychogiorgos, A. Gkelias, K. K. Leung, "Utility-proportional fairness in wireless networks," *Personal Indoor and Mobile Radio Communications (PIMRC), 2012 IEEE 23rd International Symposium on* , vol., no., pp.839,844, 9-12 Sept. 2012

[76] O. van den Biggelaar, J. Dricot, P. De Doncker, F. Horlin, "Power allocation in cognitive radio networks using distributed machine learning," *Personal Indoor and Mobile Radio Communications (PIMRC), 2012 IEEE 23rd International Symposium on* , vol., no., pp.826,831, 9-12 Sept. 2012

[77] Y. Xu, C. Fischione, "Real-time scheduling in LTE for smart grids," *Communications Control and Signal Processing (ISCCSP), 2012 5th International Symposium on* , vol., no., pp.1,6, 2-4 May 2012

[78] Z. Shen, J. G. Andrews, B, L. Evans, "Adaptive resource allocation in multiuser OFDM systems with proportional rate constraints," *Wireless Communications, IEEE Transactions on* , vol.4, no.6, pp.2726,2737, Nov. 2005

[79] T. Janevski, *Traffic Analysis and Design of Wireless IP Networks* (1st Edition) , Artech House (April 2003)

[80] 3rd Generation Partnership Project (3GPP), About 3GPP, <http://www.3gpp.org/about-3gpp/about-3gpp>, (Accessed: January, 2013)

[81] 3rd Generation Partnership Project (3GPP), 3GPP Release 8, <http://www.3gpp.org/specifications/releases/72-release-8>, (Accessed: January, 2013)

[82] 3rd Generation Partnership Project (3GPP), 3GPP Release 10, <http://www.3gpp.org/specifications/releases/72-release-10>, (Accessed: January, 2013)

[83] Y. S. Choo, J. Kim, W. Y. Yang, C-G. Kang, MIMO-OFDM Wireless Communications with Matlab (1st Edition), John Wiley & Sons (Singapore, 2010)

[84] S. Haykin, Communication Systems (4th Edition), John Wiley & Sons (New York, 2001)

[85] M. Hirsch, S. Smale, R. Devaney, *Differential Equations, Dynamical Systems & An Introduction to Chaos* (2nd Edition) , Elsevier Acadamic Press (2004)

[86] Y. Takeuchi, Global Dynamical Properties of Lotka-Volterra Systems (1st Edtion), World Scientific Pub Co Inc (Singapore, 1996)

[87] J. H. Poincaré, On curves defined by a differential equation, (1882))

[88] J. D. McCabe, Network Analysis, Architecture, and Design (3rd Edition), Elsevier Inc (Burlington, 2007)

[89] M. Rice, Digital Communications: A Discrete-Time Approach (1st Edition), Pearson Education (New Jersey, 2009)